Editor comments

E1: The main paper must give the model name and version number (or other unique identifier) in the title.

AE1: The final paper contains the model name and version number in the title.

CE1: The title is now changed.

Anonymous Referee #1

The authors use a reduced order model representation of a complex numerical wet land methane model with adaptive MCMC to estimate posterior distributions of model parameters. Because wetland methane models are complex and surface CH4 emissions are small differences between large gross fluxes, this type of calibration exercise is difficult and potentially valuable.

The authors did a nice job describing their results, given their model setup and assumptions. At this point, however, several assumptions in the approach leave me unconvinced of the reasonableness of the results, which I describe below. Also, the underlying model has not been described in the literature, and citing "Raivonen et al. (2017)" is inappropriate, since it is apparently a paper in preparation.

We thank the Anonymous Referee #1 for her/his constructive critique and we address the points raised below. Here, we would like to point out that Raivonen et al. Is in public discussion in GMD, and therefore available for consultation. The list of references that we provide at the end of the article has the old reference to "in preparation" paper, which is unfortunate. Whe have added the link, https://www.geosci-model-dev-discuss.net/gmd-2017-52/ to the references.

Changes to manuscript: Reference to Raivonen changed in the bibliography; now the entry is correct.

Major comments

R1/1. It is unclear why you need to vary the peat depth in your optimization. You apparently have measurements of the depth (lines 22-23, page 4), so you ought to use that as a non-calibratable value in the model. The high sensitivity of your parameter calibration to the peat depth implies to me that some other factor must be important and not properly resolved in your underlying model (e.g., O2 profiles below the WT depth or rooting profiles). The argument on line 31, page 6 that it is more computationally expensive to run with a deeper peat depth is not sufficient to justify this approach.

AR1/1: Peat depth of a wetland is not constant and therefore using a measured value is not as straightforward as is suggested. The peat depth affects in sqHIMMELI both production and transport. The high sensitivity of the parameter tau_C_cato suggest, as discussed, that the total catotelm decomposition rate is relatively constant as it is positively correlated with peat depth.

We changed the model to include the full 4m deep peat layer, by increasing the thickness of the lowest layer, and mention that this value is not an absolute truth but is to be looked at together with the tau_C_cato parameter, because of the variability of peat depth at any given wetland site, and the heterogeneity of the site. In MCMC experiments, 500000 sequential simulations are often needed, and the posterior estimate improves with more simulations, so in our opinion computational efficiency does matter. If the model simulation takes five seconds longer to finish, we end up spending 29 days more on the simulations.

As both referees wondered about the changing discretization level numbers, We drop the part of the study looking into that, and only concentrate on a single experiment.

CR1/1 Regarding peat depth: changes in Sec. 3.3 explain this, latexdiff p.8. l. 7-12; also the connection to the tau_C_cato parameter is mentioned there.

R1/2. Changing z_exu and Q10 on a yearly basis seems arbitrary. For Q10, I would expect much larger seasonal than interannual variations, yet you ignore that possibility. I think you need to explicitly describe the mechanisms you are proposing for the inter-annual variability of these parameters. The citation to Bergman et al 2000, who noticed change in Q10, "even within a single year", seems to bely your approach.

AR1/2 We could have added an additional model for the parameters Q10 and z_exu, but decided that a simpler approach serves us better here as we do not want to overfit the parameters. Bergman reports the following mid-July – late Sept. Q10-values for minerotrophic lawn, which is closest to the Siikaneva site (Laine et al.) whose data is used in the manuscript: 5.9, 3.7, 8.4, 4.0, 7.1, 4.1, 7.0. This suggests that the seasonal variation can be quite irregular at such sites, and in such a situation we opt for the simplest description of the variation. We would like to note here, that for the calibration we feel it is enough to be convinced that there is variation, and the mechanisms are a research question to be tackled in a separate research project. However, we note that these mechanisms are discussed in e.g. (Davidson et al., 2006), and we add a short section about it to our text.

CR1/2 Text added to Sec. 3.4, latexdiff p. 8 l.18-21

R1/3. Ignoring the temperature sensitivity of CH4 oxidation appear to be a flaw in your approach. There is substantial evidence that this temperature dependence is even larger than that for CH4 production. Further, since the net surface emission is a small balance of production and oxidation rates, and you explicitly account for the CH4 production temperature sensitivity (eq. (5)), not including Delta(E_R) in your equation (7) seems unreasonable. a. This concern propagates to the last sentence in your abstract. Oxidation often strongly affects the net CH4 emission, which is the measurement you are using to calibrate. If parameters affecting oxidation are 'not identifiable', then it seems unlikely that the production parameters are reasonable.

AR1/3 We re-performed the simulations and added Delta(E_R) in the parameters to be optimized. We add the relevant parts to the discussion and reformulate the abstract to reflect the changes. We also added the Delta_E_oxid parameter to the optimization, that regulates the temperature dependence of oxidation of the parameters. It is true that the oxidation and production terms are correlated, and this is something to beb expected. Nonetheless, also information regarding their correlation is important and as such scientifically valuable, as their mutual relationship may still be well defined.

CR1/3 The parametrers are added to Sec. 3.4, parameters no 7 and 9, latexdiff p.9 l.13 and 17. Also, they are added to the results, and tables at least to the following spots: prior information Table 3, Figs 3,4,6, and results in Table 4. Also latexdiff p.18 around l.5, p.22 l. 22, p.23 l.7, p.26 l.1, p.26 l.5.

R1/4. On line 21 of page 7, you state that V_R0 affects the rate of temperature dependent HR, but the T dependency is actually governed by Delta(E_R) which is not used in the calibration (Table 2). In general, it is unclear in your section 3.4 how the CH4 production occurs and its relationship with heterotrophic respiration.

AR1/4 This is correct, the shape of the temperature response is governed by Delta(E_R). We clarify the functions of the parameters regarding the HR in the text and also discuss the role of Delta(E_R) that was added in the new simulations.

CR1/4 This is actually covered by the description of parameter V_R0, parameter no. 6, latexdiff p.9. The short text there explains roles of both of those parameters, and the equation where they function. The parameter DeltaE_R is now part of optimization, see response CR1/3.

R1/5. In section 4.1, you say the model was linearized, but you did not show whether such a linearization is a reasonable approach. Please provide a quantitative evaluation of how appropriate this linearization

AR1/5 This was an error in the text. The linearization was done for the posterior probability density function and not to the model, and was used only in estimating the initial proposal covariance for MCMC. In the new simulations we do not use this method and hence this part of the text is dropped.

CR1/5 Sec. 4, latexdiff p. 13 l.20-21, removed text.

R1/6. Lines 22-25, page 9: Having to restart the model on January 1 of each year because realistic column gas concentrations were otherwise not predicted is a red flag for a problem in the model. The model should be able to run continuously without interruption. If this is a real problem in the model, you should rectify it. Once rectified and described in the paper, restarting each year for computational efficiency and parallelization is reasonable.

AR1/6 The concentrations are realistic and stable and the reason for the restarting is just the optimization algorithm, which allows using separate parallel simulations for different years. We wanted the peat column gas concentrations of any year in the optimizations to be in the regime of the parameters to be optimized, but since the variations are small, we actually believe, that this is more than enough. In the end the model will of course be run linearily in a single simulation, and this can be done already now with only trivial changes required to the model.

CR1/6 We believe this is adequately explained in the text, but changed the text a little, latexdiff. p.14 l. 17.

R1/7. Section 4.2.4 seems to apply that your objective function is only based on annual values, but the text implies that you use the annual values to linearize the model, and then perform the parameter calibration with observed daily CH4 emissions. Please clarify.

AR1/7 The annual component was dropped from the new simulations as they had no practical effect to the posterior. The text is updated accordingly.

CR1/7 See CR1/5, also latexdiff p.14 l.25. Additionally, removed Annual CH4 fluxes section, latexdiff p.15 l. 11-20

Smaller comments:

R1/8. Methane is the second most important anthropogenic GHG for warming (don't forget water vapor).

AR1/8 This is now mentioned in the text.

CR1/8 p.2 l.11-12

R1/9. You describe annual calibration in they abstract, but not the fact that you used a ROM and then daily fluxes for calibration (as far as I can tell). This approach should be described in the abstract.

AR1/9 The annual values were dropped, see R1/7. Also, a reduced order model was not used, and in the updated work it is not used even for covariance estimation.

CR1/9 No additional text changes needed as no ROM nor annual estimates were in the end used

R1/10. Line 13-15, page 2: cite recent methane model inter-comparisons here: Melton et al., Bohn et al.

AR1/10 Citations were added to text.

CR1/10 Latexdiff: mention added in intro, p. 2/l. 27

R1/11. Your assertion (lines 33-34, page 2 to line 4, page 3) that flawed physics representations, numerical errors, and coding errors are good reasons to calibrate a model is shocking. Calibrating a poorly constructed model is a cardinal sin of modeling, although it is regularly done. I think you might re-think the organization of this paragraph.

AR1/11 We clarify the text. However, we would like to point out that even excellent models require calibration. Model parameter optimization is effectively inverse modeling, which can improve predictive performance, reveal bottlenecks, and in the best cases provide information for analyzing the physical system. This being said, it is fully true that blindly done model calibration can lead to strange results and a worse model. We reorganize the section to better clarify our views on the topic. We also mention that proper description of the physics is important for the calibration exercise to make sense.

CR1/11 latexdiff p.3, l.13-20

R1/12. Line 5, page 3: Possibly the most mechanistic and realistic terrestrial CH4 model available today is ecosys (Grant, 2002), which you should cite.

AR1/12 Citation has been added to the text.

CR1/12 Citation added, latexdiff p.3 l.22

R1/13. Line 8, page 3: define 'multi modality'

AR1/13 The text has been clarified in regard to this.

CR1/13 latexdiff p.4 l. 26-27., text clarified.

R1/14. Your figures are cited out of order in the text (e.g., figure 11 cited just after figure 2).

AR1/14 The figures are now in order.

CR1/14 Figures and Tables are in order of appearance, and hence they are also in order in the text.

R1/15. Line 27, page 12: do you mean 'inter-annual variability' instead of 'annual variability'?

AR1/15 Yes, fixed.

CR1/15 latexdiff p.18 l. 21

R1/16. Line 9, page 12: there is no figure 6g.

AR1/16 Should have been 6 (b), fixed

CR1/16 latexdiff p.19 l. 14; (due to ordering changes of the figures and changes in the figures, the numbers are now different, and the old numbers are wrong; the cross validation figures are now 7b and 8)

R1/17. Does the model calculate the peat temperature? It is not clear from your description which T you are using to estimate your temperature sensitivity. Air T?

AR1/17 The model uses any soil temperatures that it is given. In this work we used everywhere measured soil temperatures. We clarify this point further.

CR1/17 clarified that it was measurement data that was used. latexdiff p.5 l.31-32

R1/18. What happened to a discussion of figure 10?

AR1/18A short discussion was left out and is now added.

CR1/18 This figure is now discussed: latexdiff p.21 l.24-28. The figure was already touched upon earlier, this section is latexdiff p.25 l.20-25.

R1/19. Where did the NPP come from? Describe in Methods.

AR1/19 This is explained in the appendix, but is clarified in the main text now.

CR1/19 Regression modeling of NPP is now mentioned in methods (data description section), latexdiff p.6 l.2-3. The detailed description is still left to the Appendix E.

Anonymous Referee #2

The objective of this paper is to use observed carbon flux time series in order to optimize parameters of a peatland carbon flux model. In general, this is a timely and important work. However, I found several serious issues with this manuscript including potential flaws in the method that does not allow a publication in the present form.

Please, indicate in abstract and introduction, what is the overall objective of this model e.g. in future applications? Do you want to apply it exclusively for this one peat site and for which question? Do you want to apply it on a continental to global scale, e.g. as part of a land surface scheme? In the latter case, several model assumptions are not useful (effective peat depth, C pool-independent decomposition flux), and a lot of work on parameter optimization seems to be questionable when only data from one specific site is used.

The HIMMELI model will be used in both stand-alone configurations and as parts of land surface components of regional and global models. We do not intend that the parameter optimization work here would be relevant to any wetland site – rather we look at within-site variation of parameters. The model assumption-related problems are addressed in the points below. We also further clarify the objectives of the research in the abstract and the introduction.

Changes to manuscript: Main results clarified in abstract and intro, latexdiff p.1 l. 11-17. Applicability, p.1 l. 7-9., p.3 l.11-13.

Major comments to sqHIMMELI assumptions:

R2/1 In both aerobic and anaerobic cases, organic matter decay seems to be a constant parameter not depending on substrate availability. When peat depth would have been set constant to the observed site-level value, then this could be valid for the specific site but then we do not learn anything from the parameter optimization procedure for a generally applicable dynamic model.

AR2/1 In the model, the organic matter decay (anoxic peat decomposition, Eq. A6) is not a constant parameter but depends also on the amount of peat and its temperature. And of course e.g. oxygen concentration affects the decay rates. We would like to point out for clarity that Eq. 5 in itself does not determine the reaction rate. In addition to moving appendix A into main text (as requesed in referee comment R2/15), we clarify in the text this point.

We re-performed the simulations with a 4m total peat column, which reflects our knowledge of the peat depth at the Siikaneva site (Rinne et al. 2007). Anaerobic respiration of exudates on the other hand does not depend on the peat column thickness. We clarify this in the text.

As peatlands differ widely from site to site, naturally these different types of wetlands have different parameters controlling the organic matter decay. In the manuscript we look at the decay rates for a single site and as such the parameter values are not directly generalizable everywhere. However, we believe that we could, by looking at data from other sites, calibrate the model for various types of wetlands with e.g. hierarchical Bayesian methods, and this would make it possible to e.g. use the model with land surface sceme. This is work still waiting to be done and beyond the scope of this manuscript.

CR2/1 Change of peat depth mentioned: latexdiff Sec. 3 p. 6 l. 21. For peat decay dependence, latexdiff p. 11, l.21-22.
(In fact we ended up in the end using 85% of the maximum depth of 4 meters, as the reported depth was 2-4 meters.)

R2/2 Effective peat depth: This assumption makes no sense at all. Peat depth should be a constant value corresponding to the site observation. See below for related flaws in eq 5.

AR2/2 We have changed the peat depth to 4m that roughly represents the peat depth in Siikaneva. We no longer speak about effective peat depth in the manuscript. The different simulations now refer to how deep the fine discretization of the peat column goes. Please see also the answer to R1/1.

CR2/2 Only one discretization was used in the end. Text changed everywhere to reflect that we now use an approximation of the actual peat depth, e.g. latexdiff p.8 l.7-11. All figures and tables that touched upon different peat depths are updated (new numbers): Tables 4 and 5, and Figures 4,6,7,8,10,12,13,

R2/3 A2 Anaerobic respiration producing CH4: It seems from eq. A5-A8 that you apply a CH4:CO2 ratio of 1:1 for anaerobic decomposition of root exudates. If so, please make this statement explicit and cite experimental literature showing this ratio.

AR2/3 We initially optimized the ratio along with other parameters, but due to covariability with the z_exu parameter without CO2 data, we left this parameter out as only z_exu or the ratio-determining parameter could be determined, and for the first iteration we chose 1:3. However, with CO2 flux data, we are able to constrain the parameter, and therefore we add it to the optimization and to the discussion.We now use data from (Nilsson & Öquist) to set the prior values and explicitely state the final ratios.

CR2/3 f_exu^CH4 parameter added, latexdiff p.9 l.6, p.11 l.20, p.17, l.31-33, p.21 l.20, p.26 l.19, also Figs 3,4,6, Tables 3 and 4.

R2/4 In section 3 it is also fully unclear if you consider anaerobic CO2 production or not.

AR2/4 We do. This is now also clarified in the text.

CR2/4 Mentioned in Sec. 3 first paragraph; latexdiff p. 6 l. 11

R2/5 Eq. 5: is tau(cato) the mean residence time at 273.15 K? The unit (y) in Tab 3 is not correct because in eq. 5 you do not multiply with a Cpool.

AR2/5 Equation 5 just describes a rate parameter, equation A6 is the actual peat decomposition. When tau has the units of time, A6 then has the time in the denominator which is correct.

CR2/5 We changed the presentation of the units and multiplicative factors in Table 4 (new number) to be more intuitive, eve n though we believe that it was also correct previously. See Table 4.

R2/6 I expect the Finland peat being frozen with snowpack above over long time periods of the year. What are the effects of <273K soil temperature on aerobic and anaerobic decomposition? What are the effects of soil ice on gas transport and what are the effects of snow on gas transport?

AR2/6 Ice and snow slow diffusion of gases into the atmosphere, but this has not been so far implemented in HIMMELI, except for some very preliminary and simple efforts. We tried increasing the resistance of the top soil layer when top soil temperature fell under 0 C but this did not improve the fit / change the results enough for that the change would have been reasonable to keep. We have hence not included descriptions for processes such as diffusion through snow, or release of accumulated gas bubbles under ice in spring time as described by e.g. Mastepanov et al. (2013), Sriskantharajah et al. (2012) – this will be very interesting and will hopefully be done at a later stage.

CR2/6 References and explanations added, Sec. 3, latexdiff p.6 l. 26-28

R2/7 Please include in results and discussions the exudate pool values.

AR2/7 We add the exudate pool values and briefly discuss them.

CR2/7 The exudate pool is added to Fig. 9 and there is a short description of it on p. 22 l. 1-3 in the latexdiff.

R2/8 Peat depth: Prescribing an effective peat depth will hinder any application of that model in larger dynamic models, such as land surface schemes or DGVMs. Peat depth is no parameter there that you can prescribe but included into the mass balance equations. If you define an effective peat depth then this would mean that you either introduce a fully recalcitrant carbon pool (case peat depth > effective peat) or that you "produce" CH4 and CO2 from non-existing carbon (case peat depth < effective peat depth). That is not a valid and also not useful model assumption.

AR2/8 We are not modeling for peat depth changes in this model so far. Of course, the decay in m y^-1 can be calculated in a straightforward way, but since we don't know the speed of new peat formation we don't know the change of the peat column in time. This work will be done later. We have changed the peat column depth to reflect the real depth. We have dropped the notion of effective peat depth.

CR2/8 Same changes apply as in CR1/1, CR2/1, CR2/2

Major comments on the parameter optimization:

R2/9 Tab 5: What is the reason for not including these parameters into MCMC optimization? I generally think that the information content in the data is far too low for an optimization of all model parameters, hence a selection will be useful. However, we need good reasons for such selection, either based on theory or based on a previous sensitivity analysis.

AR2/9 The selection was based on a previous preliminary analysis. This is now mentioned in the text. In practice not fixing some of the parameters may lead to ending up in local minima that are unrealistic. However, more importanly, parameters are interlinked via the model processes and in order to constrain the parameters determining the most important processes we fix some of the less important ones. We now explain for all non-included parameters why they have not been included.

CR2/9. Latexdiff p. 8 / l.21-22, and Table 2, p. 49 in latexdiff / p. 38 in the manuscript and its caption.

R2/10 I assume there is additional CO2 flux data available at the site. It is totally unclear why this data has not been used for constraining in addition to CH4 parameters such as decomposition and transport parameters as well as oxidation parameters

AR2/10 We have reperformed the simulations also utilizing CO2 flux data. The setup description, results, and the discussion have been updated.

CR2/10 The changes are wide-ranging because also methods had to be updated, including adding a further resampling step. Latexdiff p.1 l.4, p.4 l. 26, p.5 l.2-29, p.14, l.23-31, p.15, l.3-6 and 14-17, Eq. 24, p.16 l. 5, p. 19 l.3-5, 20-21, 31-33, p.30, l.7-12, 17, p.33 l.26, p. 34 l. 19-24. For the resampling, a section was added, p.35, l. 1- p.36, l.7. and p.38 l.13-20. The section (latexdiff) p. 39 l.21- p. 40 l. 5 were dropped as obsolete.

R2/11 parameter values cannot be transferred to other similar models and even not to HIMMELI because of the peat depth parameter and because of important differences in model formulations: root depth distribution, decomposition parameterization, etc. What is the scientific value of the paper then? Do you plan to use this model version in future studies and not the HIMMELI model?

AR2/11 We plan to use both sqHIMMELI and HIMMELI in future studies. The decomposition parameterization is not part of the HIMMELI model but it can still be used as a source of the anaerobic respiration, which is an input variable for HIMMELI. We believe that the results are transferrable to other models variably: the optimal values of course are not so straightforward, but correlations of the processes more so. HIMMELI is a model more suitable for integration in land surface schemes, whereas sqHIMMELI is a version of the model more designed to be used in stand-alone experiments and settings such as MCMC studies. We will in future studies also integrate features from both model version's development into each other. What model version we use for future studies will depend on the research question at hand.

CR2/11 This was clarified as indicated in changes to manuscript in response to general comments by referee #2: this document, top of p. 6. In our view no other changes to the manuscript are needed in addition to those mentioned there. (copied here: *"Main results clarified in abstract and intro, latexdiff p.1 l. 11-17. Applicability, p.1 l. 7-9., p.3 l.11-13.2"*)

R2/12 section A4: I do not understand the sentence "Due to coding mistake, the fD,a and fD,w coefficients in the aforementioned equations were set to 0.1 for gases other than CH4 in this work." Why do you set both parameters to 0.1? With a huge pore volume in peat soils I would expect a value of 0.8 or 0.9. If that is a tuning parameter then you should optimize it. These parameters are also not listed in Tab 5. Instead they are part of Fig 2 and this seems to be a real flaw in the procedure?

AR2/12 This flaw has been fixed in the new simulations.

CR2/12 p. 33 l.9 sentence removed. (Due to moving the appendix to the main text, latexdiff gets confused and this change is not properly shown in the diff.) The new corresponding place is (latexdiff) p. 12 l.23.

R2/13 For clarity, please put units on all parameters in tables and figures or when describing parameters in the text.

AR2/13 This has been done.

CR2/13 Changes all over in text, including the tables and figures. Units were added in parentheses. Manuscript Figs 3,6,13, and now Tables 1-4 have also units.

R2/14 I cannot understand the a posteriori optimized parameter values of tau_exu in the order of magnitude 0.00001 s (tab 3) when range is 3 to 30 days with a prior of 14 days (tab 2). From Fig 3 it seems there is a mistake in units in the table. I have similar problems with units of a posteriori V_0R which seems to be far too high. Zeta_exu seems to be with 0.5 also quite high and it would be good to see some comparison to literature values if available in the discussion. tau(cato) ranges from 2000 to 20000 years (unit in tab 3 wrong however) depending on peat depth just because the model invalidly does not take the carbon pool into account for calculating the decomposition flux (eq. 5).

Then of course, the deeper the peat the more C available the higher you need to have turnover time for the same flux. This is not a valid approach for a dynamic model.

AR2/14 For the units, we believe that Table 3 is correct: if tau_exu x 0.00001 = 10, then tau_exu = 10^6, which is around 11.6 days. Same is true for tau_cato and V_0R. The zeta_exu parameter is high because of a non-optimized another parameter f_methane in the model.That parameter value has been added to the optimization. We would like to note also that the decomposition flux is given by equation A6 – equation 5 gives just the reaction rate constant and if tau_cato has the units of years, the peat decomposition flux given by A6 becomes, integrated over the depth, moles per second per square meter. For the last sentence, we refer to replies to R2/1 and R2/5.

CR2/14 We changed the way the units and the magnitudes were presented, and even though we believe that it was also previously correct, we feel it is now more intuitive. See "parameter"-column in Table 4 in the manuscript. (latexdiff had serious difficulty formatting the differences in the table).

R2/15 A minor comment: I do not find it useful to have some methods description in the main text and some in appendix A but both relate so strong to each other that one understands it only when reading both together. Please move appendix A into main methods text.

AR2/15 We have moved the appendix A into the main methods text.

CR2/15 Appendix A in the old version moved to be Sec. 3.5 in the new version.

References:

Erica Davidson, Ivana Janssens, Yiqi Luo: *On the variability of respiration in terrestrial ecosystems: moving beyond Q 10,* Global Change Biology (2006) 12, 154–164, doi: 10.1111/j.1365-2486.2005.01065.x

Laine AM, Bubier J, Riutta T, Nilsson MB, Moore TR, Vasander H, Tuittila E-S. 2012. *Abundance ad composition of plant biomass as potential controls for mire net ecosystem CO2 exchange*, Botany Vol 90, 63-74.

M. Mastepanov, C. Sigsgaard, T. Tagesson, L. Ström, M. P. Tamstorf, M. Lund, and T. R. Christensen: *Revisiting factors controlling methane emissions from high-Arctic tundra*, Biogeosciences, 10, 5139–5158, 2013 doi:10.5194/bg-10-5139-2013

Nilsson & Öquist: *Partitioning Litter Mass Loss into Carbon Dioxide and Methane in Peatland Ecosystems*, Carbon Cycling in Northern Peatlands, Geophysical Monograph Series 184

Rinne, J., Riutta, T., Pihlatie, M., Aurela, M., Haapanala, S., Tuovinen, J.-P., Tuittila, E.-S., and Vesala, T.: *Annual cycle of methane emission from a boreal fen measured by the eddy covariance technique*, Tellus B, 59, 449–457, doi:10.1111/j.1600-0889.2007.00261.x, http://dx.doi.org/10.1111/j.1600-0889.2007.00261.x, 2007.

S. Sriskantharajah, R.E. Fisher, D.Lowry, T. Aalto, J. Hatakka, M. Aurela, T. Laurila, A. Lohila, E. Kuitunen: *Stable carbon isotope signatures of methane from a Finnish subarctic wetland*, Tellus B 2012, 64, 18818, http://dx.doi.org/10.3402

Calibrating ~~a~~ the sqHIMMELI v1.0 wetland methane emission model with hierarchical modeling and adaptive MCMC

Jouni Susiluoto[1,3,4], Maarit Raivonen[2], Leif Backman[1,2], Marko Laine[1], Jarmo Makela[1,4], Olli Peltola[2], Timo Vesala[2,5], and Tuula Aalto[1]

[1]Climate research, Finnish Meteorological Institute, P.O. Box 503, 00101 Helsinki, Finland
[2]Institute for Atmospheric and Earth System Research/Physics, Faculty of Science, University of Helsinki, Finland
[3]Lappeenranta University of Technology, School of Science, Finland
[4]University of Helsinki, Department of Mathematics and Statistics, Finland
[5]Institute for Atmospheric and Earth System Research/Forest Sciences, Faculty of Agriculture and Forestry, University of Helsinki, Finland

Correspondence to: jouni.susiluoto@fmi.fi

Abstract. ~~Methane~~ Estimating methane (CH_4) ~~emission estimation for~~ emissions from natural wetlands is complex and the estimates contain large uncertainties. The models used for the task are typically heavily parametrized and the parameter values are not well known. In this study we perform a Bayesian model calibration for a new wetland CH_4 emission model to improve quality of the predictions and to understand the limitations of such models.

The detailed process model that we analyze contains descriptions for CH_4 production from anaerobic respiration, CH_4 oxidation, and gas transportation by diffusion, ebullition, and the aerenchyma cells of vascular plants. The processes are controlled by several tunable parameters. We use a hierarchical statistical model to describe the parameters and obtain the posterior distributions of the parameters and uncertainties in the processes with adaptive MCMC, importance resampling and timeseries analysis techniques. For the estimation, the analysis utilizes measurement data from the Siikaneva flux measurement site in Southern Finland.

The ~~model parameters are calibrated using six different modeled peat column depths, and the~~ uncertainties related to the parameters and the modeled processes are described quantitatively. At the process level, the flux measurement data are able to constrain the CH_4 production processes, methane oxidation and the different gas transport processes. The posterior covariance structures explain how the parameters and the processes are related. Additionally, the flux and flux component uncertainties are analyzed both at the annual and daily levels. The parameter posterior densities obtained provide information regarding importance of the different processes, which is also useful for development of wetland methane emission models other than sqHIMMELI.

The hierarchical modeling allows us to assess the ~~effect~~ effects of some of the parameters on an annual basis. The results of the calibration and ~~their~~ the cross validation suggest that the early spring net primary production ~~and soil temperatures~~ could be used to predict parameters affecting the annual methane ~~emissions. The modeled peat column depth has an effect on how much the plant transport pathway dominates the gas transport, and the optimization moved most of the gas transport from the~~

diffusive pathway to plant transport. This is in line with other research, highlighting the usefulness of algorithmic calibration of biogeochemical models. production.

Modeling only 70 cm of the peat column gives the best flux estimates at the flux measurement site, while the estimates are worse for a column deeper than one meter or shallower than 50 cm. The posterior parameter distributions depend on the modeled peat depth. At the process level, the flux measurement data is able to constrain CH_4 production and gas transport processes, but for CH_4 oxidation, which is an important constituent of the total CH_4 emission , the determining parameter is not identifiable. Even though the calibration is specific to the Siikaneva site, the hierarchical modeling approach is well suited for larger scale studies and the results of the estimation pave way for a regional or global scale Bayesian calibration of wetland emission models.

1 Introduction

Methane is the second third most important gas in the atmosphere in terms of its capacity to warm the climate, after water vapor and carbon dioxide, currently with the radiative forcing power of 0.97 Wm^{-2} (IPCC, 2013). This is a sizable part of the total effect of well-mixed greenhouse gases, which is approximately 3.0 Wm^{-2}. According to IPCC (2013), the amount of CH_4 in the atmosphere has risen to its highest level in at least the last 800000 years due to human activity, and based on ice core measurements, also its growth rate is presently very likely at its highest level in the last 22000 years.

The sources of CH_4 are both anthropogenic and natural. In years 2003-2012, 60% of the global emissions were anthropogenic (range 50-65 %) and about one third came from natural wetlands. The most important source of uncertainty in the global methane budget is attributable to emissions from wetlands and other inland waters. Combining top-down and bottom-up estimates, natural wetland emissions range from 127 to 227 Tg CH_4 yr^{-1} (Saunois et al., 2016). Anthropogenic sources include rice paddies, landfills, enteric fermentation and manure, incomplete combustion of hydrocarbons, and natural gas leaks (Ciais et al., 2013).

The methane from wetlands is produced by prokaryotic archaea under anaerobic conditions. The main sink for atmospheric CH_4 is its oxidation in troposphere by OH ions and the average lifetime of a CH_4 molecule in the atmosphere is 9.1 ± 0.9 years (Prather et al., 2012; IPCC, 2013).

The wetlands in the boreal zone are a significant contributor to the total CH_4 emissions from wetlands (Kirschke et al., 2013), and for this reason the CH_4 emissions from them have been intensively studied, also with models, during the past years (Wania et al., 2010; Kaiser et al., 2016; Petrescu et al., 2015). However, major discrepancies between predictions from those models remain (Melton et al., 2013; Bohn et al., 2015).

The need for improved wetland methane emission modeling is amplified by the fact that although annual mean precipitation is projected to increase in the boreal zone (Ruosteenoja et al., 2016), changes in the frequency and duration of severe drought may follow an alternate path (Lehtonen et al., 2014), manifesting the need to study wetland responses to extreme events.

Changes to hydrological conditions such as draining or recurring low water table depth can alter the balance of greenhouse gas emissions (Frolking et al., 2011; Petrescu et al., 2015). Modeling and calibrating for such exceptional events can be difficult, as was found for instance by Mäkelä et al. (2016).

The HelsinkI Model of MEthane buiLd-up and emIssion for peatlands (HIMMELI) is a relatively full-featured wetland/peatland CH_4 emission model and it is described in detail in Raivonen et al. (2017). The model contains process descriptions for CH_4 production from anaerobic respiration, O_2 consumption and CO_2 production from oxic respiration, and gas transport processes via diffusion, ebullition, and plant transport. Modeling the concentrations of CH_4, O_2, and CO_2 in the peat column is explicitly included. The peat column depth can be set at any desired value, and the water table movement determines the part of the peat column that is favorable for CH_4 production. The version of HIMMELI in this work has additional processes, described in Sec. 3.1, and the modified model is referred to as sqHIMMELI (square root HIMMELI), as it contains a description of CH_4 production from root exudates. The sqHIMMELI model is geared towards site-level studies, whereas HIMMELI is more suited for integration directly as a component in e.g. land surface schemes.

~~Computer~~ Even well constructed computer models describing environmental processes accumulate error at many levels (Sanso et al., 2007). The sources include time- and space discretization, ~~incomplete~~ compromises in model physics and biochemistry descriptions due to computational constraints, insufficient information about the initial states of the model~~and their time evolution, numerical errors, and coding~~ , and numerical errors, along with parametrization-induced inaccuracies of the subgridsize processes. This leads to a need to calibrate and optimize models, as the physical variables do not necessarily exactly correspond to the model variables ~~perfectly and hence they cannot be often~~ and hence the model parameters cannot often be directly measured. Of course any physically insightful interpretation of calibration results makes sense only for a well-constructed physical model.

Several current CH_4 models include the important physical processes controlling both CH_4 production and transport in the peat column ~~(Kaiser et al., 2016; Lai, 2009b; Müller et al., 2015)~~(Kaiser et al., 2016; Lai, 2009b; Müller et al., 2015; Grant and Roulet, 20. The modeled peat column depth affects the total modeled CH_4 emission from the peatlands and it is directly included in some models (Lai, 2009b; Walter and Heimann, 2000). These models are in general highly sensitive to changes in the values of the parameters (van Huissteden et al., 2009). However, even though algorithmic parameter optimization has been done in some studies, the stress is often on parameter efficiencies (van Huissteden et al., 2009), or optimal values (Müller et al., 2015), and hence the full uncertainty of the values of parameters in these models is not well understood.

Methane models typically use measured values from field campaigns and parameters estimated from those studies where applicable (Lai, 2009b; Walter and Heimann, 2000; Tang et al., 2010; Riley et al., 2011), and, when needed, include extra tuning parameters for processes (Walter and Heimann, 2000). This is a practical and much used route as information regarding all of the needed parameters is not available at all sites (van Huissteden et al., 2009; Walter and Heimann, 2000). Wide variability can be expected from some parameters, such as those controlling CH_4 oxidation (Segers, 1998). Emissions from different areas of the same wetland can also vary, due to microtopography and differences between how fast the peat decomposes in different areas (Lai, 2009a; Cresto Aleina et al., 2016), making straightforward parameter value assignment difficult.

Due to these uncertainties, values of parameters vary widely from research to research. For instance for the Q_{10}-value controlling the temperature dependence of CH_4 production, Walter and Heimann (2000) use the value 6, handpicking it from the interval of 1.7-16, whereas van Huissteden et al. (2009) use a range of 3-8, and Müller et al. (2015) constrain the value between 1 and 10, with the default value of 1.33 and eventually optimizing it to the value of 1 for two of the three optimizations presented. For other parameters, such as those controlling diffusion rates in peat, the situation is similar.

Calibration done for the models is usually quite basic. Wania et al. (2010) tune their model by running it with parameters from a parameter grid, containing only three values for each of the 7 parameters tested, and Riley et al. (2011) follow a similar procedure for the wetland CH_4 model component, CLM4Me, of the Community Land Model. Such ~~crude~~ sensitivity studies obviously are not able to find out how a model is able to perform at its best. Müller et al. (2015) have further optimized the CLM4Me model using an emulator combined with a simple minimization algorithm, with respect to several different sites, which are bound to have quite different physical characteristics, and are yielding optimal values often at the borders of the prescribed allowed area of variation. In a sensitivity analysis of the PEATLAND-VU model, a derivative of the Walter-Heimann model, van Huissteden et al. (2009) look at the efficiencies of the different parameters, but do not elaborate on other qualities of the posterior. ~~Modeled peat column depth, which is included in the research at hand, is not optimized for the models generally, and for instance Walter and Heimann (2000) choose it based on expert knowledge.~~

Using hierarchical modeling to estimate annually ~~changing~~ varying parameters is sensible, since the flux measurement site has both properties that change from year to year (e.g. small changes in vegetation, plant roots, and microbe populations) and properties that are more permanent (e.g. peat quality and plant species). With fixed parameter values for all years, the model sometimes does not accurately and appropriately describe the observations. On the other hand, with different parameters for all the years, the parameters are easily overfitted, meaning that while the resulting model fits the data well, it does not accurately predict future fluxes (Gelman et al., 2013). Hierarchical modeling provides a solution for these problems.

In the present study, the sqHIMMELI model is calibrated using adaptive Markov chain Monte Carlo (MCMC) and importance resampling techniques to evaluate a hierarchical statistical model for the model parameters. The calibration is done for the boreal Siikaneva site. This study complements the work in Raivonen et al. (2017) in describing the effects of various parameters on the processes and fluxes, and analyzing what kinds of configurations best describe the studied boreal wetland.

~~Classical optimization is often misleading~~ Merely optimizing model parameters may lead to misleading results due to the ~~multi-modality~~ presence of several local minima in the objective function, as for example Müller et al. (2015) reported in a study where they used a surrogate model to calibrate the parameters of the CH_4 model component of the Community Land Model. This multi-modality can be accommodated for by using MCMC techniques. Utilizing MCMC methods for optimizing environmental models and studying their uncertainties is not new (Laine, 2008; Ricciuto et al., 2008; Hararuk et al., 2014), but to our knowledge they have not been used for wetland CH_4 model parameter estimation before. Moreover, the research that the authors are aware of does not investigate the interannual variability of parameters, as is done in this study.

The main objective of this work is to analyze the capabilities and limitations of a modern featureful wetland CH_4 model by looking into the shape of the posterior parameter distributions, parameter correlations, and the roles, identifiabilities, interdependencies, and interconnections of the parameters and the processes they control. ~~The simulations and the analyses are~~

performed with six different modeled peat depths, which allows for assessing how the modeled peat column depth affects the model behavior, and how deep a peat column is optimal based on the flux measurement data usedAs a part of this work, knowledge about how the methane and carbon dioxide flux data are able constrain the parameters and processes, is obtained.

2 Siikaneva wetland flux measurement site and model input data

Methane and carbon dioxide flux measurements were needed for estimating the model parameters, and for that purpose observational data from the Siikaneva peatland flux measurement site in southern Finland (61°50'N, 24°12'E) were used. The site is a boreal oligotrophic fen with a peat depth of up to four meters. The data collection

Measurement of ecosystem scale gas fluxes started in 2005, and in this work eddy covariance (EC) CH_4 and CO_2 flux measurements from years 2005 to 2014 were used. In the current application of the EC method, the flux was gas fluxes were calculated from the wind speed and direction, and CH_4 concentration information, both of whose sampling frequency was and CO_2 concentration information. All these variables were sampled with 10 Hz and fluxes were calculated over 30-min averaging time in order capture the whole spectrum of turbulent exchange. During the measurement period several different instruments were used for methane concentration measurements: Campbell TGA-100 (2005-2007 and 04/2010-08/2010), Los Gatos RMT-200 (01/2008-02/2014), Picarro G1301-f (04/2010-10/2011) and Los Gatos FGGA (2014). Carbon dioxide concentrations were measured throughout the period with a LI-7000 manufactured by Licor Inc. The wind velocity vector was analyzed by a USA-1 acoustic anemometer by METEK (Rinne et al., 2007). All the EC-data were post-processed in a consistent manner using an in-house software EddyUH (Mammarella et al. , 2016) (Mammarella et al., 2016). Flux data were screened for instrumental problems and for insufficient turbulent mixing. Due to instrument problems, data from 2009 was not available.

For this study daily means of CH_4 fluxes were calculated from the screened data that contained gaps. This is a viable approach, since CH_4 fluxes do not show a diel pattern at this site (Rinne et al., 2007). However, before calculating the daily values of net ecosystem exchange of CO_2, standard gap-filling methods for peatland CO_2 fluxes were applied (Aurela et al., 2001, 2007) . In short, the gap-filling algorithm estimated the CO_2 flux dependency on photosynthetic photon flux density, air temperature and water table position and the algorithm was used to fill periods when CO_2 fluxes were missing. See more details in (Aurela et al., 2001, 2007) about the gap-filling procedure. After gap-filling the daily means of CO_2 fluxes were calculated and used in this study.

For using this carbon dioxide data with the costfunction, the CO_2-flux produced by sqHIMMELI was matched with the sum of net ecosystem exchange and the net primary production of all plants. We assumed that the share of aerenchymatous plants is 70% of the total NPP. The fact that the net primary production is not a measured but modeled quantity (see below) introduces some uncertainty into the CO_2 flux against which the model is calibrated.

The required inputs for sqHIMMELI are daily soil temperatures, water table depths (WTD), net primary production (NPP), and leaf area indexes (LAI). The soil temperature profile for the grid used was generated by interpolating from measurement data between the measurement depths (-5 cm, -10 cm, -20 cm, -35 cm and -50 cm) and assuming that at -3 meters and below the temperature is a constant +7 °°C. This was the mean temperature of all the years at -50 cm depth. The WTD data used

was available as measurement data, and where data was missing, it was gap-filled by repeating the previous measured value. Net primary production cannot be measured in a direct way, and hence ~~modeled values for it~~ values obtained from a regression model were used. ~~Also~~ The methodology is explained in Appendix E and still further in Raivonen et al. (2017). Similarly for LAI, a simple model was used for obtaining the input. ~~For more details , see~~ The details are, again, given in Appendix E. A summary of the data used is given in Table 1.

3 The sqHIMMELI model

The HIMMELI (HelsinkI Model of MEthane buiLd-up and emIssion for peatlands) model (Raivonen et al., 2017) is a detailed model for estimating CH_4 emissions from wetlands. It was developed at the University of Helsinki in collaboration with the Finnish Meteorological Institute and the Max Planck Institute for Meteorology in Hamburg. The model is designed to be used as a submodel ~~for different larger~~ in different modeling environments, such as regional and global biosphere models. It contains processes describing the production of CH_4 and CO_2 including anaerobic production of CO_2, the loss of CH_4 and O_2, and transport of CH_4, O_2, and CO_2 between the soil and the atmosphere. The CH_4 transport can take place by diffusion in peat (in water and in the air), by ebullition (transport by bubble formation), and by diffusion in the porous aerenchyma tissues in vascular plants. The model is driven with peat temperature, WTD and LAI of the aerenchymatous plants. The process descriptions are mainly adopted from previous wetland CH_4 models such as Arah and Stephen (1998), Wania et al. (2010) and Tang et al. (2010). The version of the model used here differs slightly from that presented in (Raivonen et al., 2017), and is therefore called with the different name of sqHIMMELI to avoid confusion.

The model simulates the processes in a discretized peat column. The number and thickness of the peat layers can be varied, but in this work ~~a variable number of~~ six 10 cm layers is used, similarly to e.g. Kaiser et al. (2016)~~. Effectively, the total depth of the peat column changes, not the thickness of the layers~~, with one thicker bottom layer under these, so that the total modeled peat column depth is 85% of the maximum observed 4 m depth of the wetland, i.e. 3.4 m. The water table divides the column into water-filled and air-filled parts, and CH_4 is produced only in the inundated anoxic layers. In the present configuration, the NPP-related CH_4 production is allocated into the layers according to the vertical distribution of the root mass, described in Sect. 3.2. The internal time resolution of the model is dynamically adjusted depending on the model state, and the output interval is set to one day.

At present, the model does not contain descriptions for processes related to snow pack or ice such as diffusion through snow, or release of accumulated gas bubbles under ice in spring time as described by e.g. Mastepanov et al. (2013) and Sriskantharajah et al. (2012).

HIMMELI itself, as presented in Raivonen et al. (2017), does not simulate carbon uptake (photosynthesis) or peat carbon pools but instead it takes as input the rate of anoxic respiration. The differences between HIMMELI and sqHIMMELI are described below in Sec. 3.1 and 3.2 and in ~~Appendix~~ Sec. 3.1.1.

For each modeled process in sqHIMMELI, there are parameters regulating the process, affecting the concentrations of CH_4, O_2 and CO_2 in the peat column, and the wetland methane emissions. The equations describing the physics relevant to the optimized parameters are listed in section 3.4. Other relevant model equations are listed in ~~Appendix~~ Sec. 3.1.

3.1 Root exudates and peat decomposition

Methanogens prefer recently assimilated fresh carbon as their energy source, for instance the root exudates of vascular plants (Joabsson and Christensen, 2001). A connection between ecosystem productivity and CH_4 emission has been observed in several wetland studies (Bellisario et al., 1999; Whiting and Chanton, 1993). However, anoxic decomposition of litter and older peat also produces CH_4 (Hornibrook et al., 1997). Many models form CH_4 substrates by extracting directly a fraction of the net primary production (van Huissteden et al., 2009; Wania et al., 2010), and some rely on heterotrophic peat respiration only (Riley et al., 2011). In sqHIMMELI both primary production and anaerobic peat decomposition were included.

The modified sqHIMMELI model contains an exudate pool description, from which it produces methane ~~via~~ (Eq. 3 and 15). The exudate pool itself is described by Eq. 4, detailing how the modeled NPP turns into root exudates. Effectively, a fraction of NPP determined by the parameter ζ_{exu} (-) produces root exudates, which are then distributed as anaerobic respiration according to the root distribution into the peat column at the rate determined by the model parameter τ_{exu} (s). The part ending up under the water table produces CH_4 and CO_2, depending on the oxygen content of the water, and above the water table the exudates are respired into CO_2.

The second source of anaerobic respiration, the anaerobic peat decomposition, is modeled in sqHIMMELI with a simple Q_{10}-model adopted from Schuldt et al. (2013). The peat under the water table is prescribed a turnover time, based on which anaerobic respiration and CH_4 are produced according to Eq. 5 and 16.

3.2 Root distributions

The sqHIMMELI model differs from HIMMELI in the details regarding the root distribution model. Compared to measurement data of root distributions of aerenchymatous sedges from Saarinen (1996), the original root distribution $\pi(z)$, adopted from Wania et al. (2010) and described by

$$\pi(z) \propto \exp(-z/\lambda_{\mathrm{root}}), \tag{1}$$

does not describe the distribution of roots well. Here z is depth, and ~~λ_{root}~~ λ_{root} is a parameter describing the steepness of the decaying exponential curve. This formula is replaced with

$$\pi(z) \propto C_0 \exp\left[-\frac{(z-z_0)^2}{\lambda_{\mathrm{root}}^2}\frac{(z-z_0)^2}{\lambda_{\mathrm{root}}^2}\right] + C_1. \tag{2}$$

With the Gaussian shape, the new root density decreases faster with depth. Without this change, the optimization process calibrates the model to have very high root masses below 50 cm underground. The other difference between the models is that in the original model there are vanishingly few roots below the depth of one meter, but according to Saarinen (1996), sedge roots can reach to as low as 2.3 m under the surface. The term C_1 in Eq. 2 was added to remedy this.

Before starting the optimization, the parameters C_0, C_1, and z_0 were fitted to data from Saarinen (1996), resulting in values of $C_0 = 215$, $C_1 = 6$, and $z_0 = 0.105$. The different root distributions are shown in Fig. 1.

3.3 Peat depth

Methane is produced from anaerobic peat decomposition at all peat depths in the sqHIMMELI model, and its transport and oxidation affect the modeled CH_4 emission. The homogeneous model description of the peat column is highly idealized, as in reality the peat column varies from place to place with respect to CH_4 production rate, production depth, and gas transport. ~~Increasing peat depth in the model is a liability, since the deeper the column,~~ We model the ~~more expensive the model is to run (see Sect. **??**). The model calibration is run for the peat depths of 40, 50, 70, 100, 150, and 200 cm in order to find the optimal peat column depth for the model~~peat column to be 3.4 meters deep, which is 85% of the maximum observed depth of the Siikaneva wetland. Small uncertainty in the value of the parameter is acceptable since the parameter τ_{cato}, which regulates the rate of peat decomposition into CH_4, can partly compensate for this uncertainty.

3.4 Parameter descriptions for sqHIMMELI

The parameters for the optimization were chosen to constrain the processes most important for the CH_4 emission. Of the optimized parameters, all but ζ_{exu} (-) and Q_{10} ~~are constant~~ (-) are the same for all years. However, ζ_{exu} and Q_{10} change year to year to reflect the changes in the relative CH_4 input to the system from peat decomposition and NPP-based production. This will allow to analyze the year to year changes in relative importances of the production pathways. The setup is natural, as for example Bergman et al. (2000) report the Q_{10}-values changing from measurement date to another, even within a single year.

~~The parameters and~~ As the values reported for minerotrophic lawn in Bergman et al. (2000) indicate that they may vary quite irregularly within a growing season, the modeling performed here does not take intra-annual variations into account and concentrates on the year to year variation. Possible mechanisms for the parameter variations include variations in substrate supply and desiccation stress and are discussed in e.g. Davidson et al. (2006). Table 2 shows the parameters that are used in the equations below but not optimized in this work, along with their values and explanations of why they were left out. The list of calibrated parameters along with their physical meanings ~~are~~ is presented below.

CH_4 production-related parameters

1. τ_{exu} (s): Controls the decay rate of exudates, ν, from the root exudate pool P_{exu},

$$\nu = \frac{P_{\mathrm{exu}}}{\tau_{\mathrm{exu}}}. \tag{3}$$

2. ζ_{exu} (-): Fraction of NPP carbon that goes to the root exudate pool.

$$\frac{\mathrm{d}P_{\mathrm{exu}}}{\mathrm{d}t} = -\nu + \psi_t \zeta_{\mathrm{exu}}, \tag{4}$$

where ψ_t is the rate of NPP at time t, P_{exu} is size of the root exudate pool, and ν was given by Eq. 3.

3. ~~τ_{cato}~~τ_{cato} (y): Controls the base rate of peat decomposition into CH_4 in Eq. 5.

4. Q_{10} (-): Controls the temperature dependence of the rate of peat decomposition into CH_4 in anaerobic conditions via factor ~~k_{cato}~~k_{cato}, given by the equation

$$k_{\text{cato}\underline{\text{cato}}} = Q_{10}^{\frac{(T-273.15)}{10}} / \tau_{\text{cato}\underline{\text{cato}}}. \tag{5}$$

5. $f_{CH_4}^{\text{exu}}$ (-): Fraction controlling the methane production from anaerobic respiration of root exudates in Eq. 15.

$$R_{CH_4}^{\text{exu}}(z) = \frac{f_{CH_4}^{\text{exu}}}{\mathrm{d}z} \nu \frac{\pi(z)}{1 + \eta C_{O_2}(z)}.$$

Here $\pi(z)$ is the root distribution from Eq. 2, and ν is described in Eq. 3. The equation is discussed in Sec. 3.1.2.

Oxidation and respiration parameters

6. V_{R0} (mol m^{-3} s^{-1}): Respiration parameter controlling the rate of heterotrophic respiration, which consumes O_2 and produces CO_2. This affects the rate of temperature dependent heterotrophic respiration, $V_R(z)$, given by

$$V_R(z) = V_{R0} \exp\left(\frac{\Delta E_R}{R}(\frac{1}{283} - \frac{1}{T(z)})\right). \tag{6}$$

Here ΔE_R (J mol^{-1}) is a parameter affecting the temperature dependence of the heterotrophic respiration, R is the universal gas constant, and $T(z)$ is temperature at depth z.

7. ΔE_R (J mol^{-1}): Described above in context of Eq. 6.

8. V_{O0} (mol m^{-3} s^{-1}): CH_4 oxidation parameter controlling the potential rate of CH_4 oxidation V_O:

$$V_O(z) = V_{O0} \exp\left(\frac{\Delta E_{\text{oxid}}}{R}(\frac{1}{283} - \frac{1}{T(z)})\right). \tag{7}$$

~~Here ΔE_{oxid} is a parameter affecting~~

9. ΔE_{oxid}: Described in Eq. 7, affecting temperature response of CH_4 oxidation~~that is not part of the optimization~~.

Gas transport-related parameters

10. λ_{root} (m): Controls how the root mass is distributed. See Eq. 2.

11. ρ (m^2 kg^{-1}): Root-ending area per root biomass, affecting root conductance, see Eq. 8.

12. τ (m m^{-1}): Root tortuousity parameter affecting the root conductance K_R. A tortuousity of 1 means that the roots are not decreasing the conductance via their curvedness. The equation for the conductance is

$$K_R(z) = \frac{D_{\text{air}} m \rho \pi(z)}{\tau z}, \tag{8}$$

where $\pi(z)$ is the root mass density as a function of depth, over which the sum of the density is one, and m is the total root mass per square meter, set to be proportional to LAI.

13. $f_{D,a}$ (-): Fraction of the diffusion rate in air-filled peat divided by the diffusion rate in free air. The parameter affects the diffusion ~~flux~~ and the plant transport fluxes in the model: the higher this parameter is, the more there is diffusion as it takes a shorter time for the CH_4 to exit the peat reducing the possibility of oxidation and increasing the concentration gradient driving diffusion. The equation is

$$D_{\text{air}} = f_{D,a} D_{\text{air}}^{273} \left(\frac{T}{298} \right)^{1.82}, \tag{9}$$

where D_{air} is the diffusion rate in air-filled peat, D_{air}^{273} is the diffusion base rate at $273K$, and T is the temperature. ~~This parameter is also present in~~ The effect on plant transport comes via Eq. 8 .

14. $f_{D,w}$ (-): Same as above, but in water. The equation describing the peat-water diffusion rate is

$$D_{\text{water}} = f_{D,w} D_{\text{water}}^{298} \frac{T}{298}, \tag{10}$$

where the terms are analogous to the ones in ~~the previous equation~~Eq. 9.

4 ~~Model calibration and MCMC~~

~~The model calibration consisted of two steps: optimization and MCMC. Both of these steps were run separately for each different number of peat soil layers assessed (4, 5, 7, 10, 15, and 20 layers, each layer corresponding to 10 cm of peat)~~

3.1 The sqHIMMELI model equations

The version of HIMMELI presented here describes processes for CH_4 production and transport. It differs from the version presented in Raivonen et al. (2017) in that the model presented there does not contain the processes for anaerobic respiration but rather take it as input, the idea being that such input would be available when using HIMMELI as a part of a larger model. Hence the equations presented in Sec. 3.1.2 are specific to the version used in this study. The other difference between the models is the difference between the root distributions described in Sec. 3.2.

3.1.1 Governing equations

The gas concentrations of CH_4, carbon dioxide and oxygen in the peat column are governed by the equations

$$T_X(t,z) = Q_X^{\text{diff}} + Q_X^{\text{plant}} + Q_X^{\text{ebu}} \tag{11}$$

$$\frac{\partial[\text{CH}_4]}{\partial t}(t,z) = -T_{CH_4} + R_{CH_4}^{\text{exu}} + R_{CH_4}^{\text{peat}} - R_{CH_4}^{\text{oxid}} \tag{12}$$

$$\frac{\partial[\text{O}_2]}{\partial t}(t,z) = -T_{O_2} - R_{\text{aerob}}^{\text{peat}} - R_{CO_2}^{\text{exu}} - 2R_{CH_4}^{\text{oxid}} \tag{13}$$

$$\frac{\partial[\text{CO}_2]}{\partial t}(t,z) = -T_{CO_2} + R_{CO_2}^{\text{exu}} + R_{CO_2}^{\text{peat}} + R_{CH_4}^{\text{oxid}} + R_{\text{aerob}}^{\text{peat}}, \tag{14}$$

where $T_X(t,z)$ describes transport of gas X containing the diffusion, ebullition, and plant transport components, and R stands for production or consumption. The different terms in the equations are described below.

3.1.2 Anaerobic respiration producing CH_4

The equations presented in this section are specific to the version of HIMMELI used in this study. The version in Raivonen et al. (2017) takes the rate of anaerobic decomposition of carbon as input and does not treat the different sources of that carbon separately.

The carbon for methane production in this model version comes from two sources: root exudates and anaerobic peat decomposition. The methane production from anaerobic respiration of that carbon is given by the terms $R_{CH_4}^{\text{exu}}$ and $R_{CH_4}^{\text{peat}}$ described by:

$$R_{CH_4}^{\text{exu}}(z) = \frac{f_{CH_4}^{\text{exu}}}{\text{d}z}\nu\frac{\pi(z)}{1+\eta C_{O_2}(z)} \tag{15}$$

$$R_{CH_4}^{\text{peat}}(z) = k_{\text{cato}}(z) g_{CH_4}^{Q_{10}} \frac{\rho_{\text{cato}} f_{C_{\text{cato}}}}{M_C}, \tag{16}$$

where in Eq. 15 ν is the decay rate of root exudates from Eq. 3, η is an oxygen inhibition parameter, $C_{O_2}(z)$ is the oxygen concentration at depth z, and $\pi(z)$ is the normalized proportion of the total anaerobic root mass, also at depth z, given in an unnormalized form in Eq. 2. The decay rate of root exudates does not depend on the peat column thickness. The parameter $f_{CH_4}^{\text{exu}}$ (-) determines what fraction of root exudates in anaerobic conditions will turn into CH_4. Equation 15 is only used below the water table. The anoxic peat decomposition described by Eq. 16 depends on the amount of peat and its temperature, among others. The factor $g_m^{Q_{10}}$ (-) is the proportion of the anaerobic peat decomposition process producing CH_4, ρ_{cato} is the peat density in the catotelm, $f_{C_{\text{cato}}}$ is the fraction of carbon in catotelm peat, and M_C is the molar mass of carbon. The parameter $k_{\text{cato}} = Q_{10}^{\frac{(T-273.15)}{10}}/\tau_{\text{cato}}$ is described in Eq. 5, and is zero above water table.

The equations for CO_2 are similar:

$$R^{\mathrm{exu}}_{CO_2}(z) = \nu\pi(z) - R^{\mathrm{exu}}_{CH_4}(z) \tag{17}$$

$$R^{\mathrm{peat}}_{CO_2}(z) = (1 - g^{Q_{10}}_{CH_4})k_{\mathrm{cato}}(z)\frac{\rho_{\mathrm{cato}} f_{C_{\mathrm{cato}}}}{M_C}, \tag{18}$$

and the meanings of the symbols are analogous to the ones in equations for CH_4. ~~In the following, an *experiment* refers to one of these MCMC runs.~~

3.2 ~~Calibration algorithms~~

~~For optimization, an initial parameter vector was first drawn from the prior,~~

3.1.1 Peat respiration and methane oxidation

Peat respiration (aerobic respiration) is described with an equation of the Michaelis-Menten form

$$R^{\mathrm{peat}}_{\mathrm{aerob}}(z) = V_R(z)\frac{\alpha C^w_{O_2}(z)}{K_R + C^w_{O_2}(z)}, \tag{19}$$

where $C^w_{O_2}$ is the oxygen concentration in water. Above the water table we assume a water phase that is in equilibrium with the gas phase, i.e. $C^w_{O_2} = \alpha C^a_{O_2}$. The parameter α is a dimensionless Henry solubility constant for oxygen. Parameter K_R is the Michaelis-Menten constant of the process, and $V_R(z)$ is given by Eq. 6. Methane oxidation is controlled by dual-substrate Michaelis-Menten kinetics,

$$R^{\mathrm{oxid}}_{CH_4}(z) = V_O(z)\frac{C^w_{O_2}(z)}{K_{O_2} + C^w_{O_2}(z)}\frac{C^w_{CH_4}(z)}{K_{CH_4} + C^w_{CH_4}(z)}, \tag{20}$$

and here the terms are analogous to those in Eq. 19, except for that the term $V_O(z)$ is described by Eq. 7.

3.1.2 CH_4 transport

The transport term $T_X(t,z)$ in Eq. 11 consist of the following terms:

$$Q^{\mathrm{diff}}_X = D^X_{\mathrm{medium}}\frac{\partial}{\partial z}C^{\mathrm{medium}}_X \tag{21}$$

$$Q^{\mathrm{plant}}_X(z) = \frac{\rho\pi(z)D^X_{\mathrm{air}}}{\tau^2}\frac{LAI}{SLA}\frac{C_x(t,z) - C^{\mathrm{atm}}_X}{z} \tag{22}$$

$$Q^{\mathrm{ebu}}_X(z) = -k\sigma\frac{pp_{i,X}}{RT}\frac{\sum_i pp_i(z) - (P_{\mathrm{atm}} + P_{\mathrm{hyd}}(z))}{\sum_i pp_i(z)}. \tag{23}$$

The first of these is the diffusion, where the diffusion coefficients D are given by Eq. 9 and 10, and "medium" refers to either air or water. The second equation is for plant transport, with ρ ($\mathrm{m^2\ kg^{-1}}$) and τ ($\mathrm{m\ m^{-1}}$) described in context of

Eq. 8, $\pi(z)$ is the normalized root distribution mentioned above, and C_X^{atm} refers to the atmospheric partial pressure of gas X. LAI stands for the leaf area index, given as input, and SLA is the specific leaf area. The third equation is the ebullition component of the gas transport, where pp_i refers to the partial pressure of different gases indexed with i, R is the universal gas constant, k is an ebullition rate constant, and σ is the peat porosity. The parameters P_{atm} and ~~the parameters were then optimized against the costfunction described in Eq. 24. The algorithm used was the simplex-based BOBYQA, described in Powell (2009). In our tests, it was significantly faster to converge than NEWUOA (Powell, 2004), L-BFGS or Nelder-Mead (Nelder and Mead, 1965). For each experiment, the model was optimized by running 350 model~~ $P_{\mathrm{lwd}}(z)$ refer to the atmospheric pressure and hydrostatic pressure at depth z, respectively.

4 Model calibration

The model calibration consists of several steps, but can be summarized as first estimating the posterior with MCMC and then based on those results, re-calibrating the objective function and using this new formulation for importance resampling. Importance resampling is typically used for obtaining posterior distributions from minor changes to the objective function descriptions (Gelman et al., 2013). This is also its purpose here.

In more detail, first, a posterior estimate was drawn running 500000 iterations of sqHIMMELI simulations with the ~~minimization algorithm , which was enough for finding a local minimum to start the MCMC sampling from.~~

~~At the points obtained in the optimization,~~ Adaptive Metropolis Markov chain Monte Carlo algorithm with a Laplace-distributed error description and a first order autoregressive model, AR(1), for the residuals. Second, for defining the more refined costfunction for importance resampling the optimal order for an autoregressive moving average (ARMA) timeseries model for the model residuals was identified from the maximum a posteriori estimate by minimizing the Akaike and Bayesian Information Criteria with respect to the ~~model was linearized and from the Jacobian a suitable initial proposal covariance matrix for MCMC was estimated. After this the MCMC sampling was performed to estimate the posterior distribution.~~ model order. The third step was drawing a random sample of size fifty from the posterior estimate obtained with MCMC, with which the error model parameters α and γ, described in conjunction to the details of the error model in Eq. A2, were calibrated by minimizing the Kullback-Leibler divergence (Kullback and Leibler, 1951) with respect to the standard Laplace distribution for the methane and carbon dioxide separately. The median of the obtained parameters was chosen for the second costfunction used in the importance resampling. Fourth, a random sample of size 10000 was drawn from the MCMC posterior and importance resampling was performed by drawing a subsample of size 1500 utilizing weights calculated with the new costfunction values obtained from the above mentioned error model calibration as described by e.g. Gelman et al. (2013).

The need for the importance resampling arises from that the error model transformed methane and carbon dioxide residuals emerging from the maximum a posteriori and posterior mean estimates from the calibration with the AR(1) model are not fully independent and identically distributed. The recalibration of the error model, and resampling from the simulated posterior using importance resampling, remedies this problem, as can be seen in the residual histogram and autocorrelation functions in Fig. 2.

4.1 Hierarchical description of parameters

In order to be able to assess the annual parameter and CH_4 transport pathway changes, a hierarchical description for two of the parameters was used. These parameters were Q_{10} (-) controlling the temperature dependence of the peat decomposition rate, and ζ_{exu} (-), regulating the production of root exudates from NPP.

The *hyperparameters* are the means and variances defining the Gaussian priors of the hierarchical parameters Q_{10} (-) and ζ_{exu} (-). They were updated using fixed Gaussian *hyperpriors* with Gibbs sampling. The sampling distribution depends on the current values of the hyperparameters. The role of the hyperprior is to constrain the distribution from which the hyperparameters are sampled.

Technically, a *Metropolis-within-Gibbs*-method ~~Gelman et al. (2013)~~ (Gelman et al., 2013) for sampling the hierarchical parameters, non-hierarchical parameters, and the hyperparameters was used, presented briefly in Appendix C. The model parameters (i.e. everything except the hyperparameters) were sampled with the Adaptive Metropolis (AM) MCMC algorithm (Haario et al., 2001), which uses a Gaussian proposal distribution, whose covariance matrix is adapted as the chain evolves, and over time the acceptance rate gets closer to an optimal value, which is 0.23 for Gaussian targets in large dimensions (Roberts et al., 1997). If the algorithm proposes values outside the hard parameter limits listed in table 3, the model will not be evaluated and the value is rejected.

Our empirical data for the hierarchical model were the nine years from 2006 to 2014, meaning that for each of these years there were corresponding ζ_{exu} (-) and Q_{10} (-) parameters in the optimization. The model ~~needed to be~~ was spun up for each annual flux estimation in order to have a realistic column of gas concentrations available. For this reason, the previous year was always also simulated, and for the likelihood only the residuals from the latter year were included in the calculations. Therefore year 2005 did not contribute directly to the values of the objective function. The different years were run in parallel to save execution time.

4.2 Objective ~~function~~functions for MCMC and importance resampling

As in many practical ~~MCMC~~ uncertainty quantification applications, a major part of the parameter estimation problem is the proper definition of the objective function. ~~It~~ For MCMC it is defined here based on *a priori* information about the measurement uncertainties, based on information from the model residuals, and based on ~~annual flux estimates. Additionally prior informationabout the parameter values is also utilized~~additional prior information. For the importance resampling we modify the error model for the CO_2 and CH_4 residual components of the objective function based on an analysis of the MCMC results.

4.2.1 Model residuals and error model

The ~~second component~~ form of the objective function ~~contains~~ is the same for both MCMC and importance resampling. The first two components of the objective function contain the contributions from the modeled differences to the daily CH_4 and CO_2 flux measurements. ~~It~~ In the MCMC objective function it is assumed that the daily flux estimate ~~uncertainty is dependent on~~ uncertainties are dependent on approximately a fraction α of the flux measurement (Richardson et al., 2006) and some

constant error, γ (e.g. measurement device precision). The model error is expected to follow a similar form, and hence α and γ contain the contributions from both the model and measurement errors.

~~The combined error is described by a Laplace distribution. The flux observations are reported to follow a distribution of this type, rather than a Gaussian distribution (Richardson et al., 2006).~~ For importance resampling the description is the same except for that a 14-day running mean of the interannual variability is used for α. These parameters are set independently for both CH_4 and CO_2.

When determining the parameters γ and α, the resulting residuals end up being autocorrelated. Therefore they are treated as such with the AR(1)-model for MCMC and with the ARMA(2,1)-model for the importance resampling, described e.g. in Chatfield (1989). ~~Applying it, a set of Laplace-distributed residuals r^* is obtained. The error model is explained in more detail in Appendix A1.~~

4.2.2 ~~Annual CH_4 fluxes~~

~~For future climate projections, the annual total emission of the snow-free period is one of the important quantities, as cumulative emissions are what determine the radiative forcing. Therefore a Gaussian-distributed observation, G_{obs}, is included for the total annual flux , with error variance σ_G^2, where σ_G is set to 10~~Since the primary interest is in the methane fluxes, the carbon dioxide residuals are scaled down to a fifth in the importance resampling costfunction, which is enough to guide the parameter values since several years of CO_2 flux data are used. Furthermore, as the model does not contain descriptions for the effects of snow and ice on the fluxes, the fit cannot be expected to be very good in the winter months. Therefore we further only consider 20% of the ~~annual total flux for each year. The modeled total annual flux is denoted by G_M. This term keeps the annual emission estimates reasonable in the early stages of the sampling. As the annual flux estimate errors are small when sampling parameters close to the posterior mode, this term has only a minor effect at the late stages of the MCMC~~contribution of the residuals in the winter season from December to February. The obtained residuals, denoted by the ϵ-terms in the objective function, Eq. 24, are treated as Laplace-distributed. The flux observation errors are reported to follow a distribution of this type, rather than a Gaussian distribution (Richardson et al., 2006). The error model is explained in more detail in Appendix A1.

4.2.2 Prior information

The parameters affecting the CH_4 production of the wetland model are not known well, but despite this, not setting any prior distributions on parameters can lead to nonphysical parameter values in the posterior distribution.

The parameter priors are set to zero outside prescribed bounds. Within these bounds, ~~most~~ the parameters are assigned Gaussian priors, ~~and for the others the priors are~~ with the exception of one parameter whose prior is set to be flat. The prior values are based on both literature and expert knowledge and the information regarding the parameter values is summarized in Table 3.

4.2.3 The objective function

The *objective function* for the parameter optimization, $J(\boldsymbol{\theta})$, is the negative logarithm of the value of the unnormalized posterior probability density function at $\boldsymbol{\theta}$. It combines our statistical knowledge of ~~flux observations, annual flux estimates,~~ the flux observations and parameter priors presented in Sec. 4.2.1 – 4.2.2, and is given by:

$$J(\boldsymbol{\theta}) = -\log\left(p(\boldsymbol{\theta}|\boldsymbol{y})\right) = \sum_{i=1}^{N_{\text{obs}}^{\text{CH}_4}} |\epsilon_i^{\text{CH}_4}| + \sum_{j=1}^{N_{\text{obs}}^{\text{CO}_2}} |\epsilon_j^{\text{CO}_2}| + \frac{1}{2}\sum_{k=1}^{N_{par}} \frac{(\theta_k - \mu_k)^2}{\sigma_k^2} \tag{24}$$

Here ~~$|r_t^*|$~~ ϵ_i are the AR(1) or ARMA(2,1)-transformed Laplace-distributed residuals, ~~G_M, G_{obs} and σ_G^2 are the components of the annual flux term,~~ and the last term is the prior contribution, where ~~θ_i~~ θ_k is the proposed parameter value, ~~μ_i~~ μ_k is the prior mean, and ~~σ_i^2~~ σ_k^2 is its variance. For further technical details, see Appendix A1.

5 Results and discussion

The ~~experiments yielded an MCMC chain for each modeled peat depth and the final number of model simulations varied from 78000 to 391000. To look at statistics, 50% of values~~ Markov chain Monte Carlo simulations yielded a chain of 500000 samples. From these, 70% from the start of ~~each MCMC~~ the chain were discarded as warm-up ~~. The posterior covariance structures of the chains were found mostly to be similar to each other. The posterior distribution from the experiment with 70 cm of peat~~ (Fig. 3). A revised posterior distribution obtained by first sampling 10000 entries randomly from the chain, and after that obtaining 1500 entries from those with importance resampling is shown in Fig. 4, and the correlation features ~~for all peat depths~~ are shown in the upper triangle of that figure. For the different processes, Fig. 5 shows an example of the posteriors and the process correlations.

~~For each MCMC chain, three different estimates for the parameters and fluxes were looked at~~ Three different parameter estimates obtained from the posterior distribution were used to look at its features and fluxes: the maximum a posteriori (~~"MAP"~~MAP) estimate, posterior mean estimate~~("PM")~~, and a "non-hierarchical" posterior mean estimate~~("NHPM")~~, where the mean values of the parameters ζ_{exu} (-) and Q_{10} (-) over the different years were used. The "default" parameters in the text and figures refer to values adapted from Raivonen et al. (2017). If not stated otherwise, the maximum a posteriori and posterior mean estimates refer to the values obtained from the importance resampling, not from the MCMC.

5.1 Parameter values~~and modeled peat depth~~

The parameter values ~~of the MAP and PM MCMC optimizations~~ used in the analyses are shown in Table 4. ~~The catotelm carbon pool turnover time, τ_{cato} grows with the peat depth, and the reduction factor for the diffusion coefficient in air-filled peat, $f_{D,a}$, also grows slightly, increasing the diffusive permeability of the dry part of the column hence increasing conductance. The root conductance gets larger with the increasing peat depth, by the influence of the parameter ρ, which grows slightly, and the decrease in root tortuousity given by parameter τ.~~

~~The MAP estimates of the different experiments disagree~~ The MAP and posterior mean estimates agree on the value of the water-diffusion rate coefficient $f_{D,w}$ (-), and the posteriors shown in Fig. 6 (k) ~~are wide, especially for the experiments with less peat, meaning that especially in those cases this parameter is highly uncertain. However, with increasing peat depth, the mass of the posterior distribution mass moves closer to 1 compensating the decreased conductance caused by the longer distance to the surface. The~~ show that the estimates are close to the middle of the marginal distribution, and slightly above the prior value. In tests with a shallower peat column, smaller values of this variable were obtained (not shown).

Contrary to this, the air diffusion rate coefficient $f_{D,a}$ ~~shows similar behavior, but with lower values as it is constrained by the prior. For the 40-cm peat column optimization, the MAP estimate for $f_{D,w}$ is far from the others. This can be explained by that in that particular case there is not much~~ (-) finds its best values lower and the variability of the parameter is larger than for the diffusion rate coefficient in water-filled peat~~in the model leaving the parameter with less effect on the results.~~.

The root distribution parameter, ~~λ_{root}~~λ_{root}, is optimized larger than expected, and ~~is closer to the prior value only in the optimization with 15 and 20 layers. This is also true for the MAP estimates implying~~ again the MAP estimate is close to the posterior mean. This implies that the model optimizes best when the CH_4 produced from the photosynthesis-induced exudate production goes relatively far below the surface: with a value of 0.3, 49% of the roots are deeper than 25cm, 15% of the roots are deeper than 50cm, and just 2.5% are deeper than 75cm, see Fig. 1. In relation to these numbers, the water table depth is most of the time above the depth of -20 cm. Additionally, a larger ~~λ_{root}~~ λ_{root} will facilitate the emission of the CH_4 produced by peat decomposition in the catotelm. ~~The small values for the two experiments with the thickest peat column make the model behave differently from how it functions with 40-100 cm of peat.~~

~~The results in Table 4 reveal that the parameter regulating~~

The values of the exudate pool turnover time ~~, τ_{exu} , slightly decreases with the peat column depth implying a shorter period between photosynthesis and methane emission with morepeat~~are close to the default value of two weeks, with the MAP estimate at a little under 14 days and the posterior mean at two and a half days more. The results from the importance resampling show that the spread is around three days around this posterior mean value. However, the value of $\overline{\zeta_{\text{exu}}}$ controlling ~~the amount of methane produced from exudates gets smaller until 100 cm, and the values for 150 and 200 cm of peat are markedly larger. This implies, that CH_4 production from exudates is closely linked to the depth of the root mass and λ_{root}.~~

~~The non-hierarchical parameter V_{O0} controlling the amount of CH_4 oxidation taking place does not show a trend with respect to the modeled peat column depth in the PM estimate, but there is a clear trend in the MAP estimates, shallow peat depths favoring larger parameters and inducing more CH_4 oxidation. The effect of the parameter on the total CH_4 oxidation is substantial, which is evident from part (a) of Fig. 12 With all peat depths,~~ amount of exudates produced from photosynthesis, is smaller than the default value at roughly 0.15-0.45 with the ~~chains traverse in regions of both high and low V_{O0} as shown~~ MAP and posterior mean estimates at 0.343 and 0.292 respectively. In contrast to this and balancing the effect of a relatively low $\overline{\zeta_{\text{exu}}}$, the parameter $f_{CH_4}^{\text{exu}}$ (-), controlling how much methane is produced from anaerobic decomposition of exudates, has a skewed posterior marginal distribution with most of the mass above the value of 0.7, as can be seen in Fig. 6~~(f). Another parameter indirectly affecting~~ .

The non-hierarchically optimized parameter V_{Q0} (mol m^{-3} s^{-1}) controlling the amount of CH_4 oxidation ~~, the heterotrophic respiration parameter V_{R0}~~ taking place is close to the minimum allowed value at one fifth of the default value. This is also true for the parameter controlling heterotrophic respiration, ~~drifts in all experiments~~ V_{R0} (mol m^{-3} s^{-1}), whose all optimized estimates reside close to its minimum value reducing the amount of heterotrophic respiration taking place. The posteriors are very narrow. In contrast to these narrow posteriors, the parameters ΔE_{oxid} (J mol^{-}1) and ΔE_R (J mol^{-1}), which are present in the same equations as the V_{Q0} and V_{R0}-parameters, have slightly wider posterior distributions, with the former slightly under and the latter slightly above the default values.

Table 4 shows that the ~~hierarchical~~ hierarchically optimized parameter Q_{10} (-), controlling the temperature dependence of the CH_4 production from peat decomposition, ~~increases with peat column depth: the more peat there is, the stronger the peat decomposition process responds to soil temperature changes. Contrasting with this, the~~ has slightly different values for the MAP and posterior mean estimates, with the Gibbs-sampled mean value (mean of those values in the case of the posterior mean) at 5.72 and 4.43 respectively.

The parameter τ_{cato} (y), also controlling the peat decomposition rate in the catotelm~~increases with peat depth compensating for changes in total peat volume and keeping the production volumes reasonable. Part (d) of Fig. 12 shows how increasing the peat depth and keeping parameters constant drastically increases the total methane production~~, compensates for the differences of $\overline{Q_{10}}$ between the MAP and posterior mean estimates by having a faster turnover time for the posterior mean than the MAP estimate. That parameter has a wide posterior, ranging from around 10000 to 30000, which was the value used by Raivonen et al. (2017) and the upper limit of the parameters in our work. Our posterior density goes to zero towards the higher limit, and the posterior mean is found at the value of 22690 years.

~~The annual~~

The inter-annual variability of Q_{10} ~~is similar across all peat depths~~(-) is mostly similar for both MAP and posterior mean estimates. For instance ~~years 2013 and 2014 (and sometimes 2011) are years of high Q_{10}, whereas in~~ the years of the smallest values are 2007 and 2008 in both cases, and the values of the years 2006~~the parameter gets its lowest or second-lowest value for all depths in the PM simulations.~~ , 2011, and 2014 are the largest in both cases. For the other ~~hierarchical~~ hierarchically calibrated parameter, ζ_{exu} ~~, these patterns~~ (-), these similarities do not exist.

5.2 Costfunction values and ~~annual discrepancies~~model fit

~~The minimum costfunction values and annual biases provide information about how well the different configurations of the model performed in the model calibration task.~~

Table 4 lists the costfunction values for the MAP and posterior mean estimates, and the annual errors for the MAP, ~~PM, and NHPM estimates~~ posterior mean, and non-hierarchical posterior mean estimates and default parameter values are shown for each ~~MCMC experiment~~ parameter set in Fig. 7. ~~Among the MAP estimates, the~~ The costfunction value is ~~lowest with 7 layers of peat (259) and then gradually higher for 10 (262), 15 (267), 20 (269), 5 (274), and 4 layers (295), the last of these being significantly worse than the first ones. Figure 7 suggests that for the MAP and PM estimates, the annual total CH_4 flux estimates are less steady with only 40 or 50 cm of peat.~~ unsurprisingly lower for the MAP estimate than for the posterior mean estimate,

indicating a better fit in terms of the error model. In figure Fig. 7 (~~g) the NHPM~~ b) the non-hierarchical posterior estimate shows a ~~very~~ large variance of the annual errors, with early years having a ~~sizable~~ positive bias, and later years having a ~~similar~~ negative bias. Incidentally the ~~averages~~ average discrepancy from observations over the whole period for ~~NHPM are small~~ the non-hierarchical posterior mean is small for both methane and carbon dioxide, as Fig. 8 ~~(b) indicates.~~ indicates. However, the variation for methane is the largest, implying that the annual variation is not reflected well. The model estimates of the annual fluxes are good ~~and~~ in that the variance of ~~its~~ the errors is small for both MAP and ~~PM~~ posterior mean experiments, especially~~for peat column depths of at least 50 cm~~, even though the estimates show a negative bias of 25%. Compared to the default parameters, ~~the~~ which strongly underestimate methane emissions (and even more overestimate the carbon dioxide emissions), the flux estimates are much improved. This is to be expected as the results shown are not for an independent validation dataset. Rather, the motivation with the MAP and posterior mean estimates is to see ~~,~~ how the model fit looks like for optimized parameters and how the features differ from the unoptimized ones. It is, however, worth noting that the target objective function did not aim at minimizing annual discrepancies but daily residuals that were considered correlated.

A cross validation of the regression modeling in terms of the annual errors is shown ~~for the experiments with 70 cm and 100 cm peat columns~~ in Fig. ~~8 (g) and~~ 7 (b) and 8. While the annual estimates are ~~worse than the estimates with the optimized parameters, compared to the NHPM estimate and the default parameter values~~ not on average better than the ones from the simulation with the non-hierarchically obtained posterior mean, the spread of the errors are ~~smaller~~acceptable, particularly if the strong negative bias in 2007, which is mostly due to lack of observations during the season, is disregarded. Additionally the overall biases are ~~as good as~~ surprisingly slightly better than with the optimized parameters, due to effects of the prior, different data resolution in the costfunction, and the non-trivial error model used. The cross validation is described in Sec. 5.6.

The positive bias in the CO_2 may partly be due to the assumption that 70% of the NPP comes from the aerenchymatous plants, and this affected the data that the sqHIMMELI model results were matched with.

~~Almost all~~ All years of hierarchically optimized experiments show at least a small negative annual bias in the methane flux when compared to the available observations. This can be due to the high day to day variability of the summertime fluxes, which dominate year-round total fluxes, and the fact that the model can not, without data about the fine structure and heterogeneity of the wetland, match the high variability fluxes. The proportional model-data residual error component $\alpha\, y_t$ (Appendix A1) allows the model to underestimate the high peaks more than the low flux values. The error model favors the baseline of the lower values during periods when observed variance is very high, for instance in the peak emission season of 2010. This is also true for periods of increased ebullition, and such fluxes are very difficult to fit into. These periods contribute to both the costfunction values and the underestimation of the total methane flux. Any temporal shifts of peaks of seasons are penalized heavily, and the optimized parameter values rather produce less peaks than right size peaks at a slightly wrong time.

Another reason is that the carbon dioxide fluxes are overestimated by the model, leading to need to balance between the two, and as methane production in the wetland also produces carbon dioxide, the optimization algorithm will find a middle ground between the conflicting needs of minimizing carbon dioxide and maximizing methane production.

Additionally, the wintertime methane fluxes are underestimated systematically, and the emissions start slightly late in early summer, which produces a negative bias to the total flux even though visually the fit is good, as can be seen in Fig. 9. This figure

also reveals that the observations for the vast majority fall within the confidence margins suggested by the ARMA model for the residual. The variation from the full posterior is higher because the uncertainty shown in Fig. 9 does not take the parameter variations into account.

The input data has a role in affecting the model fit to the data, and since NPP is a modeled quantity, there is some additional uncertainty stemming from that modeling involved. For LAI we note that even though in reality it is not identical every year, in the model it follows the same pattern, (see Appendix E). The parameter calibration must then favor parameters producing a good fit in terms of average model performance.

5.3 Parameter values and processes in sqHIMMELI

The sqHIMMELI model produces the CH_4 from anaerobic respiration that originates from peat decay and the decay of root exudates. These production components, along with the different output pathways, CH_4 oxidation and model residuals, are plotted as functions of water table depth in Fig. 10 for the ~~optima of various MCMC experiments, and for the unoptimized~~ MAP, posterior mean, non-hierarchical posterior mean, and default parameter values. The process correlations and covariances are shown for the year ~~2008 from the experiment with 70 cm of peat~~ 2012 in Fig. 5.

In the following, *all ebullition* refers to any ebullition in the peat column regardless to whether the bubbles reach the peat column surface. *Ebullition* refers to the part of "all ebullition" which reaches the surface. Most of the time the water table is under the peat surface, and at those times "ebullition" is zero, although "all ebullition" can be substantial. In that case the ebullition flux does not go directly into the atmosphere, but into the first air-filled peat layer above the ~~WTD~~water table level, and continues from there via other pathways. The reason for this separation comes from implementation details of HIMMELI. In all experiments, ebullition reaching the surface is minor fraction of the total CH_4 emission.

For the ~~PM estimatewith the 100 cm column depth~~posterior mean estimate, the flux components and oxidation are shown as time series in Fig. 11. ~~Having only four layers of peat leads to peat decay being inhibited when the water table is low as the volume of the modeled catotelm decreases (~~Optimizing the model leads to increased production of methane from peat decay, as can be seen in Fig. 10 (f)~~). The~~ . A similar effect is seen also in the plant transport component in Fig. 10 (b). ~~Plant transport becomes proportionally more important with increasing depth of the peat column with MAP, PM, and NHPM estimates (Fig. 7 (a-c)), even though the differences get quite small and the system seems to mostly stabilize already at 7 layers. For the default parameters, however, the trend is opposite (Fig. 7 (d)) as increasing the peat depth dramatically increases CH_4 production and as the default parameter set favors ebullition and diffusion over plant transport.~~

Comparing results from simulations with optimized parameters to results using the default parameter values (~~prior mean values,~~ shown in Table ~~3~~4) shows that the optimization ~~drastically increases~~ somewhat decreases the role of the plant transport pathway ~~at the expense~~ in favor of the diffusion pathway~~.~~ , especially for years 2010, 2011, and 2013. Diffusion and all ebullition fluxes are closely tied to each other, as can be seen in Fig. 7 (~~a-d~~a), in that in ~~all cases~~ many years (2007-2008, 2012-2014) their values are close to each other for all estimates. This is also visible in the flux component time series in Fig. 11.

5.3.1 Methane production and oxidation

Figures 12 and 5 show, that there is considerable ~~annual~~ inter-annual variation in the production of CH_4 from both of the production processes. Year 2007 has a high amount of production from peat decomposition, whereas year 2006 shows a lot less, even though the ζ_{exu}-controlled proportion does not change ~~much. This is not a general trend~~equally much. Generally, though, ~~and instead~~ in years of high emissions the amount of CH_4 from both of the production sources is increased. The shape of the NPP input, shown in Fig. 9, does not change remarkably from year to year, but the emissions change considerably, as the model state and input affect the production non-linearly. For example in times of low WTD in the peak emission season, the root exudates do not contribute to CH_4 production as much as during slightly wetter times, as much of the roots are located in the dry part of the peat column and the exudates are deposited there (Fig. 10 (e)). Another explanation for changes in CH_4 production comes through the production-determining parameters, whose variation is in ~~Sect~~Sec. 5.6 found to be related to the springtime temperature and NPP.

The NPP-based CH_4 production controlled by the parameter ζ_{exu} ~~is~~ (-) is not strongly constrained by its hyperprior as can be seen in Fig. 6 (b) and the ~~values accepted in the chain are from the higher side of the Gaussian hyperprior, whose mean and standard deviation are both 0.2~~MAP and posterior mean estimates. The posterior means in table 4 are between ~~0.27 and 0.38, with standard deviations of 0.17-0.18~~0.182 and 0.323 for the different years. For the MAP values the ~~deviations are even~~ values are slightly higher, leading to ~~wider fluctuations in the characteristics of the modeled wetland. As mentioned in Table 3, the prior for~~ a larger input to the root exudates pool. The effect of ζ_{exu} ~~was set quite low, and actually even these~~ on the exudate pool sizes can be seen by comparing the posterior mean values to the exudate pool sizes in Fig. 9. The values obtained here are ~~on the low side of the spectrum~~ in line of values reported by Walker et al. (2003), who gives a range of ~~0.2-0.84~~ roughly 0.15-0.65 in terms of our ζ_{exu}-parameter~~. Our result hence agrees with~~, when also considering the mean value of the $f_{exu}^{CH_4}$. This parameter finds its maximum a posteriori value at 0.729, which is close to the prescribed upper limit of 0.77. The posterior mean is at 0.736. From these results we can conclude that a relatively large portion of the photosynthesized sugar is respired into methane.

The year to year variation of the posterior distributions of the ζ_{exu}-parameter, shown in Fig. 13, is large and this difference has an important role in driving the annual CH_4 production. For especially the years 2007, 2008, 2012 and 2014 the importance resampling has the effect of increasing the value of the parameter, correspondingly increasing the production of methane. This effect is not visible for the other hierarchically modeled production-related parameter, the Q_{10}, whose posterior is not affected by the resampling despite the more permissive prior.

The methane produced by the action of ζ_{exu} is distributed according to the root distribution, whose form is determined by λ_{root} (m). The posterior means reveal, that that the contribution of the prior component of λ_{root} to the costfunction is large. Its values might well be larger with a wider prior and more permissive prior, but in regard to how root distributions are in reality (Fig. ~~3.2~~1), larger values for the parameter would make its interpretation difficult. This parameter affects both how exudates are allocated in the column and how deep the fast plant transportation reaches. Clearly there is a need to reach further down, implying that the model performs more optimally when it transports CH_4 faster to the atmosphere.

The exudate pool size follows the net primary production in Fig. 9 with a delay, as one could expect. According to the modeling, the pool sizes are up to 0.5 moles per square meter, and the exudate pool is depleted from December until the start of the growing season.

The methane production from decomposition of peat in anaerobic conditions is aided by the rather strongly correlated parameters Q_{10} (-) and the catotelm carbon decay half-life τ_{cato} (y) as seen in Fig. 4. ~~Unlike with ζ_{exu}, the~~ The prior means of Q_{10} (-) are mostly inside the 1-σ bounds of the hyperprior, and the temperature dependence of the anaerobic respiration from peat decomposition is close to what was *a priori* expected. The MCMC utilized a rather strict prior, which constrained the parameter exploration somewhat. Despite this, also very low values were proposed.

~~All years of the PM simulations have very little oxidation taking place with over 70 cm of peat and in the experiments with up to 70 cm of peat~~ Methane oxidation is quite steady between the different estimates as can be seen in Fig. 12 - except for the default parameters values, with which the amount of oxidation is ~~higher (Fig. 12 (b)). In our analysis no easy explanation was found for this feature and it is suspected that multiple processes involving the parameters governing the root distributions and the availability of oxygen are behind the phenomenon. The MAP simulations (~~several tens of percents more. However, there is considerable inter-annual variability, which seems to be related to the varying production from exudates, as seems to be suggested by Fig. 5, and also by Fig. 12~~(a)), however, show that the CH_4 oxidation reduces gradually with the modeled peat depth, and that the simulations with the deepest modeled peat columns have parameter estimates with the lowest V_{O0}-parameters. The correlation between oxidation and the value of V_{O0} is high, at 0.8 for the year 2008~~.

The stronger oxidation with ~~70 cm peat. With more modeled peat, the methane transportation time from the lower parts of the catotelm increases, and to compensate for this~~ the default parameter values can be for it part also linked to the larger V_{O0} ~~in the MAP covaryingly reduces CH_4 oxidation so that the amount coming to the surface varies only a little (Table 4). This is also supported by that methane oxidation and production from root exudates covary negatively, as shown in~~ (mol m^{-3} s^{-1}) parameter, despite that the other parameter determining oxidation in Eq. 7, ΔE_{oxid}, is slightly lower (50000 vs. 53580 for map and 55750 for posterior mean).

The process correlation figure, Fig. 5 ~~. That figure also shows ,~~ also shows that the exudate and peat decomposition based methane production terms are ~~strongly~~ negatively correlated, and that ~~either of the terms can dominate production of CH_4 within the~~ the exudate based production is roughly 50% ~~confidence interval, even though in 2008 the 70 cm experiment shows overall dominance of the peat decomposition process.~~ stronger than the peat decay source.

~~The production and oxidation related parameters τ_{cato}, and V_{O0} correlate (Fig. 4), and ζ_{exu} and Q_{10} are affected via their correlations with τ_{cato}. These parameters covary producing a total emission that minimizes the likelihood but this yields a posterior, where some parameters like V_{O0} have wide marginal distributions (Fig. 6 (f)), as in the presence of several covarying parameters any of those covarying ones can to some degree compensate for the movement of the others. The~~

The hard prior bounds of V_{O0} (mol m^{-3} s^{-1}) were tight and for example Segers (1998) reports that potential CH_4 oxidation can vary across three orders of magnitude. Hence, ~~higher~~ also lower proportions of CH_4 oxidation could have been seen with a more permissive prior. This would have then ~~resulted in wider posteriors also for the covarying parameters.~~ also altered the posteriors of the weakly covarying parameters, most notably λ_{root}.

~~Curiously,~~ The parameter V_{R0} (mol m^{-3} s^{-1}) controlling heterotrophic respiration correlates ~~negatively in all experiments weakly~~ positively with CH_4 production via ζ_{exu}, ~~and positively with parameter τ_{cato}. Removing oxygen from the column reduces CH_4 oxidation and in order to maintain the overall level of CH~~τ_{exu} (s) (smaller value enhances methane production), but the correlations with $\overline{Q_{10}}$ and τ_{cato} seem to cancel out each other. The correlations of $\overline{\zeta_{\mathrm{exu}}}$ are weak implying that that process is well constrained by the combined CO_2 and CH_4 ~~emission, production is reduced. The wide posterior of~~ data. There is also a weak anticorrelation between V_{R0} ~~in Fig. 6 implies that the day to day variation in the emissions and the combined effects of other parameters dominate. In the MAP estimates, however, the parameter is close to the lower bound~~and ΔE_R, which is to be expected based on Eq. 6.

5.3.2 Plant transport

The amount of plant transport in the calibrated models, shown in Fig. 7 ~~, is close to 90~~(a), is between 75% and 95% which is ~~slightly over the upper end of~~ just slightly higher than the range of 68-85% reported in Wania et al. (2010) in a study simulating CH_4 emissions for seven boreal peatlands. ~~This is opposite to what was obtained with sqHIMMELI with the default (prior mean) parameter values and 100 cm modeled peat, where the simulation routed 71% of the flux via diffusion.~~

The high optimized share of plant transport is mainly due to the ~~deep roots and high root conductance from the~~ high values of the root depth controlling parameter λ_{root} ~~and the~~ (m) and some of the difference between the MAP and posterior mean estimates in Fig. 7 (a) may be explained by the higher root ending cross section ~~parameter~~ area in the MAP estimate, controlled by parameter ρ ~~, and the low values of root tortuousity parameter τ. These parameters are close to the limits of what the priors allow, and are the reason for that plant transport dominates the gas transport.~~ (m^2 kg^{-1}). Wania et al. (2010) used the parametrization from Eq. 1 with $\lambda_{\mathrm{root}} = 0.2517$, and the root ~~distributions from the PM estimates are~~ distribution from the posterior mean estimate is shown alongside that distribution in Fig. 1. Compared with measurements from Saarinen (1996), the amount of roots at 20-60 cm is exaggerated by all of the optimized parameter values. The model provides a better fit to the data when the root conductance is ~~maximized.~~

~~The parameter posteriors of λ_{root} in the MCMC with 15 and 20 peat layers are apart from the others~~ high. However, the posterior distribution of the root tortuousity parameter in Fig. 6 ~~, implying that an optimal rooting depth is an ambiguous notion. The root distribution depths also correlate differently with other parameters in different depths - there is a negative correlation between $\overline{\zeta_{\mathrm{exu}}}$ and root depth (Fig. 4), which gets stronger with increasing peat column depth suggesting that more exudates are needed for shallow roots, which is reasonable since the exudates above the water table are respired aerobically. The other parameters affecting plant transport,~~ is almost identical to the prior, so obviously there is no need to maximize plant transport at any cost.

Since the parameters ρ (m^2 kg^{-1}) and τ ~~both~~ (m m^{-1}) both affect plant transport and are included in Eq. 8~~and~~ , one could expect them to be tightly coupled. In the posterior, however, they are only slightly correlated, with ~~coefficients~~ the correlation coefficient of only 0.12 in Fig. 4~~from 0.16 to 0.31. The strict priors may play a role, as root tortuousity cannot go below the value of 1.~~. This might be due to ρ having the tendency to be close to its the lower limit. The root-ending area parameter ρ has

a notable negative correlation with the air-diffusion coefficient $f_{D,a}$ (-). This follows directly from that increased root ending area increases root conductance, as does faster diffusion through the air-filled aerenchyma cells, via Eq. 8.

5.3.3 Diffusion

The masses of the diffusion coefficient parameters $f_{D,a}$ (-) and $f_{D,w}$ (-) in the posterior distributions (Fig. 6 (j) and (k)) are above the priors. This is true especially for within the rather permissive priors having the values of 0.8. The parameter $f_{D,w}$, which optimizes to is optimized close to the upper limit of one, specifically for the experiments with 100 - 200 cm of peat. Kaiser et al. (2016) note that these parameters are not well known, and use for both of them the value of 0.8, in which light the prior for $f_{D,a}$ looks narrow. The PM estimates for $f_{D,a}$ in Table 4 are between 0.50 and 0.65 for the depths of 40 - 100 cm.

The parameter $f_{D,a}$ is correlated negatively with the root-ending area parameter ρ. This is because the air diffusion parameter also affects the speed of CH_4 transport in plant stems via Eq. 8, and by negatively correlating the two parameters the model can compensate for one of them by moving the other. Additionally, a smaller root conductance implies that more of the CH_4 needs to come out via the diffusive flux , which is also seen in the negative correlation of λ_{root} and $f_{D,w}$, especially in experiments with peat depths of 70 and 100 cm.

Diffusion is correlated strongly with peat decay-based CH_4 production and negatively with exudate-based production (Fig. 5), and these correlations extend to the hierarchical parameters defining the CH_4 production (not shown). This is related to the strong connection between diffusion and ebullition, and that decaying peat produces CH_4 lower in the peat column than decaying exudates, production from which is more likely transported by plants (Fig. 5).

In general, the calibrations tend to end up facilitating the total CH_4 transport as the depth increases, by the action of the parameters ρ and τ affecting plant transport, and $f_{D,a}$, and $f_{D,w}$ affecting diffusion, implying that there is a regime of optimal conductance. Pertaining to this, Fig. 8 shows how the more modeled peat there is, the less important the diffusive component becomes. Going deeper down, plant transport becomes more competitive compared to diffusion in the MAP estimates.

. Constraining the model with the CO_2 flux measurements results in the diffusion component not correlating with the amount of methane produced via anaerobic peat decomposition.

5.3.4 Ebullition

Ebullition is very strongly tied to diffusion in the flux estimates with parameters from the posterior, as is shown for the 70 cm experiment in Fig. 5. The flux component timeseries in Fig. 11 shows that ebullition to the surface is a small fraction (circa 0-3% with optimized parameters), of the total flux, and Fig. 8 shows, that the more there is peat, the less important the ebullition flux is, including the part emitted as part of the diffusive flux. Similarly, Wania et al. (2010) report almost virtually no ebullition to the surface. This result is highly dependent on the type of the wetland as for instance Kaiser et al. (2016) report high ebullition fluxes for a polygonal tundra in the Siberian permafrost region, where the ice-free soil layer reaches only about 30 cm depth during summer. Variation between different sites is very large and depends on whether the water reaches the surface at times of high CH_4 emission.

Contrasting with this, in the simulations with the ~~default parametersand 100 cm of peat~~non-hierarchically optimized parameters, a major part of the diffusive flux, which comprises around 30% of the total flux for most years, is transported by ebullition (Fig. 8) and diffusion is ~~the dominating~~ a major flux component, even though ebullition to the surface accounts for only 5% of the total flux. Since ebullition is a fast timescale process, it was not directly constrained in the optimization with parameters, as preliminary tests revealed that daily data resolution would not be sufficient for this. While finer time resolution data would have been available, using it would not have been feasible as there is not enough knowledge about the fine structure of the wetland and micrometeorological conditions affecting the footprint area of the flux tower. It is reasonable to believe that the deviations from the daily averaged fluxes at a finer time resolution would only look like noise in the residuals not improving our parameter posterior. Despite this, ebullition is controlled indirectly by letting CH_4 production and transport parameters control when the water column has enough CH_4 available for ebullition. This happens when the sum of the partial pressures of dissolved gases is larger than the sum of atmospheric and hydrostatic pressures as shown in Eq. 23. The high ebullition-related proportion of the diffusive flux strengthens the argument that the likelihood formulation results in model optimizing towards parameter values that support rapid CH_4 transport.

~~The results show that with deep roots and high root conductances the wet part of the peat column rarely creates the conditions for ebullition to happen. Hence with less peat the amount of "all ebullition" increases, (Fig. 7 (b), 8 (a), and 10 (d)), as the produced CH_4 needs to be stored in a smaller volume increasing its concentration. This way the modeled peat depth has a major effect on how the model transports gases.~~

5.4 Parameter and process identifiability

The priors of the hierarchical CH_4 production-related parameters Q_{10} (-) and ζ_{exu} (-) in Fig. 6 (b) and (d) are constrained by the data, as are the hierarchical parameters themselves, shown in Fig. 13. The priors of these distributions are wider than their posteriors, which is also the case for the other production-related parameters τ_{exu} (s) and τ_{cato} ~~. The different posteriors of the catotelm peat turnover time τ_{cato} are disjoint from each other as increasing simulated peat column depth is compensated for by reducing the peat decomposition rate per volume~~(y). Both process descriptions for obtaining the anaerobic respiration are clearly needed for a good model fit, because the parameter posteriors do not have remarkable mass in the regions minimizing either of these processes (hierarchical parameters at the lower bounds or turnover rate parameters τ_{exu} and τ_{cato} at the upper bound). The covariances in Fig. ~~5~~ 4 and Fig. ~~4~~ 5 show that the two production processes covary slightly, with correlation coefficient -0.32, and hence they are ~~partly~~ to that extent interchangeable. Reasonable identifiability of the Q_{10}-parameters is not obvious, as for example Müller et al. (2015) optimizing a corresponding parameter end up with the parameter at the lower bound of their prescribed range. However, half of the mass of the production terms in the process correlation plot, Fig. 5, lies within a region that for production from exudates is roughly 10% of the total production and for the production from peat decay of the order of 35%,, and hence the production processes can be said to be well constrained.

The posterior distributions of V_{R0} (mol m^{-3} s^{-1}) show, that sqHIMMELI performs better when the heterotrophic respiration is close to being minimized, ~~but still away from the lower bound. With 100 cm of peat, the parameter has a clear mode further from the lower bound, suggesting that the flux measurement data used also constrains this process, and that the prior does not~~

~~indisputably rule out the best values. However, the oxidation parameter~~ which is also aided by a posterior mean value of ΔE_R (J mol^{-1}) that is lower than the prior mean. For the oxidation parameters V_{O0} ~~is not identifiable, and as the strong correlation with the peat decay related parameter τ_{cato} shows, its function is partly to calibrate the total CH_4 output of the the model and to spread the posteriors of the covarying parameters. With this model and data, methane oxidation rates at the Siikaneva site cannot be estimated without further constraints for e.g. the CH_4 production~~(mol m^{-3} s^{-1}) and ΔE_{oxid} the situation is different: the former has the tendency of being very small - but the temperature response has the tendency of being stronger with posterior mean and MAP values above the prior mean.

~~All~~

Whereas the fraction of plant transport is stable and high, but still constrained, not all the parameters affecting root conductivity are constrained by the data ~~to maximize the conductance~~as the root tortuousity posterior distribution follows very closely the prior form. The root ~~tortuousity parameter τ has narrow posteriors close to the lower bound of one, the root depth parameter λ_{root} is above its prior, and the root-ending area parameter ρ optimizes to very high values compared to the prior distribution~~(ending cross sectional area, however, is constrained to its lower side despite there being mass also above the prior mean value. For this parameter the importance resampling resulted in a changed posterior in that there is a lot more mass at the higher end of the distribution, as can be seen in Fig. 6 (~~g-i)). The diffusion-related parameters $f_{D,a}$ and $f_{D,w}$ are optimized to high values and identifiable with the exception that with the shallowest peat depths the water diffusion rate coefficient has little role and a wide posterior spanning all values from 0 to 1. Transport pathway shares are stable between the MAP and PM optimizations~~ h). In addition to this difference, the effects of the resampling were mostly minor. Still, the resampling informed that the roots should reside slightly higher in the peat column than suggested by the MCMC, and that the $f_{CH_4}^{\mathrm{exu}}$ is constrained to a higher value by the data than suggested by the initial MCMC run.

The transport pathways are well identified as can be seen in the ranges of variation in the transport characteristics in Fig. ~~8 (a), and their annual variation is small, implying that the existence of the different pathways helps to optimize the model fit~~5. Notably the transport processes do not strongly anticorrelate implying that they are not obviously interchangeable with each other. The correlation between oxidation and plant transport suggest that uncertainty in oxidation is a major part of the uncertainty in the plant transport portion. On the other hand, there is uncertainty in the absolute magnitude of the total flux (in terms of the posterior uncertainty) and this is reflected in the strong positive correlation between plant transport and the total flux. Similar but weaker positive correlations exist between the total flux and diffusion and ebullition, which is to be expected. The variation of oxidation is around ten percent of the total flux.

5.5 Low WTD in 2006, 2010, and 2011

The calibrated sqHIMMELI model is ~~not able to estimate~~ able to describe the CH_4 flux correctly in times of low water table~~in the 40 and 50 cm peat depth configurations. This is not unique to this particular model - also~~ , which is not obvious as other studies have indicated the challenges in parametrizations of emission models ~~in response~~ with respect to the water table depth (e.g. Zhu et al. (2014)). ~~Figures 10 (b) and (f) reveal that in July 2006~~ Figure 10 shows how the model processes are described under water stress. In times of a very low water table, the plant transport component and ~~CH_4 production from peat decay~~

go effectively to zero during the period of the lowest WTD. This effect is not visible in the simulations with more peat, and already the PM estimate with 7 layers gives a very nice fit for July 2006 (not shown) as the deeper peat column provides for more freedom for flux adjustment. The underestimation of the emission is visible comparing the plant transport pathways and total model residuals with respect to the water table depth at different depths in Fig. 10 (b), (f), and (h).

Other extended periods of low water table occur during the years 2010 and 2011, which explains why those years tend to be accentuatedly underestimated with respect to the observed flux with shallow simulated peat columns, as is shown methane production from root exudates are decreased somewhat, as is methane oxidation. This results directly from how the model is constructed as exudate deposition to the peat column is allocated depth-wise according to the root density profile. That the model continues to perform well during these years, implies that this method of regulating methane emissions during dry seasons is realistic. The residuals in Fig. 7 (f) , even though curiously the 50 cm MAP estimate also performs well. The lowest water table depth of the simulation period is in 2006, when on the 26$^{\text{th}}$ of August the water table drops to 38 cm below the surface. In 2011 the WTD goes below 20 cm for a total of 77 days in a row, and in 2010 it recedes to -17 cm for a period of 71 days, the average of the period being -23 cm. Years 2010 and 2011 have the strongest tendency to underestimate the total annual CH_4 emission compared with the observations. A sufficiently deep peat column to accommodate for CH_4 emissions during the low WTD periods is needed for making accurate predictions 10 (h) further show that there is a only a slight positive emission bias at the times of the very lowest water table levels.

5.6 Optimal modeled peat depth for sqHIMMELI

Even though most of the parameters and processes are identifiable, all of the parameter posteriors vary with peat depth, the most striking example of which is τ_{cato} (Fig. 6 (c)). For this reason, the validity and meaning of the parameter values must be understood in each particular model setting.

The objective function incorporating prior knowledge can be used to evaluate what peat column depth best represents the data and still retains the physical interpretation of the parameters, information about which is in the prior parameter distributions. In the MAP estimations, the costfunction values (Table 4) and the annual flux estimate errors (Fig. 8) are smaller starting with the depth of 70 cm and especially the 40 cm optimizations are systematically worse in this respect than the others, due to worse handling of periods of low WTD (Fig. 10). These problems do not exist with the 70 or 100 cm simulations, and are less pronounced already with 50 cm of peat.

With 150 or 200 cm of peat the correlations of the parameters shown in Fig. 4 show markedly different patterns from the correlations with shallower modeled columns. For these thick peat columns the costfunction values are higher, the correlations are not easy to explain, annual negative biases are not better, and model integration is more costly in terms of CPU time. For these reasons there is no reason to believe that modeling deeper peat columns than 100 cm in sqHIMMELI would be superior. Rather, the optimal thickness lies between 50 and 100 cm.

5.6 Predicting emissions with sqHIMMELI

Modeled CH_4 flux estimates may have large errors as was shown in Fig. 8 ~~(b)~~ with the default parameter set. The negative biases ~~of less than ten percent~~ in the calibration phase that were found with the ~~PM~~ maximum a posteriori and posterior mean estimates are reasonable since the quality of the modeled input data from e.g. a land surface scheme will also contribute to the uncertainty in the model predictions. Additionally, a known constant bias can be relatively easily accounted for if the inter-annual variability is correctly modeled.

Compared to the estimate with the optimized annual variations of the ~~Q_{10}~~ methane production related parameters, the non-hierarchical posterior mean estimate ~~without the hierarchical parameters (NHPM) does not produce very good good~~ produces reasonable flux estimates over the assessment period~~(Fig. 7 (g)). With all peat depths, the total CH_4 emission of the first years is overestimated by up to 30 percents and for the last years there is a similar negative bias.~~ , with twice the variability in fluxes compared to the posterior mean estimate, even though the average of the errors is closer to zero. The variability is seen in Fig. 7. The hierarchical posterior mean ~~(PM)~~ on the other hand does produce very steady estimates of the CH_4 flux ~~,~~ compared with observations ~~, and for these estimates the model dynamics are similar between the estimates for the peat depths of up to 100 cm.~~ even though there is a downward bias of 23%, and the smaller inter-annual variance implies better predictive skill. The same is true to a lesser extent also for the maximum a posteriori estimate.

In order to be able to utilize the ~~PM estimates~~ information regarding the annual variability in the posterior mean estimate for the future prediction of CH_4 emissions, the values of the hierarchical parameters need to be estimated for the simulation years. A simple regression analysis of the hierarchical variables with respect to relevant input data was performed in order to find out if such estimation is possible. As the explaining variables, means, minimums, and maximums of NPP, water table depth, and soil temperature at different depths and over different periods of time were looked at. These time periods were June, July, August, and various different amounts of days from the start of the year.

The analysis revealed that the mean soil temperature of the first 10 weeks (70 days) of the year at the depth of 30-40 cm, denoted here by $\overline{T^{70}_{30-40}}$, is the best single-variable predictor of the Q_{10}-value for that year, and for ζ_{exu}, it is the sum of NPP from the first 130 days of the year, denoted by NPP^{130}. This is hardly surprising, since the peat decomposition process regulated by the parameter Q_{10} is driven by soil temperature, and the anaerobic respiration from exudates controlled by the parameter ζ_{exu} is driven by the NPP input. These variables also indicate that the timing of the start of the growing season might play a role in determining the parameters. Possible mechanisms could include e.g. effects of the start of growing season on development of the microbe populations in the spring. However, further analysis would be needed to confirm this..

The p values summarizing the reliabilities of the regressions and the r^2 values, which are the coefficients of determination of the fit, are presented in table 5. The r^2 values explain what fraction of the variance of the dependent (predicted) variable is explained by the independent (explaining) variables.

~~For the MCMC experiment with 40 cm of peat the p value of the regression is better when looking at the 20-30 cm average soil temperature ($p = 0.075$, $r^2 = 0.38$), than with the 30-40 cm temperature ($p = 0.13$, $r^2 = 0.30$). It is understandable that~~

estimating Q_{10} gets more difficult with a shallow peat column depth, because the parameter has less effect as in the summer a majority of the whole peat column is dry. For the simulations with 150 or 200 cm of peat the regression for Q_{10} does not give meaningful results and the The $p$values are large, implying that a deep active peat column might pose an additional degree of difficulty for performing the CH_4 emissions.

The best experiments in terms of the predictability of the hierarchical variables are those with 70 - and 100 cm of peat, which also were the best performing peat column depths among the model calibration results (Table 4). For those depths, the r^2-values uncover that the hierarchical modeling reveals a clear-cut reliable relationship between the early NPP and the optimal ζ_{exu}-parameter ($p = 5 \times 10^{-6}$, $r^2 = 0.957$). This provides new insight into future model development and exemplifies why such a hierarchical description of variables is valuable in Bayesian optimization in a geophysical model context.

For the other inter-annually changing parameter, Q_{10}, the soil temperatures explain only slightly over half of the variation ($p = 0.0185$, $r^2 = 0.571$). Since the effect of this parameter is very important for the total methane flux, this results leaves lots of room for further analysis.The hierarchical parameters Q_{10} and ζ_{exu} for each year can be estimated with

$$Q_{10}^{7\mathrm{l}} = 3.27 + 1.71\zeta_{\mathrm{exu}}^{7\mathrm{l}} = -56000 NPP^{130} + 0.468 Q_{10}^{7\mathrm{l}} = 2.60 + 2.67\zeta_{\mathrm{exu}}^{10\mathrm{l}} = -68300 NPP^{130} + 0.480, \quad (25)$$

$$Q_{10} = 3.86\,\overline{T_{30-40}^{70}} + 1.76 \quad (26)$$

$$\zeta_{\mathrm{exu}} = -46500 NPP^{130} + 0.431 \quad (27)$$

where the upper indexes 7l and 10l refer to the number of 10 cm peat layers, temperatures are in °C, and the units of NPP are mol $\mathrm{m}^{-2}\ \mathrm{s}^{-1}$.

The lower p and higher r^2 values for the 70 and 100 cm models suggest that also in terms of predictive skill these configurations are superior as the hierarchically varying variables can be more robustly estimated. A leave one out-cross validation (LOO-CV, see e.g. Gelman et al. (2013)) of the predicted fluxes was therefore performed on the 70 cm and 100 cm models by optimizing them regression modeling was performed by optimizing the hierarchical parameters with respect to the costfunction in Eq. 24 leaving one year at a time out, calculating the estimates for the hierarchical parameters based on the results obtained for other years, and predicting the CH_4 emissions for the year that was left out. The algorithm (BOBYQA) and the number of iterations completed (350) were the same as before the MCMC and for the hierarchical parameters the priors were defined by the values defining the hyperprior. The results of the cross validation are shown in Fig. 7 (gb) and 8(b). Compared to the NHPM estimateand the default parameter values the annual errors were reduced . The cross-validated results are comparable in terms of annual performance to the non-hierarchical posterior mean. Despite the relatively good performance of the non-hierarchical posterior mean simulation, we note that the cross-validated result should be more relied on for prediction, since the well-predictable ζ_{exu}-parameters contain useful information that is not available in the non-hierarchical posterior mean estimate. A hybrid between these approaches could be also used, using the regression modeled values for the ζ_{exu}-parameters and the mean annual errors were -4.95% and -3.01% with the standard deviations of 13.6% and 13.4 %, for

the ~~70 cm and 100 cm peat column depths respectively. In comparison to the NHPM estimate the annual errors were reduced for six out of the nine years. These results are promising, and as the analysis performed was extremely simple, there is room for further development.~~ Q_{10}, to minimize the risk of major annual biases due to unsuccessful prediction of the Q_{10}-parameters.

As Fig. 7 (b) shows, much of the error in the cross validation actually comes from challenges estimating year 2007, which is missing the peak season observations, and therefore the error percentage (in terms of the annual observed flux) is easily high, especially as the start of season is modeled with a delay, which is readily apparent in Fig. 9, and in this sense the negative bias in Fig. 7 gives an unnecessarily pessimistic view of the model performance. For the CO_2 fluxes, it can be noted that there is a persistent positive bias of some tens of percents, but the observations are very noisy and due to the processing for the use in the costfunction, they might have biases. The effect of a small bias on the parameter posterior distribution is, however, minor, since the carbon dioxide observations were given less weight in the costfunction than the methane observations. Hence, given their uncertainty the optimized fit to the measurement data can, also in the cross-validation as in the other experiments, be seen as acceptable.

6 Conclusions

In this study, Bayesian calibration of a new process-based wetland CH_4 emission model, sqHIMMELI, was performed using ~~MCMC methodsagainst observations~~ Markov chain Monte Carlo methods, hierarchical statistical modeling of methane production related parameters, Box-Jenkins-type timeseries modeling, and importance resampling, against daily methane and carbon dioxide flux data from the Siikaneva flux measurement site in Finland. The results show that the modeled processes and the estimated parameters are identifiable with the flux data~~, with the exception of CH_4 oxidation. The depth of the modeled peat column, for which an optimal range was found at around 70 cm, strongly affects the posterior distributions of the parameters, and the optimal model functioning in terms of the gas transport pathway fractions and the relative importances of the sources of the anaerobic respiration. Such dependence on the chosen model setup suggests that using strict measurement-based priors can cause the model to behave in an unintended manner.~~ . The parameter correlations and process correlations from random sampling the posterior reveal that there are no redundant processes in the model description. However, a few strong correlations between parameters exist reminding of the difficulty of strictly interpreting parameter values to be connected to isolated physical processes. The optimized model fits well to the data in that the modeled fluxes fit within a range from the data that is expected based on the error modeling.

Preliminary results obtained also suggest that estimation of the ~~annually varying CH_4 production-related parameters~~ annual variation of the parameters controlling methane production from anaerobic respiration of root exudates is feasible and may help to improve the future estimates of the boreal wetland CH_4 emissions.

~~Since the flux observations were not enough to constrain the oxidation rates, a possible path forward is to estimate model and parameter states assimilating column concentrations with a method such as the one presented in Hakkarainen et al. (2012) . Along that path~~

For future studies, combining observations from several sites and optimizing them together with the methods presented here in conjunction with independent validation can provide valuable information about the uncertainties related to wetland emission modeling and about how to best improve the quality of predicting wetland methane emissions in land surface schemes of climate models.

7 Code availability

The HIMMELI source code is available as a supplement to the publication Raivonen et al. (2017).

8 Data availability

The model input data and the flux measurement data are available upon a reasonable request from the lead author.

Appendix A: ~~The sqHIMMELI~~ Error model ~~equations~~for residuals

~~The version of HIMMELI presented here describes processes for CH_4 production and transport. It differs from the version presented in Raivonen et al. (2017) in that the model presented there does not contain the processes for anaerobic respiration but rather take it as input, the idea being that such input would be available when using HIMMELI as a part of a larger model. Hence the equations presented in Sec. 3.1.2 are specific to the version used in this study. The other difference between the models is the difference between the root distributions described in Sec. 3.2.~~

A1 ~~Governing equations~~

~~The gas concentrations of CH_4, carbon dioxide and oxygen in the peat column are governed by the equations~~

$$T_X(t,z) = Q_X^{\mathrm{diff}} + Q_X^{\mathrm{plant}} + Q_X^{\mathrm{ebu}} \frac{\partial[\mathrm{CH_4}]}{\partial t}(t,z) = -T_{CH_4} + R_{CH_4}^{\mathrm{exu}} + R_{CH_4}^{\mathrm{peat}} - R_{CH_4}^{\mathrm{oxid}} \frac{\partial[\mathrm{O_2}]}{\partial t}(t,z) = -T_{O_2} - R_{\mathrm{aerob}}^{\mathrm{peat}} - R_{CO_2}^{\mathrm{exu}} - 2R_{CH_4}^{\mathrm{oxid}} \frac{\partial[\mathrm{C}}{}$$

(A1)

~~where $T_X(t,z)$ describes transport of gas X containing the diffusion, ebullition, and plant transport components, and R stands for production or consumption. The different terms in the equations are described below.~~

A1 ~~Anaerobic respiration producing CH_4~~

~~The equations presented in this section are specific to the version of HIMMELI used in this study. The version in Raivonen et al. (2017) takes the rate of anaerobic decomposition of carbon as input and does not treat the different sources of that carbon separately.~~

The carbon for methane production in this model version comes from two sources: root exudates and anaerobic peat composition. The methane production from anaerobic respiration of that carbon is given by the terms $R^{\text{exu}}_{CH_4}$ and $R^{\text{peat}}_{CH_4}$ described by:

$$R^{\text{exu}}_{CH_4}(z) = \frac{f^{\text{exu}}_{CH_4}}{\mathrm{d}z}\nu\frac{\pi(z)}{1+\eta C_{O_2}(z)} R^{\text{peat}}_{CH_4}(z) = k_{\text{cato}}(z) g^{Q_{10}}_{CH_4}\frac{\rho_{\text{cato}} f_{C_{\text{cato}}}}{M_C}, \tag{A2}$$

where in Eq. 15 ν is the decay rate of root exudates from Eq. 3, η is an oxygen inhibition parameter, $C_{O_2}(z)$ is the oxygen concentration at depth z, and $\pi(z)$ is the normalized proportion of the total anaerobic root mass, also at depth z, given in an unnormalized form in Eq. 2. The parameter $f^{\text{exu}}_{CH_4}$ is a constant determining what fraction of root exudates in anaerobic conditions will turn into CH_4. Equation 15 is only used below the water table. In Eq. 16, $g^{Q_{10}}_m$ is the proportion of the anaerobic peat decomposition process producing CH_4, ρ_{cato} is the peat density in the catotelm, $f_{C_{\text{cato}}}$ is the fraction of carbon in catotelm peat, and M_C is mass of carbon. The parameter $k_{\text{cato}} = Q_{10}^{\frac{(T-273.15)}{10}}/\tau_{\text{cato}}$ is described in Eq. 5, and is zero above water table.

The equations for CO_2 are similar:

$$R^{\text{exu}}_{CO_2}(z) = \nu\pi(z) - R^{\text{exu}}_{CH_4}(z) R^{\text{peat}}_{CO_2}(z) = (1-g^{Q_{10}}_{CH_4})k_{\text{cato}}(z)\frac{\rho_{\text{cato}} f_{C_{\text{cato}}}}{M_C}, \tag{A3}$$

and the meanings of the symbols are analogous to the ones in equations for CH_4.

A1 Peat respiration and methane oxidation

Peat respiration (aerobic respiration) is described with an equation of the Michaelis-Menten form

$$R^{\text{peat}}_{\text{aerob}}(z) = V_R(z)\frac{\alpha C^x_{O_2}(z)}{K_R + C^x_{O_2}(z)}, \tag{A4}$$

where α is a dimensionless Henry solubility constant for oxygen above the water table, and one below it, see Tang et al. (2010). The factor $C^x_{O_2}$ refers to $C^w_{O_2}$ below the water table, and to $C^a_{O_2}$ above it. Here w In section 4.2.1 we described the error models as AR(1) / ARMA(2,1) models where the residuals are Laplace-distributed. Intuitively these models can be thought of as characterizing the "inertia" or "memory" in the model-observation discrepancy. Formally the observation equation for our statistical inference problem can be written as

$$\boldsymbol{y}_t = \boldsymbol{x}_t + \boldsymbol{r}^*_t \tag{A5}$$

$$\boldsymbol{x}_t = M(\boldsymbol{x}_{t-1}, \boldsymbol{z}_{t-1}, \boldsymbol{\theta}) \tag{A6}$$

The vector notation for $\boldsymbol{y}$ and $\boldsymbol{r}^*$ in Eq. A5 refers to that at each time t there can be observations of both methane and carbon dioxide, and a refer to whether the concentration is in the gaseous or in the liquid phase. Parameter K_R is the Michaelis-Menten constant of the process, and $V_R(z)$ is given by Eq. 6.

Methane oxidation is controlled by dual-substrate Michaelis-Menten kinetics,

$$R^{\text{oxid}}_{CH_4}(z) = V_O(z)\frac{C^x_{O_2}(z)}{K_{O_2}+C^x_{O_2}(z)}\frac{C^x_{CH_4}(z)}{K_{CH_4}+C^x_{CH_4}(z)}, \tag{A7}$$

and here α factors similar to the one M in Eq. 19 have been absorbed into the concentration terms - otherwise the terms are analogous to those in Eq. 19, except for that the term $V_O(z)$ is described by Eq. 7.

A1 CH_4 transport

The transport term $T_X(t,z)$ in Eq. 11 consist of the following terms:

$$Q^{\text{diff}}_X = D^X_{\text{medium}}\frac{\partial}{\partial z}C^{\text{medium}}_X \qquad Q^{\text{plant}}_X(z) = \frac{\rho\pi(z)D^X_{\text{air}}}{\tau^2}\frac{LAI}{SLA}\frac{C_x(t,z)-C^{\text{atm}}_X}{z} \qquad Q^{\text{ebu}}_X(z) = -k\sigma\frac{pp_{i,X}}{RT}\frac{\sum_i pp_i(z)-(P_{\text{atm}}+P_{\text{hyd}}(z))}{\sum_i pp_i(z)}. \tag{A8}$$

The first of these is the diffusion, where the diffusion coefficients D are given by Eq. 9 and 10, and "medium" refers to either air or water. Due to coding mistake, the $f_{D,a}$ and $f_{D,w}$ coefficients in the aforementioned equations were set to 0.1 for gases other than CH_4 in this work.

The second equation is for plant transport, with ρ and τ described in contextof Eq. 8, $\pi(z)$ is the normalized root distribution mentioned above, and C^{atm}_X refers to the atmospheric partial pressure of gas X. LAI stands for the leaf area index, given as input, and SLA is the specific leaf area. The note above regarding the $f_{D,a}$ values is also valid for plant transport, as it is a factor determining D^X_{air}.

The third equation is the ebullition component of the gas transport, where pp_i refers to the partial pressure of different gases indexed with iA6 denotes the model (sqHIMMELI) advancing the model state $\boldsymbol{x}_{t-1}$ forward in time. The term $\boldsymbol{z}_{t-1}$ is the external model forcing data. In this context, R is the universal gas constant, k is an ebullition rate constant, and σ is the peat porosity. The parameters P_{atm} and $P_{\text{hyd}}(z)$ refer to the atmospheric pressure and hydrostatic pressure at depth z, respectively.

Table 2 shows the parameters that are used in the equations above but not optimized in this work, along with their values.

Appendix B: Error model for residuals

In section 4.2.1 we described the error model as an AR(1) model where the residuals are Laplace-distributed. The error of each measurement was described as a fraction α on the absolute value of the observation at that time, plus a constant error component, $\gamma$the *error model* that is referred to in text refers to how the $\boldsymbol{r}^*_t$-terms are modeled. The modeling is different for the MCMC and importance resampling steps.

Residuals terms for MCMC

Let $\boldsymbol{y}' = \max(\boldsymbol{c},\boldsymbol{y})$, where $\boldsymbol{c}$ For both CO_2 and CH_4, let $y'_t = \max(c_t, y_t)$, where c_t is the 14-day running mean of the gap-filled CH_4 flux observations $\boldsymbol{y}$, and where the maximum is understood to be taken over each pair separately. Let M be the model

~~, $\boldsymbol{x}_t$ the model state, and $\boldsymbol{z}_t$ the forcing input data at time t. Then the~~ flux observations y_t. Due to the heteroscedasticity of the model error, we scale the residuals for error modeling by dividing each model prediction and observation with $\alpha|y'_t| + \gamma$, where α and γ are pre-determined constants. The error-scaled residual at time t is

$$r_t = \frac{y_t - M(\boldsymbol{x}_{t-1}, \boldsymbol{z}_t, \boldsymbol{\theta})}{\delta_t}, \tag{A1}$$

~~where $\delta_t = \alpha|y'_t| + \gamma$.~~ then

$$r_t = \frac{r^*_t}{\alpha|y'_t| + \gamma}. \tag{A2}$$

Let ϕ denote the lag-1 autocorrelation coefficient, meaning the correlation of the residual timeseries with the same residual timeseries one day later. The AR(1)-corrected residual for time t then becomes

$$r^*_t = r_t - \phi\, r^*_{t-1}. \tag{A3}$$

~~The motivation~~

$$r_t = \phi\, r_{t-1} + \epsilon_t. \tag{A4}$$

The reason for the way of constructing $\boldsymbol{y}'$ above ~~is~~ was to allow for a reasonable amount of error both in the case when there is an emission spike upwards and when the same happens downwards, avoiding the problems ~~where~~ when if in the summer there is suddenly a day with zero CH_4 emissions, ~~and the likelihood would take the observation~~ the observation would be taken to be extremely precise (as $\alpha\, y_t$ would be small) ~~because of the low absolute value~~ even though the low value is rather due to noise.

~~The model was fitted against the data with a crude least-squares likelihood in order to determine α and γ. The AR(1)-transformed residuals obtained follow the Laplace distribution with mean 0 and scale 1, when $\alpha = 0.08$, and $\gamma = 0.00025\ \mu$ mol s^{-1} m^{-2}. The AR(1) parameter ϕ was set to 0.2. The~~

The MCMC experiment was performed with a costfunction that permissively allowed for exploration of the parameter ~~δ_t in Eq. A2 and the annual flux term in Eq. 24 were finally scaled so that the contribution from the residuals was 80%, and the contributions from the annual fluxes and prior were 10% each in terms of the number of summands. This was done to prevent being overconfident with the parameter estimates and to account for that the value of 0.2 for ϕ was on the low side, since the transformed residuals still are autocorrelated with~~ space. The α and γ were 0.4 and 0.00075 for CH_4 and 1.0 and 0.029 for CO_2, respectively, and the lag-1 ~~correlation coefficient between 0.45 and 0.65 for the PM and MAP estimates. Other uncertainties motivating such treatment are~~ autocorrelation coefficient used was 0.6. Uncertainties motivating such a permissive error description include uncertainties in the NPP model, inadequacies in the model description of the peat column and lack of spatial heterogeneity in the model description, filled gaps in the water table depth data, errors from interpolation of the soil temperature data and heat transfer, and other unknown error sources. The same model error description was used for all MCMC model simulations.

~~The residual histograms of the 70 cm PM estimates show that the error model transformed unscaled residuals closely~~

Residuals for importance resampling

The sum of the absolute values of the ϵ_t-terms appears in the objective function, Eq. 24, but the AR(1)-modeled values are in the end not independent and do not accurately follow the Laplace distribution, in part because generous values were chosen for α and γ that allowed for easier exploration of the parameter space. The objective function used for importance resampling fixes these problems.

For choosing the order of autoregressive moving average model (the ARMA(p, q) model), the different models up to order $p = q = 4$ were fitted, and the one whose fitting yielded the lowest Bayesian Information Criterion was picked. After making sure that the fitted residuals are independent by calculating the Durbin-Watson statistic, the order of $(p, q) = (2, 1)$ was chosen. In place of Eq. A4, the error model for the residuals is then written as

$$r_t = \phi_1 r_{t-1} + \phi_2 r_{t-2} + \theta\epsilon_{t-1} + \epsilon_t, \tag{A5}$$

where the ϕ-parameters are the AR model parameters and the θ is the MA-part. ~~There is a slight extra concentration of mass on the lower side, which is explainable with the overall negative bias of a few percents in~~

The scaling of the ~~emission estimate,which was~~ model residuals for choosing the ARMA parameters and the values for α and γ above (separately for the CH_4 and CO_2 timeseries) was done by effectively calculating the 2-week running mean of the variances of the flux from observations for each day of year. More explicitly, let

$$\hat{y}_t = \sqrt{(\mathbb{V}_{\mathrm{doi}=t}[y_t])} \tag{A6}$$

denote the standard deviation of the observed fluxes for a given day of year over the whole observation dataset. Then the residuals are scaled as before by

$$r_t = \frac{r_t^*}{\alpha \boldsymbol{h}^T \hat{\boldsymbol{y}}_t + \gamma} \tag{A7}$$

where $\boldsymbol{h}^T$ is a vector of length 14 with each element having value $\frac{1}{14}$ and $\hat{\boldsymbol{y}}_t$ is the vector with elements $\hat{y}_{t-7}, \ldots, \hat{y}_{t+6}$. Let $\Psi(b_i)$ denote the value of a discretization of the standard Laplace distribution at point $b_i \in \{b_1, \ldots, b_{N_b}\}$, and let $S^{\tilde{\phi}_1, \tilde{\phi}_2, \tilde{\theta}}_{\alpha,\gamma}(b_i)$ denote the empirical probability density function of the set of the transformed residual terms, the ϵ_t-terms in Eq. A5, again at point b_i. The parameters $\tilde{\phi}_1, \tilde{\phi}_2$, and $\tilde{\theta}$ are the optimized ARMA model parameters from fitting the model.

The ARMA(2,1) model parameters and the parameters α and γ are determined for the importance resampling by minimizing the *Kullback-Leibler divergence*,

$$D_{KL}(\Psi \| S^{\tilde{\phi}_1, \tilde{\phi}_2, \tilde{\theta}}_{\alpha,\gamma}) = -\sum_{i=1}^{i=N_b} \log \Psi(b_i) \frac{S^{\tilde{\phi}_1, \tilde{\phi}_2, \tilde{\theta}}_{\alpha,\gamma}(b_i)}{\Psi(b_i)}, \tag{A8}$$

which is a measure of similarity between distributions. Effectively we fit the error model parameters to make sure that the modeled residuals really are Laplace-distributed and independent. The parameters α and γ are then chosen to be

$$\alpha, \gamma = \underset{\alpha,\gamma}{\operatorname{argmin}}\, D_{KL}(\Psi \| S^{\tilde{\phi}_1, \tilde{\phi}_2, \tilde{\theta}}_{\alpha,\gamma}), \tag{A9}$$

and the ARMA-parameters are chosen to be the ones from the model fit with those parameters α and γ minimizing the KL-divergence. The BOBYQA optimization algorithm (Powell, 2009) was used to carry out the minimization. The procedure was performed for 50 parameters vectors randomly sampled from the posterior of the MCMC run and the medians of these values, which were for all parameters narrowly distributed, were the final ones picked for the likelihood used in importance resampling. The actual values of these parameters for methane were: $\alpha^{\mathrm{CH_4}} = 0.594$, $\gamma^{\mathrm{CH_4}} = 1.38 \times 10^{-6}$, $\phi_1^{\mathrm{CH_4}} = 1.30$, $\phi_2^{\mathrm{CH_4}} = -0.325$, and $\theta^{\mathrm{CH_4}} = -0.770$; correspondingly for carbon dioxide $\alpha^{\mathrm{CO_2}} = 0.443$, $\gamma^{\mathrm{CO_2}} = 3.96 \times 10^{-3}$, $\phi_1^{\mathrm{CO_2}} = 1.21$, $\phi_2^{\mathrm{CO_2}} = -0.242$, and $\theta^{\mathrm{CO_2}} = -0.738$. The histograms of the ϵ_t-values and the autocorrelation functions are shown in Fig. 82.

Appendix B: A basic outline of MCMC

~~Markov Chain~~ Markov chain Monte Carlo (MCMC) methods are a class of Bayesian methods that can be used for obtaining the probability distribution $p(\boldsymbol{\theta}|\boldsymbol{y})$ for a parameter vector $\boldsymbol{\theta} \in \boldsymbol{R}^n$ given data $\boldsymbol{y} \in \boldsymbol{R}^k$. According to Bayes' theorem~~from 1763~~, this can be written as

$$p(|) = \frac{p(\boldsymbol{y}|\boldsymbol{\theta})p(\boldsymbol{\theta})}{p(\boldsymbol{y})}, \tag{B1}$$

$$p(\boldsymbol{\theta}|\boldsymbol{y}) = \frac{p(\boldsymbol{y}|\boldsymbol{\theta})p(\boldsymbol{\theta})}{p(\boldsymbol{y})}, \tag{B2}$$

where $p(\boldsymbol{y}|\boldsymbol{\theta})$ is the *likelihood* (in this work the first two terms on the right hand side of Eq. ~~4.2.3~~24), and ~~$p(\boldsymbol{y})$~~ $p(\boldsymbol{\theta})$ is the *prior* (the last term). The *evidence*, $p(\boldsymbol{y})$ is often very difficult to evaluate, but in MCMC this is not needed, because MCMC algorithms evaluate ratios of successive evaluations of $p(\boldsymbol{\theta}|\boldsymbol{y})$, making the denominators to cancel out and hence the evidence term can be dropped.

MCMC sampling starts by taking some starting value $\boldsymbol{\theta}$ ~~,~~ and calculating the objective function (also known as *costfunction*) value ~~$J(\boldsymbol{\theta}) \in \boldsymbol{R}$~~$J(\boldsymbol{\theta}) \in \mathbb{R}$ - the notation here is the same as in Eq. 24. The algorithm then draws a new sample of the parameter vector, $\boldsymbol{\theta}'$ from a prescribed *proposal distribution* $q(\boldsymbol{\theta})$, and evaluates $J(\boldsymbol{\theta}')$. It accepts the new parameter vector with a probability that depends on the value of $J(\boldsymbol{\theta}')$ and the objective function value of the previous accepted parameter, $J(\boldsymbol{\theta})$. If the value is accepted, the chain will move to position $\boldsymbol{\theta}'$ (setting $\boldsymbol{\theta} \leftarrow \boldsymbol{\theta}'$), and if $\boldsymbol{\theta}'$ is rejected, the value $\boldsymbol{\theta}$ will be repeated in the chain. After this a new value, sampled from $q(\boldsymbol{\theta})$ (which is possibly a different distribution from the one used at the previous iteration as $\boldsymbol{\theta}$ may have changed) will be proposed and the whole process is repeated. In the end the procedure will produce a chain of parameter values.

~~This chain of parameter vectors will theoretically, given infinitely many iterations, converge to the~~ According to Markov chain theory, the sampled parameter values will eventually follow the *target distribution* ~~of the Markov process,~~ $p(\boldsymbol{\theta}|\boldsymbol{y})$ meaning, that in such a case picking a random element from the chain amounts to drawing a sample directly from the target distri-

bution. As real-life Markov chains are of finite length, the *posterior distribution* obtained from the chain is an approximation of the underlying target distribution.

In practice this means, that with MCMC it is possible to find a good approximation of the probability density function of the parameter vector $\boldsymbol{\theta}$ in cases, where the model is ~~too complicated~~ not suitable for analytical treatment. From this probability density function, valuable information such as modes, variances, and correlations of the parameters can be analyzed. The posterior also reveals, what parameters are constrained by the data, and what are not.

For efficient convergence of the chain to the posterior distribution a good estimate of $q(\boldsymbol{\theta})$ is needed. The Adaptive Metropolis algorithm automatically calibrates the proposal during the MCMC.

Appendix C: Metropolis within Gibbs sampling of the parameters

The hierarchical parameters Q_{10}^{year} and $\zeta_{\mathrm{exu}}^{\mathrm{year}}$ are denoted here generically by θ^i, where i refers to the different years. The priors of these parameters are defined by the *hyperparameters* μ_i and σ_i that determine the prior of θ^i by

$$\theta^i \sim N(\mu_i, \sigma_i^2). \tag{C1}$$

$$\theta^i \sim N(\mu_i, \sigma_i^2). \tag{C2}$$

The unknown hyperparameters μ_i and σ_i^2 have probabilistic models

$$\mu_i \sim N(\mu_0, \tau_0^2) \sigma_i^2 \sim \text{Inv-}\chi^2(n_0, \sigma_0^2), \tag{C3}$$

$$\mu_i \sim N(\mu_0, \tau_0^2) \tag{C4}$$

$$\sigma_i^2 \sim \text{Inv-}\chi^2(n_0, \sigma_0^2), \tag{C5}$$

where μ_0 and τ_0^2 define the mean and variance of the hyperprior of μ_i, ~~$n_0 \in \mathbf{N}$~~ $n_0 \in \mathbb{N}$ defines the number of degrees of freedom of the Inv-χ^2 distribution, and σ_0^2 is the expected value of the scaled Inv-χ^2 distribution.

In Gibbs sampling the full conditional posterior distributions of the hyperparameters and the parameters θ_i are sampled in turns. Due to the conjugacy of the normal distribution and the scaled Inv-χ^2 distribution, closed form expressions exists for sampling from $p(\mu_i|\sigma^2, \mu_0, \sigma_0^2, \theta^i)$ and $p(\sigma_i^2|\sigma_0^2, n_0, \theta^i)$, where μ is the current mean of the parameters θ_i and σ^2 is their variance. The Gibbs sampling therefore consists of three steps:

1. Draw μ_i from

$$\mu_i|\mu, \sigma^2 \sim N\frac{\frac{n_i\overline{\theta^i}}{\sigma^2} + \frac{\mu_0}{\tau_0^2}}{\frac{n_i}{\sigma^2} + \frac{1}{\tau_0^2}}, \frac{1}{\frac{n_i}{\sigma^2} + \frac{1}{\tau_0^2}}, \tag{C6}$$

$$\mu_i|\mu,\sigma^2 \sim N\left(\frac{\frac{n_i\overline{\theta^i}}{\sigma^2}+\frac{\mu_0}{\tau_0^2}}{\frac{n_i}{\sigma^2}+\frac{1}{\tau_0^2}}, \frac{1}{\frac{n_i}{\sigma^2}+\frac{1}{\tau_0^2}}\right), \tag{C7}$$

2. draw σ_i^2 from

$$\sigma_i^2|, \sim \text{Inv-}\chi^2 n_0+n_i, \frac{\sigma_0^2 n_0+\sum_{j=1}^{n_i}(\theta_j^i-\mu_j)^2}{n_0+n_i}, \text{and} \tag{C8}$$

$$\sigma_i^2|\boldsymbol{\theta},\boldsymbol{\mu} \sim \text{Inv}-\chi^2\left(n_0+n_i, \frac{\sigma_0^2 n_0+\sum_{j=1}^{n_i}(\theta_j^i-\mu_j)^2}{n_0+n_i}\right), \text{and} \tag{C9}$$

3. draw the parameters θ_i (and the non-hierarchical parameters) with MCMC, since closed-form expression for $p(\boldsymbol{\theta}|\phi,\boldsymbol{y})$, where ϕ denotes all the different hyperparameters, is not available.

In this work, the value of the parameter τ_0^2 was set to the value of σ_0^2, n_i is the number of years, and the value of n_0 was set to 9. The means and variances obtained this way describe the interannual variability of the parameters, and not including them as parameters in the MCMC sampling reduces the dimension of space that the MCMC sampler needs to explore, speeding up convergence of the posterior distribution.

Appendix D: Importance resampling

Importance resampling is a method for obtaining samples from a desired (unnormalized) distribution $q(\boldsymbol{\theta})$ by re-evaluating samples from a similar distribution from which it is know how samples are generated, $p(\boldsymbol{\theta})$. It is usually remarkably faster than for instance re-performing an MCMC experiment.

The samples $\boldsymbol{\theta}_1 \ldots \boldsymbol{\theta}_N$ are first drawn from $p(\boldsymbol{\theta})$ (in our case randomly picked from the MCMC chain), and at these points the new posterior density $q(\boldsymbol{\theta})$ is evaluated. For each of these, the *weights* are defined by $w(\boldsymbol{\theta}_i) = \frac{q(\boldsymbol{\theta}_i)}{p(\boldsymbol{\theta}_i)}$. The samples from the distribution $q(\boldsymbol{\theta})$ are then generated by sampling according to the set of normalized weights, $\tilde{w}(\boldsymbol{\theta}_i) = \frac{w(\boldsymbol{\theta}_i)}{\sum_{j=1}^{N} w(\boldsymbol{\theta}_j)}$. The sampling is performed without replacement. For further details, see e.g. Gelman et al. (2013).

Appendix E: NPP and LAI

We estimated the net photosynthesis rate, P_n, of vascular plants of Siikaneva for years 2005-2014 by utilizing regression models of gross photosynthesis, P_g, and autotrophic respiration R_a formulated for peatland vegetation (Riutta et al., 2007a, b; Raivonen et al., 2015). The model of the P_g of sedge and dwarf shrub canopy (Riutta et al., 2007a) simulates the carbon uptake driven by photosynthetically active radiation (PAR), WTD and air temperature. The model of R_a (Raivonen et al., 2015) simulates the respiration rate driven by air temperature and WTD and was parameterized for sedges only.

Both P_g and R_a models simulate the carbon fluxes per soil surface area and the rate depends on the LAI. We simulated the LAI using a lognormal function presented by (Wilson et al., 2007). Parameter values of the LAI model were obtained by averaging the values reported by (Wilson et al., 2007) for the vascular species abundant at Siikaneva. For the growing season peak LAI we used the maximum LAI observed at the eddy covariance footprint area, viz. approximately 0.4 m^2 m^{-2} (Riutta et al., 2007b). We also included a constant wintertime LAI since a significant green sedge biomass may overwinter, approximately 15% of the maximum (Saarinen, 1998; Bernard and Hankinson, 1979). The overwintering LAI at Siikaneva would thus be 0.05 m^2 m^-2 . The same LAI was used for all the years and this LAI also was given as the input for the CH_4 transport model.

The daily averages of P_n were calculated by subtracting R_a from P_g. The models were run with measured meteorological data. We determined the photosynthetically active seasons based on snowmelt dates in spring or arrival of snowcover in autumn from the reflected PAR data, or based on air temperature (~~permenently~~ permanently greater than 5 °C assumed to be the growing season). After the calculation, we compared the resulting P_n of vascular vegetation of year 2005 to eddy covariance CO_2 fluxes from Siikaneva. We used the GPP derived from the measured NEE by (Aurela et al., 2007). ~~This was the only available year of processed CO_2 flux data.~~ The GPP was on average 4.5-fold compared with our P_n , with a R^2 of 0.9. GPP also includes the photosynthesis of *Sphagnum* mosses as well as CO_2 released in autotrophic respiration. *Sphagnum* accounted for 20-40% of the GPP in the study by (Riutta et al., 2007a) and autotrophic respiration has been observed to be roughly 50% of GPP (Gifford, 1994). Consequently, the NPP of vascular vegetation can be estimated by multiplying the GPP with 0.7×0.5. This estimate was still 1.56-fold compared with the P_n for the year 2005. Since the P_n also was lower than generally reported for peatlands, we chose to trust the eddy covariance measurement and scaled the P_n of all the years upwards by multiplying with 1.56. For further details, please consult Raivonen et al. (2017).

Appendix F: ~~Supplementary information~~

E1 ~~Details regarding the AM algorithm usage~~

~~In order to infer about the posterior distribution, the MCMC chain needs to be long enough, and converged to produce the right statistics. The MCMC chains driven by the AM algorithm mixed well, example of which as can be seen in Fig. **??** showing the chain from the experiment with 100 cm of peat. The proposal distribution of the AM algorithm was adapted when the iteration number was a square of an integer, and for the adaptation 20% from the start of the chain was discarded. In the early stages of each experiment, the initial approximation for the proposal covariance, calculated from the Jacobians of the model, was allowed to dominate until after accepting enough proposed points there was sufficient data to start the proposal covariance adaptation procedure.~~

E1 ~~Computational requirements~~

~~Even though the model runs fast, in around five to thirty seconds for the ten-year period on a multicore laptop, due to the large number of simulations, the MCMC experiments needed to be performed on a CRAY XC-20 supercomputer using a single node for a single MCMC chain and running all the experiment in the RAM of the computer minimizing hard drive utilization. Shared-memory parallellization was used to run the different years at the same time and the MCMC experiments were run for a month during which all the MCMC experiments completed between 78000 and 391000 forward model simulations.~~

Author contributions. JS designed the study with help from the co-authors, programmed the algorithms, performed the model simulations, analyzed the results, and prepared the manuscript and the figures. MR provided and validated the input data and helped with the interpretation of the results. LB contributed several model subroutines and helped to interpret the results. ML provided assistance with getting the technical aspects of the Bayesian analysis right. OP provided insight into the data used. JM, TV, and TA provided helpful critical comments and suggestions that helped to improve the manuscript substantially.

Competing interests. The authors state that they are free from any conflicting interests.

Acknowledgements. We would like to thank the University of Helsinki researchers M.Sc. Pavel Alekseychik, and Dr. Ivan Mammarella, and Prof. Janne Rinne from Lund University for valuable comments and input regarding the Siikaneva measurement site data. We would also like to thank Prof. Heikki Haario from Lappeenranta University of Technology, Dr. Janne Hakkarainen from Finnish Meteorological Institute, and Prof. Samuli Siltanen from University of Helsinki for comments regarding the mathematical aspects of the study.

This work has been supported by the EU LIFE+ project MONIMET LIFE12 ENV/FI/000409, and the EU FP7 project EMBRACE. We additionally acknowledge funding from the RED platform of the Lappeenranta University of Technology, and thank the Academy of Finland Center of Excellence (272041), CARB-ARC (285630), ICOS Finland (281255) ICOS-ERIC (281250), NCoE eSTICC (57001), EU-H2020 CRESCENDO (641816) and Academy Professor projects (284701) and (282842).

References

Arah, J. R. M. and Stephen, K. D.: A Model of the Processes Leading to Methane Emission from Peatland, Atmospheric Environment, 32, 1998.

Aurela, M., Tuovinen, J.-P., and Laurila, T.: Net CO2 exchange of a subarctic mountain birch ecosystem, Theoretical and Applied Climatology, 70, 135–148, doi:10.1007/s007040170011, https://doi.org/10.1007/s007040170011, 2001.

Aurela, M., Riutta, T., Laurila, T., Tuovinen, J.-V., Vesala, T., Tuittila, E.-S., Jinne, J., Haapanala, S., and Laine, J.: CO2 exchange of a sedge fen in southern Finland—the impact of a drought period, Tellus B, 59, 826–837, doi:10.1111/j.1600-0889.2007.00309.x, http://dx.doi.org/10.1111/j.1600-0889.2007.00309.x, 2007.

Bellisario, L. M., Bubier, J. L., Moore, T. R., and Chanton, J. P.: Controls on CH4 emissions from a northern peatland, Global Biogeochemical Cycles, 13, 81–91, doi:10.1029/1998GB900021, http://dx.doi.org/10.1029/1998GB900021, 1999.

Bergman, I., Klarqvist, M., and Nilsson, M.: Seasonal variation in rates of methane production from peat of various botanical origins: effects of temperature and substrate quality, FEMS Microbiology Ecology, 33, 181–189, doi:10.1111/j.1574-6941.2000.tb00740.x, http://dx.doi.org/10.1111/j.1574-6941.2000.tb00740.x, 2000.

Bernard, J. M. and Hankinson, G.: Seasonal Changes in Standing Crop, Primary Production, and Nutrient Levels in a Carex rostrata Wetland, Oikos, 32, 328–336, http://www.jstor.org/stable/3544743, 1979.

Bohn, T. J., Melton, J. R., Ito, A., Kleinen, T., Spahni, R., Stocker, B. D., Zhang, B., Zhu, X., Schroeder, R., Glagolev, M. V., Maksyutov, S., Brovkin, V., Chen, G., Denisov, S. N., Eliseev, A. V., Gallego-Sala, A., McDonald, K. C., Rawlins, M. A., Riley, W. J., Subin, Z. M., Tian, H., Zhuang, Q., and Kaplan, J. O.: WETCHIMP-WSL: intercomparison of wetland methane emissions models over West Siberia, Biogeosciences, 12, 3321–3349, doi:10.5194/bg-12-3321-2015, https://www.biogeosciences.net/12/3321/2015/, 2015.

Chatfield, C.: The analysis of time series: an introduction, Chapman and Hall, 4th edn., 1989.

Ciais, P., Sabine, C., Bala, G., Bopp, L., Brovkin, V., Canadell, J., Chhabra, A., DeFries, R., Galloway, J., Heimann, M., Jones, C., LeQuere, C., Myneni, R., Piao, S., and Thornton, P.: Carbon and Other Biogeochemical Cycles, book section 6, p. 465–570, Cambridge University Press, Cambridge, United Kingdom and New York, NY, USA, doi:10.1017/CBO9781107415324.015, www.climatechange2013.org, 2013.

Cresto Aleina, F., Runkle, B. R. K., Brücher, T., Kleinen, T., and Brovkin, V.: Upscaling methane emission hotspots in boreal peatlands, Geoscientific Model Development, 9, 915–926, doi:10.5194/gmd-9-915-2016, http://www.geosci-model-dev.net/9/915/2016/, 2016.

Davidson, E. A., Janssens, I. A., and Luo, Y.: On the variability of respiration in terrestrial ecosystems: moving beyond Q10, Global Change Biology, 12, 154–164, doi:10.1111/j.1365-2486.2005.01065.x, http://dx.doi.org/10.1111/j.1365-2486.2005.01065.x, 2006.

Frolking, S., Talbot, J., Jones, M. C., Treat, C. C., Kauffman, J. B., Tuittila, E.-S., and Roulet, N.: Peatlands in the Earth's 21st century climate system, Environmental Reviews, 19, 371–396, doi:10.1139/a11-014, http://dx.doi.org/10.1139/a11-014, 2011.

Gedney, N., Cox, P. M., and Huntingford, C.: Climate feedback from wetland methane emissions, Geophysical Research Letters, 31, n/a–n/a, doi:10.1029/2004GL020919, http://dx.doi.org/10.1029/2004GL020919, l20503, 2004.

Gelman, A., Carlin, J., Stern, H., Dunson, D., Vehtari, A., and Rubin, D.: Bayesian Data Analysis, Chapman and Hall/CRC, 3rd edn., 2013.

Gifford, R. M.: The Global Carbon Cycle: a Viewpoint on the Missing Sink, Functional Plant Biology, 21, 1–15, http://dx.doi.org/10.1071/PP9940001, 1994.

Grant, R. F. and Roulet, N. T.: Methane efflux from boreal wetlands: Theory and testing of the ecosystem model Ecosys with chamber and tower flux measurements, Global Biogeochemical Cycles, 16, 2–1–2–16, doi:10.1029/2001GB001702, http://dx.doi.org/10.1029/2001GB001702, 1054, 2002.

Haario, H., Saksman, E., and Tamminen, J.: An Adaptive Metropolis Algorithm, Bernoulli, 7, 223–242, 2001.

Hakkarainen, J., Ilin, A., Solonen, A., Laine, M., Haario, H., Tamminen, J., Oja, E., and Järvinen, H.: On closure parameter estimation in chaotic systems, Nonlin. Processes Geophys., pp. 127–143, doi:10.5194/npg-19-127-2012, 2012.

Hararuk, O., Xia, J., and Luo, Y.: Evaluation and improvement of a global land model against soil carbon data using a Bayesian Markov chain Monte Carlo method, Journal of Geophysical Research: Biogeosciences, 119, 403–417, doi:10.1002/2013JG002535, http://dx.doi.org/10.1002/2013JG002535, 2013JG002535, 2014.

Hornibrook, E. R., Longstaffe, F. J., and Fyfe, W. S.: Spatial distribution of microbial methane production pathways in temperate zone wetland soils: Stable carbon and hydrogen isotope evidence, Geochimica et Cosmochimica Acta, 61, 745 – 753, doi:http://dx.doi.org/10.1016/S0016-7037(96)00368-7, http://www.sciencedirect.com/science/article/pii/S0016703796003687, 1997.

Iiyama, I. and Hasegawa, S.: Gas Diffusion Coefficient of Undisturbed Peat Soils, Soil Science and Plant Nutrition, 51, 431–435, doi:10.1111/j.1747-0765.2005.tb00049.x, http://dx.doi.org/10.1111/j.1747-0765.2005.tb00049.x, 2005.

IPCC: Summary for Policymakers, book section SPM, p. 1–30, Cambridge University Press, Cambridge, United Kingdom and New York, NY, USA, doi:10.1017/CBO9781107415324.004, www.climatechange2013.org, 2013.

Joabsson, A. and Christensen, T. R.: Methane emissions from wetlands and their relationship with vascular plants: an Arctic example, Global Change Biology, 7, 919–932, doi:10.1046/j.1354-1013.2001.00044.x, http://dx.doi.org/10.1046/j.1354-1013.2001.00044.x, 2001.

Juottonen, H.: Archaea, Bacteria, and methane production along environmental gradients in fens and bogs, Ph.D. thesis, University of Helsinki, 2008.

Kaiser, S., Beer, C., Göckede, M., Castro-Morales, K., Knoblauch, C., Ekici, A., Kleinen, T., Zubrzycki, S., Sachs, T., and Wille, C.: Process-based modelling of the methane balance in periglacial landscapes with JSBACH, Geoscientific Model Development Discussions, 2016, 1–47, doi:10.5194/gmd-2016-103, http://www.geosci-model-dev-discuss.net/gmd-2016-103/, 2016.

Kirschke, S., Bousquet, P., Ciais, P., Saunois, M., Canadell, J. G., Dlugokencky, E. J., Bergamaschi, P., Bergmann, D., Blake, D. R., Bruhwiler, L., Cameron-Smith, P., Castaldi, S., Chevallier, F., Feng, L., Fraser, A., Heimann, M., Hodson, E. L., Houweling, S., Josse, B., Fraser, P. J., Krummel, P. B., Lamarque, J. F., Langenfelds, R. L., Le Quere, C., Naik, V., O'Doherty, S., Palmer, P. I., Pison, I., Plummer, D., Poulter, B., Prinn, R. G., Rigby, M., Ringeval, B., Santini, M., Schmidt, M., Shindell, D. T., Simpson, I., Spahni, R., Steele, L. P., Strode, S. A., Sudo, K., Szopa, S., van der Werf, G. R., Voulgarakis, A., van Weele, M., Weiss, R. F., Williams, J. E., and Zeng, G.: Three decades of global methane sources and sinks, Nature Geoscience, 6, 813–823, doi:10.1038/ngeo1955, <GotoISI>://WOS:000325003700010, n/a, 2013.

Kullback, S. and Leibler, R. A.: On Information and Sufficiency, Ann. Math. Statist., 22, 79–86, doi:10.1214/aoms/1177729694, https://doi.org/10.1214/aoms/1177729694, 1951.

Lai, D.: Methane Dynamics in Northern Peatlands: A Review, Pedosphere, 19, 409 – 421, doi:http://dx.doi.org/10.1016/S1002-0160(09)00003-4, http://www.sciencedirect.com/science/article/pii/S1002016009000034, 2009a.

Lai, D. Y. F.: Modelling the effects of climate change on methane emission from a northern ombrotrophic bog in Canada, Environmental Geology, 58, 1197–1206, doi:10.1007/s00254-008-1613-5, http://dx.doi.org/10.1007/s00254-008-1613-5, 2009b.

Laine, M.: Adaptive MCMC methods with applications in environmental and geophysical models, Ph.D. thesis, Lappeenranta University of Technology, 2008.

Lehtonen, I., Ruosteenoja, K., and Jylhä, K.: Projected changes in European extreme precipitation indices on the basis of global and regional climate model ensembles, International Journal of Climatology, 34, 1208–1222, doi:10.1002/joc.3758, http://dx.doi.org/10.1002/joc.3758, 2014.

Mäkelä, J., Susiluoto, J., Markkanen, T., Aurela, M., Järvinen, H., Mammarella, I., Hagemann, S., and Aalto, T.: Constraining ecosystem model with adaptive Metropolis algorithm using boreal forest site eddy covariance measurements, Nonlinear Processes in Geophysics, 23, 447–465, doi:10.5194/npg-23-447-2016, http://www.nonlin-processes-geophys.net/23/447/2016/, 2016.

Mammarella, I., Peltola, O., Nordbo, A., Järvi, L., and Rannik, U.: Quantifying the uncertainty of eddy covariance fluxes due to the use of different software packages and combinations of processing steps in two contrasting ecosystems, Atmospheric Measurement Techniques, 9, 4915–4933, doi:10.5194/amt-9-4915-2016, http://www.atmos-meas-tech.net/9/4915/2016/, 2016.

Mastepanov, M., Sigsgaard, C., Tagesson, T., Ström, L., Tamstorf, M. P., Lund, M., and Christensen, T. R.: Revisiting factors controlling methane emissions from high-Arctic tundra, Biogeosciences, 10, 5139–5158, doi:10.5194/bg-10-5139-2013, https://www.biogeosciences.net/10/5139/2013/, 2013.

Melton, J. R., Wania, R., Hodson, E. L., Poulter, B., Ringeval, B., Spahni, R., Bohn, T., Avis, C. A., Beerling, D. J., Chen, G., Eliseev, A. V., Denisov, S. N., Hopcroft, P. O., Lettenmaier, D. P., Riley, W. J., Singarayer, J. S., Subin, Z. M., Tian, H., Zürcher, S., Brovkin, V., van Bodegom, P. M., Kleinen, T., Yu, Z. C., and Kaplan, J. O.: Present state of global wetland extent and wetland methane modelling: conclusions from a model inter-comparison project (WETCHIMP), Biogeosciences, 10, 753–788, doi:10.5194/bg-10-753-2013, https://www.biogeosciences.net/10/753/2013/, 2013.

Müller, J., Paudel, R., Shoemaker, C. A., Woodbury, J., Wang, Y., and Mahowald, N.: CH_4 parameter estimation in CLM4.5bgc using surrogate global optimization, Geoscientific Model Development, 8, 3285–3310, doi:10.5194/gmd-8-3285-2015, http://www.geosci-model-dev.net/8/3285/2015/, 2015.

Nedwell, D. B. and Watson, A.: CH4 production, oxidation and emission in a U.K. ombrotrophic peat bog: Influence of SO42- from acid rain, Soil Biology and Biochemistry, 27, 893 – 903, doi:http://dx.doi.org/10.1016/0038-0717(95)00018-A, http://www.sciencedirect.com/science/article/pii/003807179500018A, 1995.

Nelder, J. A. and Mead, R.: A Simplex Method for Function Minimization, The Computer Journal, 7, 308–313, doi:10.1093/comjnl/7.4.308, http://comjnl.oxfordjournals.org/content/7/4/308.abstract, 1965.

Nilsson, M. and Öquist, M.: Partitioning Litter Mass Loss into Carbon Dioxide and Methane in Peatland Ecosystems, pp. 131–144, American Geophysical Union, doi:10.1029/2008GM000819, http://dx.doi.org/10.1029/2008GM000819, 2013.

Petrescu, A. M. R., Lohila, A., Tuovinen, J.-P., Baldocchi, D. D., Desai, A. R., Roulet, N. T., Vesala, T., Dolman, A. J., Oechel, W. C., Marcolla, B., Friborg, T., Rinne, J., Matthes, J. H., Merbold, L., Meijide, A., Kiely, G., Sottocornola, M., Sachs, T., Zona, D., Varlagin, A., Lai, D. Y. F., Veenendaal, E., Parmentier, F.-J. W., Skiba, U., Lund, M., Hensen, A., van Huissteden, J., Flanagan, L. B., Shurpali, N. J., Grünwald, T., Humphreys, E. R., Jackowicz-Korczyński, M., Aurela, M. A., Laurila, T., Grüning, C., Corradi, C. A. R., Schrier-Uijl, A. P., Christensen, T. R., Tamstorf, M. P., Mastepanov, M., Martikainen, P. J., Verma, S. B., Bernhofer, C., and Cescatti, A.: The uncertain climate footprint of wetlands under human pressure, Proceedings of the National Academy of Sciences, 112, 4594–4599, doi:10.1073/pnas.1416267112, http://www.pnas.org/content/112/15/4594.abstract, 2015.

Powell, M. J. D.: The NEWUOA software for unconstrainedoptimization without derivatives, Tech. rep., 2004.

Powell, M. J. D.: The BOBYQA algorithm for bound constrained optimization without derivatives, Tech. rep., 2009.

Prather, M. J., Holmes, C. D., and Hsu, J.: Reactive greenhouse gas scenarios: Systematic exploration of uncertainties and the role of atmospheric chemistry, Geophysical Research Letters, 39, n/a–n/a, doi:10.1029/2012GL051440, http://dx.doi.org/10.1029/2012GL051440, l09803, 2012.

Raivonen, M., Mäkiranta, P., Lohila, A., Juutinen, S., Vesala, T., and Tuittila, E.-S.: A simple {CO2} exchange model simulates the seasonal leaf area development of peatland sedges, Ecological Modelling, 314, 32 – 43, doi:http://dx.doi.org/10.1016/j.ecolmodel.2015.07.008, http://www.sciencedirect.com/science/article/pii/S0304380015003142, 2015.

Raivonen, M., Smolander, S., Backman, L., Susiluoto, J., Aalto, T., Markkanen, T., Mäkelä, J., Rinne, J., Peltola, O., Aurela, M., Lohila, A., Tomasic, M., Li, X., Larmola, T., Juutinen, S., Tuittila, E.-S., Heimann, M., Sevanto, S., Kleinen, T., Brovkin, V., and Vesala, T.: HIMMELI v1.0: HelsinkI Model of MEthane buiLd-up and emIssion for peatlands, Geoscientific Model Development, 10, 4665–4691, doi:10.5194/gmd-10-4665-2017, https://www.geosci-model-dev.net/10/4665/2017/, 2017.

Rezanezhad, F., Price, J. S., Quinton, W. L., Lennartz, B., Milojevic, T., and Cappellen, P. V.: Structure of peat soils and implications for water storage, flow and solute transport: A review update for geochemists, Chemical Geology, 429, 75 – 84, doi:http://dx.doi.org/10.1016/j.chemgeo.2016.03.010, http://www.sciencedirect.com/science/article/pii/S0009254116301243, 2016.

Ricciuto, D. M., Davis, K. J., and Keller, K.: A Bayesian calibration of a simple carbon cycle model: The role of observations in estimating and reducing uncertainty, Global Biogeochemical Cycles, 22, n/a–n/a, doi:10.1029/2006GB002908, http://dx.doi.org/10.1029/2006GB002908, gB2030, 2008.

Richardson, A. D., Hollinger, D. Y., Burba, G. G., Davis, K. J., Flanagan, L. B., Katul, G. G., Munger, J. W., Ricciuto, D. M., Stoy, P. C., Suyker, A. E., Verma, S. B., and Wofsy, S. C.: A multi-site analysis of random error in tower-based measurements of carbon and energy fluxes, Agricultural and Forest Meteorology, 136, 1 – 18, doi:http://dx.doi.org/10.1016/j.agrformet.2006.01.007, http://www.sciencedirect.com/science/article/pii/S0168192306000281, 2006.

Riley, W. J., Subin, Z. M., Lawrence, D. M., Swenson, S. C., Torn, M. S., Meng, L., Mahowald, N. M., and Hess, P.: Barriers to predicting changes in global terrestrial methane fluxes: analyses using CLM4Me, a methane biogeochemistry model integrated in CESM, Biogeosciences, 8, 1925–1953, doi:10.5194/bg-8-1925-2011, http://www.biogeosciences.net/8/1925/2011/, 2011.

Rinne, J., Riutta, T., Pihlatie, M., Aurela, M., Haapanala, S., Tuovinen, J.-P., Tuittila, E.-S., and Vesala, T.: Annual cycle of methane emission from a boreal fen measured by the eddy covariance technique, Tellus B, 59, 449–457, doi:10.1111/j.1600-0889.2007.00261.x, http://dx.doi.org/10.1111/j.1600-0889.2007.00261.x, 2007.

Riutta, T., Laine, J., Aurela, M., Rinne, J., Vesala, T., Laurila, T., Haapanala, S., Pihlatie, M., and Tuittila, E.-S.: Spatial variation in plant community functions regulates carbon gas dynamics in a boreal fen ecosystem, Tellus B, 59, 838–852, doi:10.1111/j.1600-0889.2007.00302.x, http://dx.doi.org/10.1111/j.1600-0889.2007.00302.x, 2007a.

Riutta, T., Laine, J., and Tuittila, E.-S.: Sensitivity of CO2 Exchange of Fen Ecosystem Components to Water Level Variation, Ecosystems, 10, 718–733, doi:10.1007/s10021-007-9046-7, http://dx.doi.org/10.1007/s10021-007-9046-7, 2007b.

Roberts, G. O., Gelman, A., and Gilks, W. R.: Weak convergence and optimal scaling of random walk Metropolis algorithms, Ann. Appl. Probab., 7, 110–120, doi:10.1214/aoap/1034625254, http://dx.doi.org/10.1214/aoap/1034625254, 1997.

Ruosteenoja, K., Jylhä, K., and Kämäräinen, M.: Climate Projections for Finland Under the RCP Forcing Scenarios, Geophysica, 51, 17–50, 2016.

Saarinen, T.: Biomass and production of two vascular plants in a boreal mesotrophic fen, Canadian Journal of Botany, 74, 934–938, doi:10.1139/b96-116, http://dx.doi.org/10.1139/b96-116, 1996.

Saarinen, T.: Demography of Carex rostrata in boreal mesotrophic fen: shoot dynamics and biomass development, Ann. Bot. Fennici, pp. 203–209, 1998.

Sanso, B., Forest, C., and Zantedeschi, D.: Inferring Climate System Properties Using a Computer Model, Tech. rep., 2007.

Saunois, M., Bousquet, P., Poulter, B., Peregon, A., Ciais, P., Canadell, J. G., Dlugokencky, E. J., Etiope, G., Bastviken, D., Houweling, S., Janssens-Maenhout, G., Tubiello, F. N., Castaldi, S., Jackson, R. B., Alexe, M., Arora, V. K., Beerling, D. J., Bergamaschi, P., Blake, D. R., Brailsford, G., Brovkin, V., Bruhwiler, L., Crevoisier, C., Crill, P., Covey, K., Curry, C., Frankenberg, C., Gedney, N., Höglund-Isaksson, L., Ishizawa, M., Ito, A., Joos, F., Kim, H.-S., Kleinen, T., Krummel, P., Lamarque, J.-F., Langenfelds, R., Locatelli, R., Machida, T., Maksyutov, S., McDonald, K. C., Marshall, J., Melton, J. R., Morino, I., Naik, V., O'Doherty, S., Parmentier, F.-J. W., Patra, P. K., Peng, C., Peng, S., Peters, G. P., Pison, I., Prigent, C., Prinn, R., Ramonet, M., Riley, W. J., Saito, M., Santini, M., Schroeder, R., Simpson, I. J., Spahni, R., Steele, P., Takizawa, A., Thornton, B. F., Tian, H., Tohjima, Y., Viovy, N., Voulgarakis, A., van Weele, M., van der Werf, G. R., Weiss, R., Wiedinmyer, C., Wilton, D. J., Wiltshire, A., Worthy, D., Wunch, D., Xu, X., Yoshida, Y., Zhang, B., Zhang, Z., and Zhu, Q.: The global methane budget 2000–2012, Earth System Science Data, 8, 697–751, doi:10.5194/essd-8-697-2016, http://www.earth-syst-sci-data.net/8/697/2016/, 2016.

Schuldt, R. J., Brovkin, V., Kleinen, T., and Winderlich, J.: Modelling Holocene carbon accumulation and methane emissions of boreal wetlands – an Earth system model approach, Biogeosciences, p. 1659–1674, 2013.

Segers, R.: Methane production and methane consumption: a review of processes underlying wetland methane fluxes, Biogeochemistry, 41, 23–51, doi:10.1023/A:1005929032764, http://dx.doi.org/10.1023/A:1005929032764, 1998.

Sriskantharajah, S., Fisher, R. E., Lowry, D., Aalto, T., Hatakka, J., Aurela, M., Laurila, T., Lohila, A., Kuitunen, E., and Nisbet, E. G.: Stable carbon isotope signatures of methane from a Finnish subarctic wetland, Tellus B: Chemical and Physical Meteorology, 64, 18 818, doi:10.3402/tellusb.v64i0.18818, https://doi.org/10.3402/tellusb.v64i0.18818, 2012.

Stephen, K., Arah, J., Thomas, K., Benstead, J., and Lloyd, D.: Gas diffusion coefficient profile in peat determined by modelling mass spectrometric data: implications for gas phase distribution, Soil Biology and Biochemistry, 30, 429 – 431, doi:http://dx.doi.org/10.1016/S0038-0717(97)00118-1, http://www.sciencedirect.com/science/article/pii/S0038071797001181, 1998.

Szafranek-Nakonieczna, A. and Stepniewska, Z.: Aerobic and anaerobic respiration in profiles of Polesie Lubelskie peatlands, International Agrophysics, 28, 219–229, doi:doi: 10.2478/intag-2014-0011, 2014.

Tang, J., Zhuang, Q., Shannon, R. D., and White, J. R.: Quantifying wetland methane emissions with process-based models of different complexities, Biogeosciences, 7, 3817–3837, doi:10.5194/bg-7-3817-2010, http://www.biogeosciences.net/7/3817/2010/, 2010.

van Huissteden, J., Petrescu, A. M. R., Hendriks, D. M. D., and Rebel, K. T.: Sensitivity analysis of a wetland methane emission model based on temperate and arctic wetland sites, Biogeosciences, 6, 3035–3051, doi:10.5194/bg-6-3035-2009, http://www.biogeosciences.net/6/3035/2009/, 2009.

Vile, D., Garnier, E., Shipley, B., Laurent, G., Navas, M.-L., Roumet, C., Lavorel, S., Díaz, S., Hodgson, J. G., Lloret, F., Midgley, G. F., Poorter, H., Rutherford, M. c., Wilson, P. J., and Wright, I. J.: Specific Leaf Area and Dry Matter Content Estimate Thickness in Laminar Leaves, Annals of Botany, 96, 1129, doi:10.1093/aob/mci264, +http://dx.doi.org/10.1093/aob/mci264, 2005.

Walker, T. S., Bais, H. P., Grotewold, E., and Vivanco, J. M.: Root Exudation and Rhizosphere Biology, Plant Physiology, 132, 44–51, doi:10.1104/pp.102.019661, http://www.plantphysiol.org/content/132/1/44.short, 2003.

Walter, B. P. and Heimann, M.: A process-based, climate-sensitive model to derive methane emissions from natural wetlands: Application to five wetland sites, sensitivity to model parameters, and climate, Global Biogeochemical Cycles, 14, 745–765, doi:10.1029/1999GB001204, http://dx.doi.org/10.1029/1999GB001204, 2000.

Wania, R.: Modelling northern peatland land surface processes, vegetation dynamics and methane emissions, Ph.D. thesis, University of Bristol, 2007.

Wania, R., Ross, I., and Prentice, I. C.: Implementation and evaluation of a new methane model within a dynamic global vegetation model: LPJ-WHyMe v1.3.1, Geoscientific Model Development, 3, 565–584, 2010.

Watson, A., Stephen, K. D., Nedwell, D. B., and Arah, J. R.: Oxidation of Methane in Peat: Kinetics of CH4 and O2 Removal and the Role of Plant Roots, Soil Biol. Biochem., 29, 1997.

Whiting, G. J. and Chanton, J. P.: Primary production control of methane emission from wetlands, Nature, 364, 794–795, doi:10.1038/364794a0, http://dx.doi.org/10.1038/364794a0, 1993.

Wilson, D., Alm, J., Riutta, T., Laine, J., Byrne, K. A., Farrell, E. P., and Tuittila, E.-S.: A high resolution green area index for modelling the seasonal dynamics of CO2 exchange in peatland vascular plant communities, Plant Ecology, 190, 37–51, doi:10.1007/s11258-006-9189-1, http://dx.doi.org/10.1007/s11258-006-9189-1, 2007.

Zhu, Q., Liu, J., Peng, C., Chen, H., Fang, X., Jiang, H., Yang, G., Zhu, D., Wang, W., and Zhou, X.: Modelling methane emissions from natural wetlands by development and application of the TRIPLEX-GHG model, Geoscientific Model Development, 7, 981–999, doi:10.5194/gmd-7-981-2014, http://www.geosci-model-dev.net/7/981/2014/, 2014.

Table 1. Description of the data used

Data	Description	Usage	Units	Source	Comments
LAI	leaf area index	input	-	modeled	Gaussian curve to approximate the seasonal cycle
WTD	water table depth	input	m	measured	gap-filled at various times
NPP	net primary prod.	input	mol m^{-2} s^{-1}	modeled	generated by a separate NPP model
~~T_{soil}~~ T_{soil}	soil temperature	input	°C	measured	interpolated from fewer observation depths
CH_4	CH_4 flux	objective function	mol m^{-2} s^{-1}	measured	used in the objective function formulation
CO_2	CO_2 flux	objective function	mol m^{-2} s^{-1}	measured	used in the objective function formulation

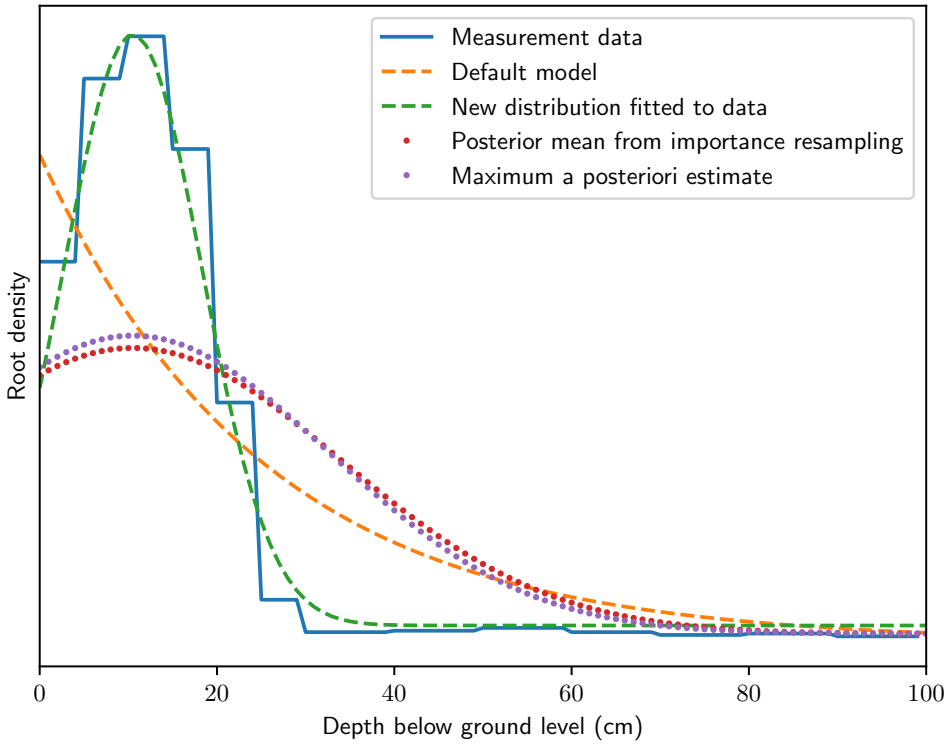

Figure 1. The different root distribution descriptions. The original description is shown as the decaying exponential, and the graph with discrete steps shows measurement data from Saarinen (1996). The new root distribution curve with optimized parameters are shown along with the curves resulting from the MCMC optimization. The original distribution gives more root mass to depths of 50-80cm, than the MCMC-optimized curves of the new root distribution. All curves are normalized to the same total root mass.

Table 2. Parameters that were not calibrated. Based on an initial sensitivity analysis, the Michaelis-Menten parameters K were not constrained by the data enough strongly and consistently to include them in the optimization. The same applies for the ebullition half-life, which is understandable given the temporal resolution of the observed data. The peat porosity was dropped from optimization in favor of the diffusivity parameters $f_{D,w}$ and $f_{D,a}$, and the specific leaf area was not chosen for optimization since the optimized parameters τ (m m^{-1}) and ρ (m^2 kg^{-1}) are already part of the equation 22 where SLA appears. The parameter $g_{CH_4}^{Q_{10}}$ was left out in favor of parameter τ_{cato}, despite their functions regarding CO_2 being different, but trusting the prior value.

Parameter	Equation	Value	Units	Description	Source
$g_{CH_4}^{Q_{10}}$	16	0.4	-	peat decay to CH_4 fraction	Schuldt et al. (2013)
K_R	19	0.022	mol m^{-3}	Michaelis-Menten coeff.	Nedwell and Watson (1995)
K_{CH_4}	20	0.044	mol m^{-3}	Michaelis-Menten coeff.	Nedwell and Watson (1995)
K_{O_2}	20	0.033	mol m^{-3}	Michaelis-Menten coeff.	Nedwell and Watson (1995)
SLA	22	23	$m^2 kg^{-1}$	specific leaf area	Vile et al. (2005)
k	23	$\log(2)/1800$	s^{-1}	ebullition rate constant	-
σ	23	0.5	-	peat porosity	Rezanezhad et al. (2016)

	Low	High	Units	Prior μ	Prior σ	Source
$f_{D,a}$	0.01	1.0	-	~~0.1~~ 0.8	0.2	~~(Iiyama and Hasegawa, 20~~
$f_{D,w}$	~~0.1~~ 0.01	1.0	-	~~(0.5)~~ 0.8	~~-~~ 0.2	~~-~~ (Raivonen et al., 2017)
V_{R0}	~~2×10^{-5}~~ 2×10^{-6}	~~3×10^{-4}~~ 1×10^{-4}	mol m^{-3} s^{-1}	~~4×10^{-5}~~ 1×10^{-5}	2×10^{-5}	(Nedwell and Watson, 199
V_{O0}	~~2×10^{-5}~~ 2×10^{-6}	3×10^{-4}	mol m^{-3} s^{-1}	~~1×10^{-4}~~ 1×10^{-5}	~~6×10^{-4}~~ 2×10^{-5}	~~Order of magnitude from (~~
λ_{root}	0.01	0.4	m	0.125	0.05	Fitted to data in (Saarinen,
τ	1.0	5.0	m m^{-1}	1.5	~~0.5~~ 0.2	(Stephen et al., 1998)
ρ	0.05	0.4	m^2 kg^{-1}	0.085	0.0425	(Stephen et al., 1998)
τ_{exu}	3	30	days	14	2.5	(Wania, 2007)
~~τ_{cato}~~ τ_{cato}	1000	30000	years	~~(11111)~~ -	-	~~Value affected by peat dep~~
ΔE_R	5000	200000	J mol^{-1}	50000	5000	(Nedwell and Watson, 199
ΔE_{oxid}	5000	200000	J mol^{-1}	50000	5000	(Nedwell and Watson, 199
$f_{CH_4}^{\text{exu}}$	0.5	0.77	-	0.635	0.06	(Nilsson and Öquist, 2013)
Q_{10}	1.7	16.0	-	5.9	~~2.0~~ 0.5*	(Juottonen, 2008; Gedney
ζ_{exu}	0.01	0.99	-	~~0.2~~ 0.5	0.2*	~~Lower bound of~~ (Walker et

Table 3. Parameter limits and prior distribution parameters. The priors are truncated Gaussian, with mean values μ and standard deviations σ, truncated at the values in the columns *low* and *high*. ~~The~~ *For importance resampling, the hierarchical modeled parameters' (Q_{10} (-) and ζ_{exu} (-)) priors were relaxed by a factor of three, to allow for a more data-constrained resampling, and to accommodate the low values ~~in~~ of Q_{10} reported by Szafranek-Nakonieczna and Stepniewska (2014). Note that the ~~"Prior μ" column are used as~~ values ~~in~~ of the ~~"default" simulations, results from which are shown in e.g. Fig. 10 and 7~~prior for these two parameters were sampled at each iteration with Gibbs sampling.

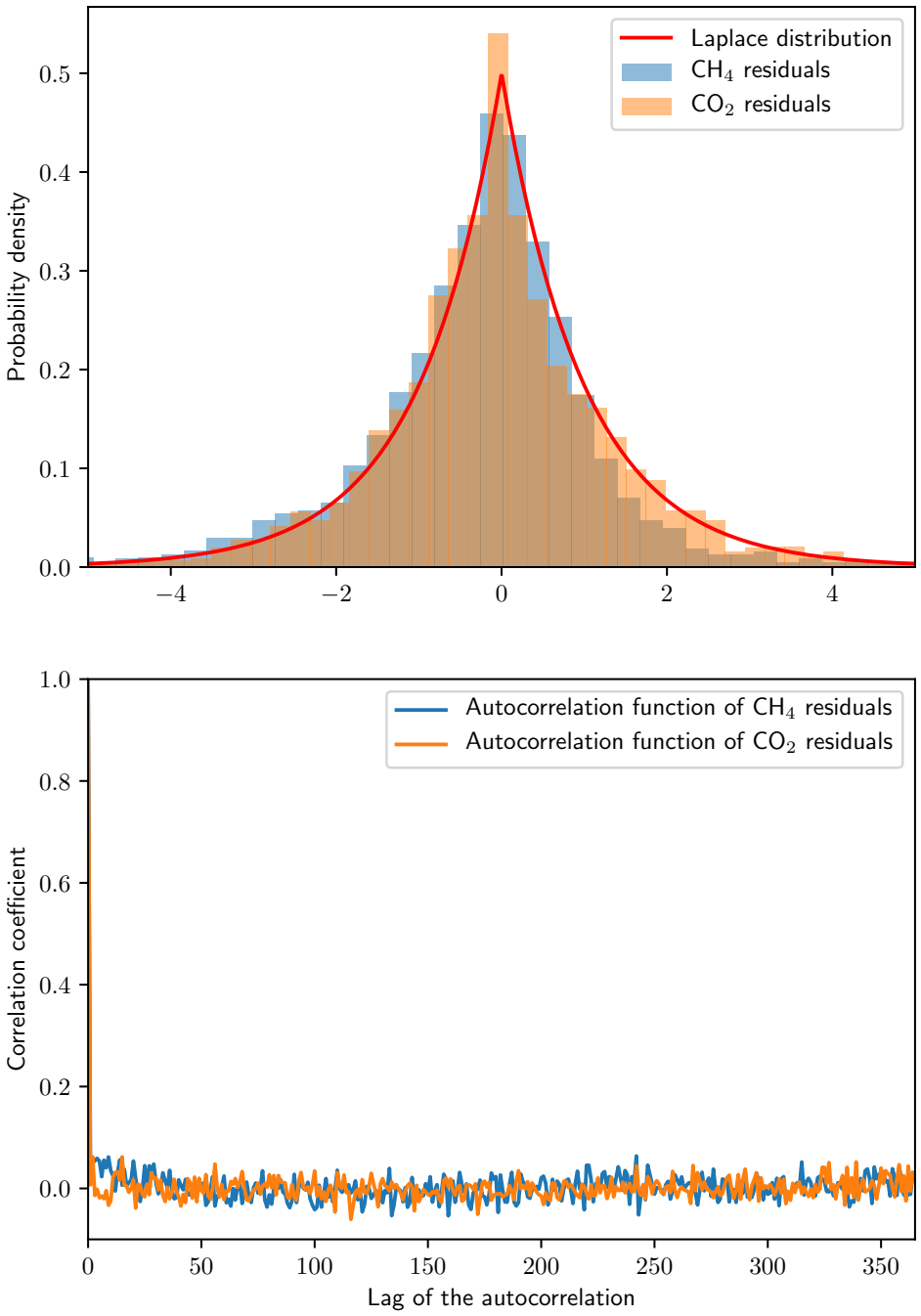

Figure 2. Residual histograms and autocorrelation functions of the error terms ϵ_t in the objective function, Eq. 24, show that neither the CO_2 nor the CH_4 residuals are autocorrelated and that they closely follow the Laplace-distribution. The results shown are for the residuals from the posterior mean estimate.

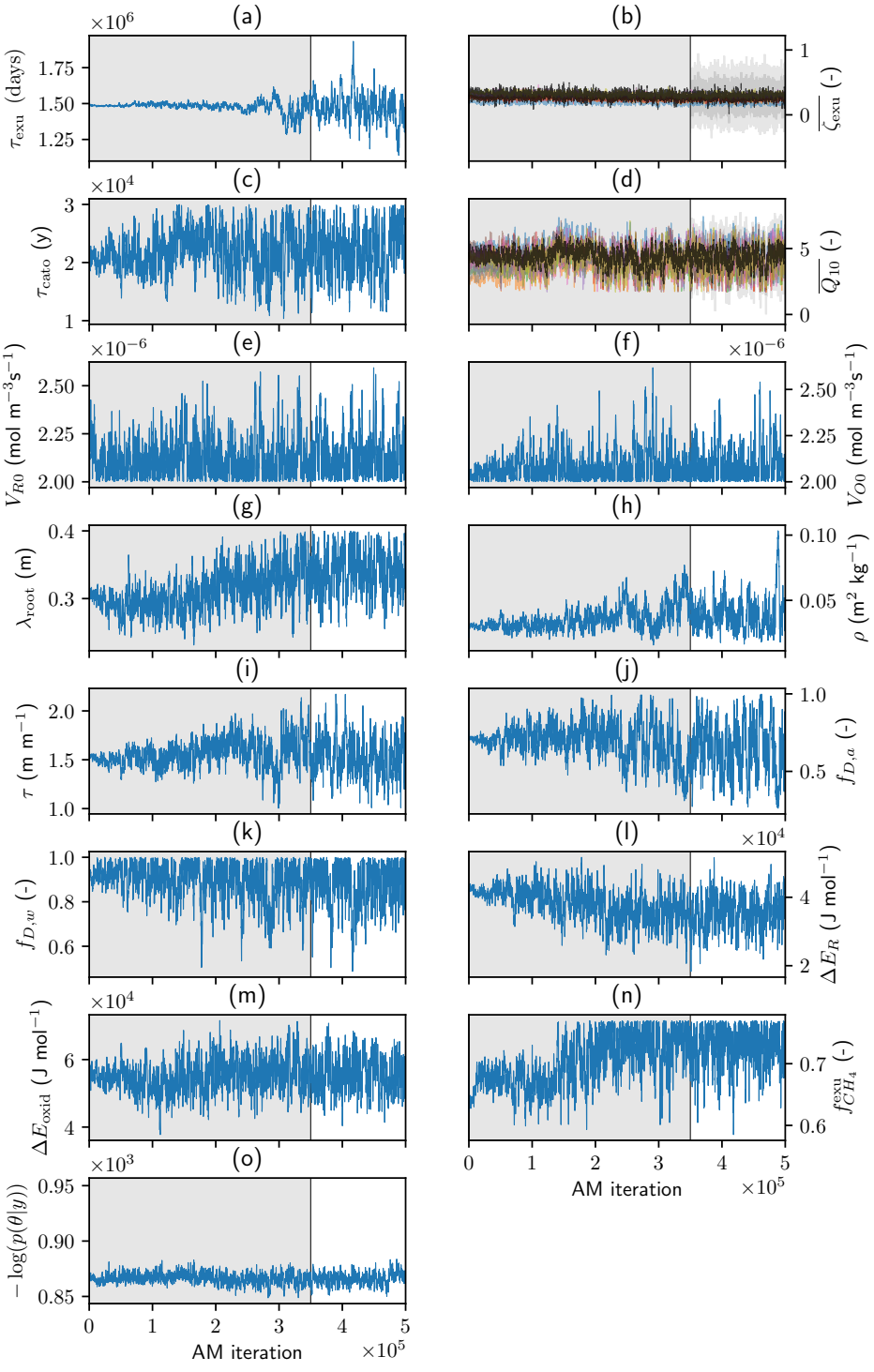

Figure 3. MCMC chains showing a thinned sample of the half million values in the chain. The first 70% was discarded for the analyses as warm-up and is grayed out in the figures. The hierarchical parameters in (b) and (d) show the mean value in the middle as a black mass, and the colorful surroundings are the values of the parameters for the individual years. The last figure (o) shows the value of the objective function.

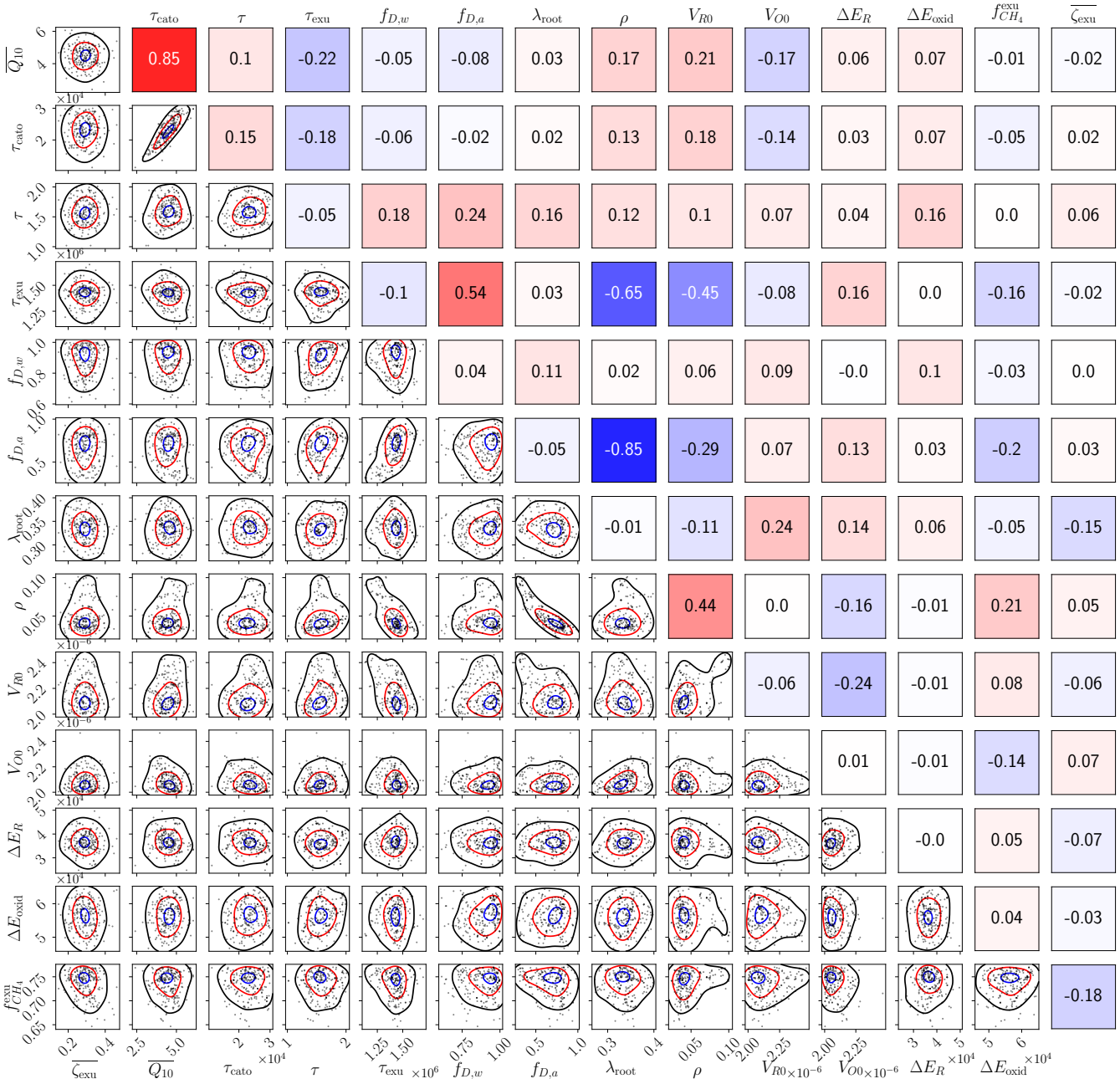

Figure 4. Posterior distributions of the parameters from the ~~MCMC~~importance sampling. The two-dimensional marginal distributions of the posterior distribution ~~from the experiment with 70 cm peat depth are~~ is shown in the triangle on the lower left (labels on the left and at the bottom), and the correlations between parameters are shown in the upper triangle on the right (labels on the left and ~~on~~ at the top). The images in the lower left triangle show the 90% (black) 50% (red), and 10% (blue) contours, and ~~roughly~~ a ~~one-thousandth of the~~ points ~~sampled. The first 50% of each chain was discarded as~~ from a ~~warm-up period~~random sample of the posterior (black dots). On the upper right, each plot shows correlation coefficients between parameters~~for all experiments~~, color-coded to show negative correlations in blue and positive in red. ~~Left-to-right and top to bottom in each color-coded square, the depths are 40, 50, 70, 100, 150, and 200 cm of peat.~~ The ~~values from the posterior of the 7-layer experiment, referring to 70 cm peat and shown also in the lower left part of the figure,~~ units are ~~marked~~ listed in ~~boldface~~Table 4.

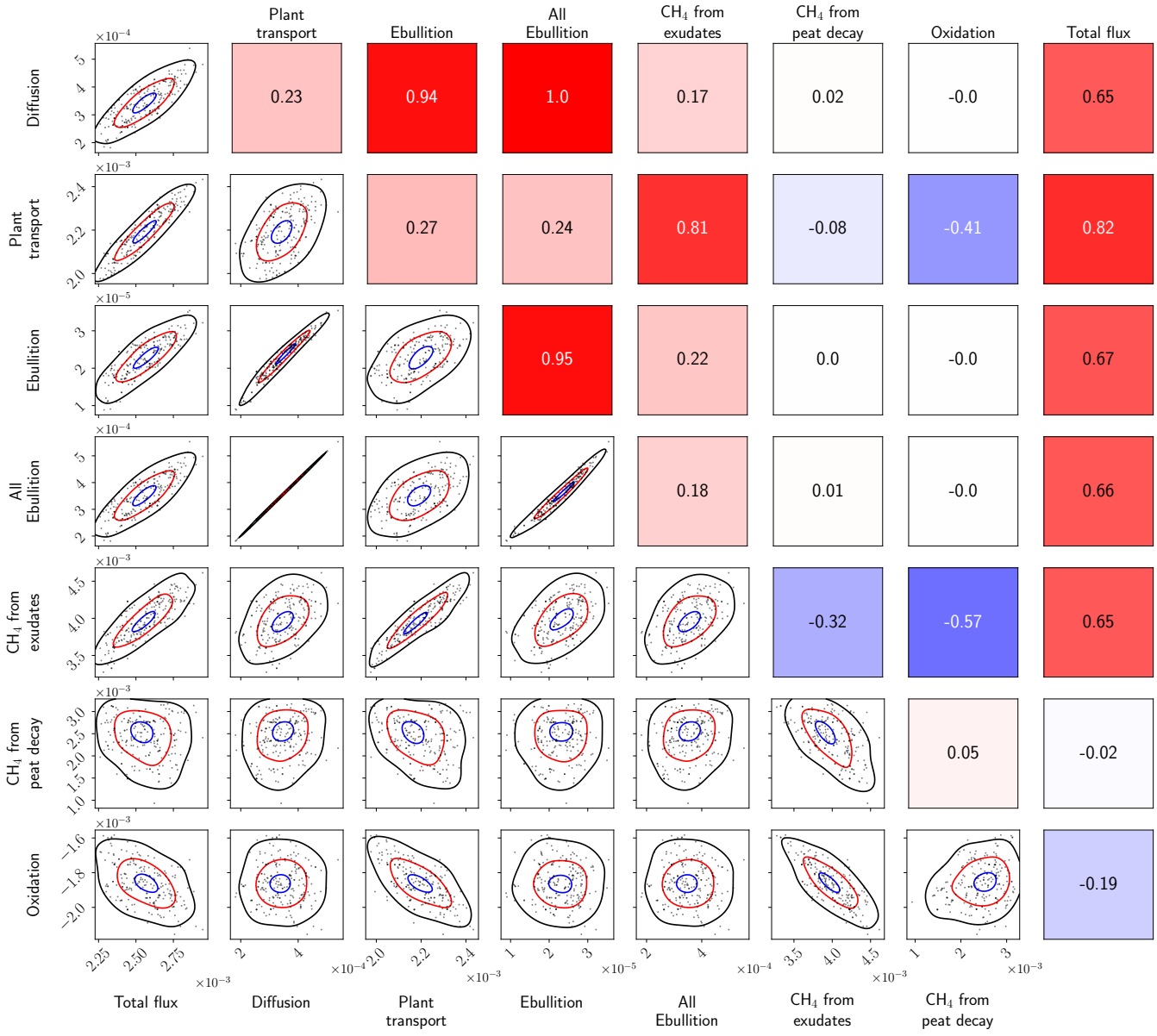

Figure 5. Posterior distributions and correlations of the annual means of the output from the modeled processes for the year 2012. The dynamics for the other years are mostly similar but the strengths of the correlations vary somewhat. The results shown are based on 1000 random samples from the parameter posterior distribution. The two-dimensional marginal distributions in the triangle on the lower left have their labels on the left and at the bottom, and the correlations between the processes in the upper triangle on the right have their labels on the left and on the top. The images in the lower left triangle show the 90% (black) 50% (red), and 10% (blue) contours. The all ebullition and diffusion fluxes correlate almost fully showing that the "diffusion"-flux has a strong contribution from underground ebullition.

Table 4. Parameter values obtained in the optimization of the ~~models~~ sqHIMMELI model with ~~the different peat depths~~importance resampling. ~~Values shown are for the~~ The maximum a ~~posteriori (MAP) /~~ posterior, posterior mean, non-hierarchical mean (~~PM~~mean values used for hierarchically varying parameters)~~estimates~~, and values from Raivonen et al. (2017) are shown. The horizontal line in the middle separates the hierarchically optimized parameters (including their priors) from the others.

~~Peat depth 40 cm 50 cm~~ Parameter	~~70 cm~~ MAP	~~100 cm~~ Posterior mean	~~150 cm~~ Nor
~~$\tau_{\mathrm{cato}} \times 10^{-3}$~~ ($\tau_{\mathrm{cato}}$ ($\times 10^4$ y)	~~2.35 / 3.02 3.02 / 4.00 5.10 / 6.04~~ 2.872	~~9.12 / 10.1~~ 2.269	~~15.9 / 15~~
τ (m m^{-1})	~~1.29 / 1.31 1.13 / 1.28 1.18 / 1.19~~ 1.462	~~1.05 / 1.14~~ 1.581	~~1.01 / 1.~~
~~$\tau_{\mathrm{exu}} \times 10^{-5}$ (s) 11.6 / 10.8 9.86 / 9.73~~ τ_{exu} ($\times 10^6$ s)	~~8.67 / 8.83~~ 1.187	~~9.47 / 8.75~~ 1.411	~~8.56 / 8.~~
$f_{D,w}$ (-)	~~0.78 / 0.55 0.55 / 0.56 0.65 / 0.64~~ 0.866	~~0.74 / 0.81~~ 0.887	~~0.99 / 0.~~
$f_{D,a}$ (-)	~~0.58 / 0.50 0.55 / 0.54 0.52 / 0.54~~ 0.427	~~0.72 /~~ 0.65	~~0.86 / 0.~~
λ_{root} (m)	~~0.30 / 0.30 0.28 / 0.29 0.33 / 0.32~~ 0.314	~~0.34 / 0.35~~ 0.333	~~0.21 / 0.~~
ρ (m^2 kg^{-1})	~~0.14 / 0.15~~ 0.081	~~0.15 / 0.15~~ 0.049	~~0.15 / 0.~~
V_{R0} ($\times 10^{-6}$ mol m^{-3} s^{-1})	~~0.23 / 0.24~~ 2.366	~~0.24 / 0.22~~ 2.153	2.1
~~$V_{R0} \times 10^5$~~ V_{O0} ($\times 10^{-6}$ mol m^{-3} s^{-1})	~~2.86 / 3.92~~ 2.013	~~2.15 / 3.63~~ 2.09	~~3.97 / 3.~~
ΔE_R ($\times 10^4$ J mol^{-1})	~~2.86 / 3.31~~ 3.478	~~2.52 / 4.43~~ 3.647	3.6
~~$V_{O0} \times 10^4$~~ ΔE_{oxid} ($\times 10^4$ J mol^{-1})	~~2.87 / 1.31~~ 5.358	~~1.63 / 1.50~~ 5.575	~~2.95 / 1.~~
$f^{\mathrm{exu}}_{CH_4}$ (-)	~~0.866 / 1.06~~ 0.729	~~0.233 / 1.51~~ 0.736	0.7
$\overline{\zeta_{\mathrm{exu}}}$ (-)	~~0.49 / 0.38 0.38 / 0.31 0.34 / 0.28~~ 0.343	~~0.31 / 0.26~~ 0.292	~~0.38 /~~
$\zeta^{\mathrm{std}}_{\mathrm{exu}}$ (-)	~~0.15 / 0.18 0.12 / 0.17 0.13 / 0.17~~ 0.128	~~0.15 / 0.18~~ 0.157	~~0.26 /~~
$\overline{Q_{10}}$ (-)	~~1.85 / 3.80 3.59 / 4.58 3.81 / 4.85~~ 5.721	~~4.22 / 5.15~~ 4.425	~~5.22 /~~
Q^{std}_{10} (-)	~~1.55 / 1.70 1.88 / 1.74 1.35 / 1.73~~ 0.587	~~1.11 / 1.70~~ 0.616	~~1.26 /~~
$\zeta^{2006}_{\mathrm{exu}}$ (-)	~~0.53 / 0.34 0.40 / 0.28 0.25 / 0.24~~ 0.212	~~0.23 / 0.17~~ 0.182	~~0.30 / 0.~~
$\zeta^{2007}_{\mathrm{exu}}$ (-)	~~0.44 / 0.24 0.17 / 0.18 0.13 / 0.13~~ 0.251	~~0.10 / 0.10~~ 0.244	~~0.09 / 0.~~
$\zeta^{2008}_{\mathrm{exu}}$ ~~0.48 / 0.35 0.40 / 0.31 0.37 / 0.27~~ (-)	0.28 ~~/ 0.25~~	~~0.33 / 0.31~~ 0.276	~~0.19 / 0.~~
$\zeta^{2009}_{\mathrm{exu}}$ (-)	~~0.51 / 0.42 0.52 / 0.30 0.29 / 0.31~~ 0.202	~~0.37 / 0.29~~ 0.243	~~0.34 / 0.~~
$\zeta^{2010}_{\mathrm{exu}}$ (-)	~~0.65 / 0.50 0.52 / 0.37 0.35 / 0.35~~ 0.34	~~0.48 / 0.33~~ 0.314	~~0.32 / 0.~~
$\zeta^{2011}_{\mathrm{exu}}$ (-)	~~0.55 / 0.45 0.52 / 0.37 0.31 / 0.31~~ 0.251	~~0.27 / 0.25~~ 0.258	~~0.18 / 0.~~
$\zeta^{2012}_{\mathrm{exu}}$ (-)	~~0.50 / 0.37 0.42 / 0.32 0.39 / 0.34~~ 0.327	~~0.32 / 0.30~~ 0.324	~~0.33 / 0.~~
$\zeta^{2013}_{\mathrm{exu}}$ (-)	~~0.59 / 0.51 0.59 / 0.42 0.45 / 0.38~~ 0.368	~~0.55 / 0.44~~ 0.313	~~0.54 / 0.~~
$\zeta^{2014}_{\mathrm{exu}}$ (-)	~~0.43 / 0.39 0.59 / 0.30 0.29 / 0.30~~ 0.334	~~0.32 / 0.26~~ 0.323	~~0.40 / 0.~~
Q^{2006}_{10} (-)	~~1.87 / 2.88 2.42 / 3.50 3.19 / 3.90~~ 5.946	~~3.95 / 4.57~~ 4.488	~~4.18 / 3.~~
Q^{2007}_{10} (-)	~~2.33 / 3.96 4.02 / 4.28 4.11 / 4.38~~ 4.882	~~4.67 / 4.74~~ 3.857	~~5.25 / 4.~~
Q^{2008}_{10} (-)	~~2.29 / 3.24 2.96 / 3.67 3.09 / 4.14~~ 4.017	~~3.97 / 4.23~~ 3.684	~~3.57 / 3.~~
Q^{2009}_{10} (-)	~~2.82 / 3.77 2.81 / 5.02 4.27 / 4.89~~ 5.469	~~4.31 / 5.02~~ 4.14	~~4.98 / 4.~~
Q^{2010}_{10} (-)	~~2.29 / 3.34 3.38 / 4.64 4.49 / 4.86~~ 5.337	~~4.11 / 5.16~~ 4.284	~~5.99 / 5.~~
Q^{2011}_{10} (-)	~~2.58 / 3.41 2.90 / 4.26 4.37 / 4.71~~ 6.306	~~4.92 / 5.49~~ 4.305	~~6.73 / 6.~~
Q^{2012}_{10} (-)	~~2.89 / 3.53 3.34 / 4.15 3.82 / 4.40~~ 5.377	~~4.65 / 5.00~~ 4.193	~~5.96 / 4.~~
Q^{2013}_{10} (-)	~~4.43 / 4.82 3.76 / 5.72 5.05 / 6.30~~ 5.219	~~4.17 / 5.72~~ 4.211	~~5.71 / 5.~~
Q^{2014}_{10} (-)	~~3.46 / 3.76 2.56 / 4.96 4.99 / 5.29~~ 6.438	~~4.82 / 5.93~~ 4.332	~~5.24 / 4.~~
Costfunction value	~~294.85 / - 274.37 / -~~ 1205.22	~~258.93 / -~~ 1227.01	~~261.~~
~~Model simulations 391000 340000 277000 171000 92000 78000~~			

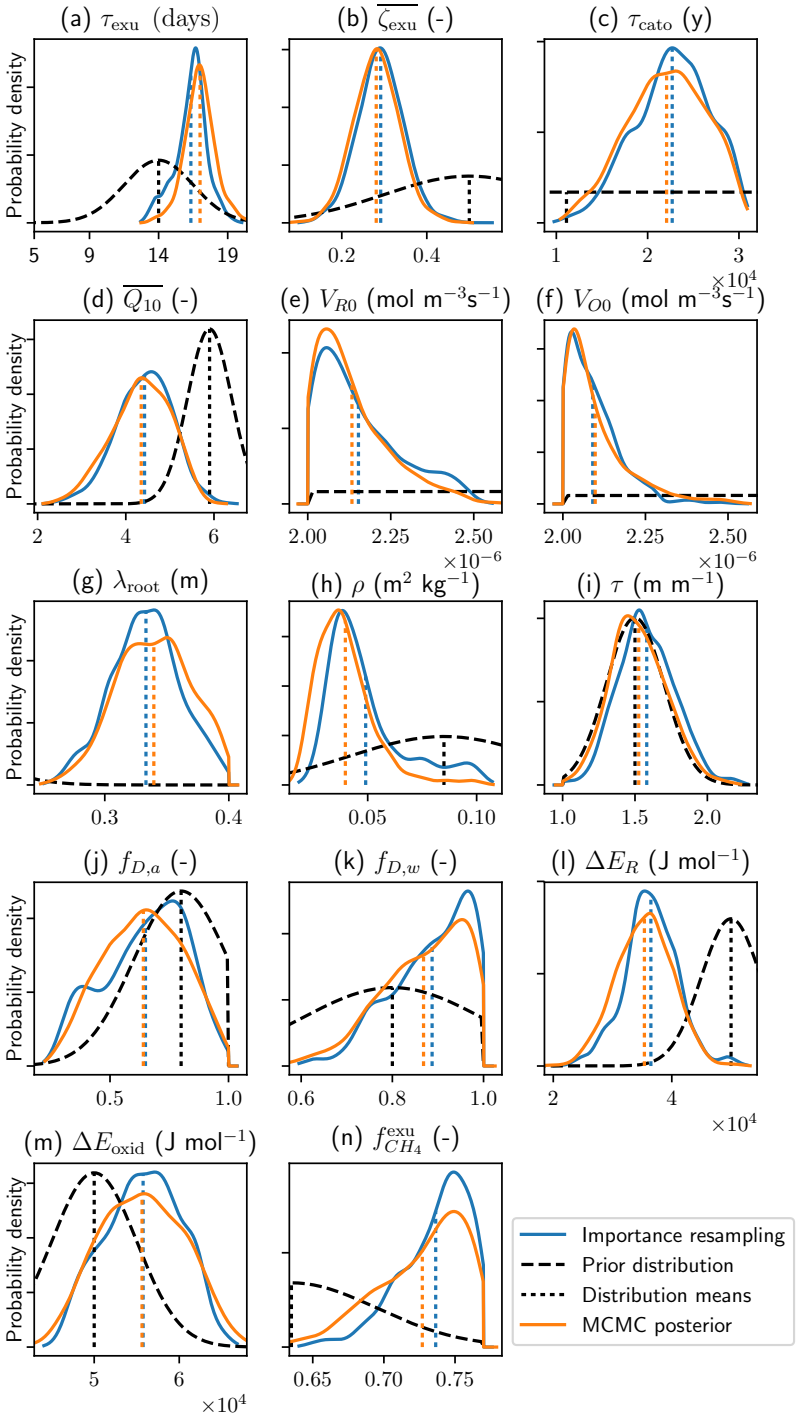

Figure 6. Posterior marginal and prior distributions ~~for all~~ from MCMC ~~experiments~~ and importance resampling for all parameters: (a-d) and (n) are the production-related, (e-f) and (l-m) the respiration and oxidation related, and (g-k) the gas transport related parameters. The blue and orange curves shown ~~for the MCMC experiments~~ are smoothed slightly using Gaussian kernel estimates for readability. To make these figures, ~~50~~70% from the start of ~~each~~ the MCMC chain was discarded as warm-up (orange line). The dotted vertical lines show the ~~default parameter~~ prior mean values and the sample means from both MCMC and importance sampling. For the parameters $\overline{\zeta_{\text{exu}}}$ (b) and $\overline{Q_{10}}$ (d), the prior distribution drawn is the hyperprior.

~~Annual CH_4 production in g m^{-2} from root exudates (colored part) and peat decomposition (white part). Oxidized CH_4 is shown as gray and negative. (a) shows MAP estimate, (b) the posterior mean, (c) the non-hierarchical posterior mean estimate, and (d) the results with the default parameter values.~~

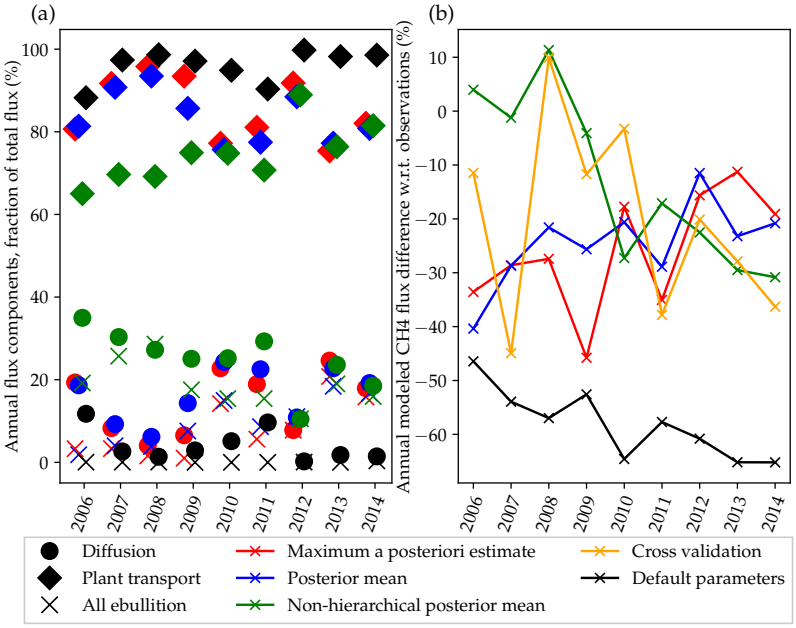

Figure 7. On the left side~~(a-d)~~: proportions of flux components as a function of the year. Diamonds are for plant transport, ~~dots are~~ balls for the diffusion flux, and crosses describe the total ebullition taking place. The ~~figures~~ figure on the right ~~(e-h) show~~ shows the annual model-observation mismatch in percents for the methane flux, where only residuals from days with observation data available have been taken into account. The ~~x-axes of sub-figures~~ data in sub-figure (~~a-~~da) ~~have~~ has been spread slightly for readability in the x-axis direction. The ~~dashed lines~~ orange line in sub-figure (~~g~~b) represent the results from the cross validation discussed in Sec. 5.6. Note that the optimization target was not to directly fit annual emissions.

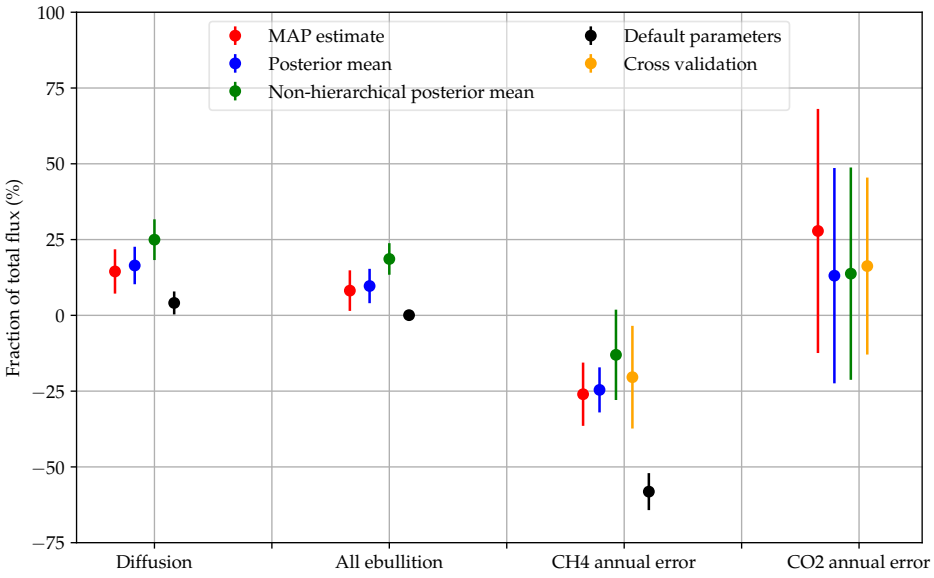

Figure 8. ~~(a)~~ Fractions of the annual diffusive fluxes of the total fluxes. Means and 1-σ error bars are shown. Almost all ebullition takes place when the water table is below the peat surface and hence it is emitted to the atmosphere as part of the diffusion flux. Plant transport is not shown, as it is very close to the complement of the diffusive flux: together these two streams add up to more than 98% of the total flux. Plant transport variation is very close to that of diffusion. ~~Part (b) shows~~ On the right side of the figure the average annual errors ~~with similar 1-σ errorbars~~ are shown for the interannual variation of the fluxes. The results of the cross validation of the regression modeling of the hierarchically varying parameters, discussed in Sec. 5.6, are drawn in orange. The "Default" parameters produce carbon dioxide fluxes that are above the upper limit of the chart.

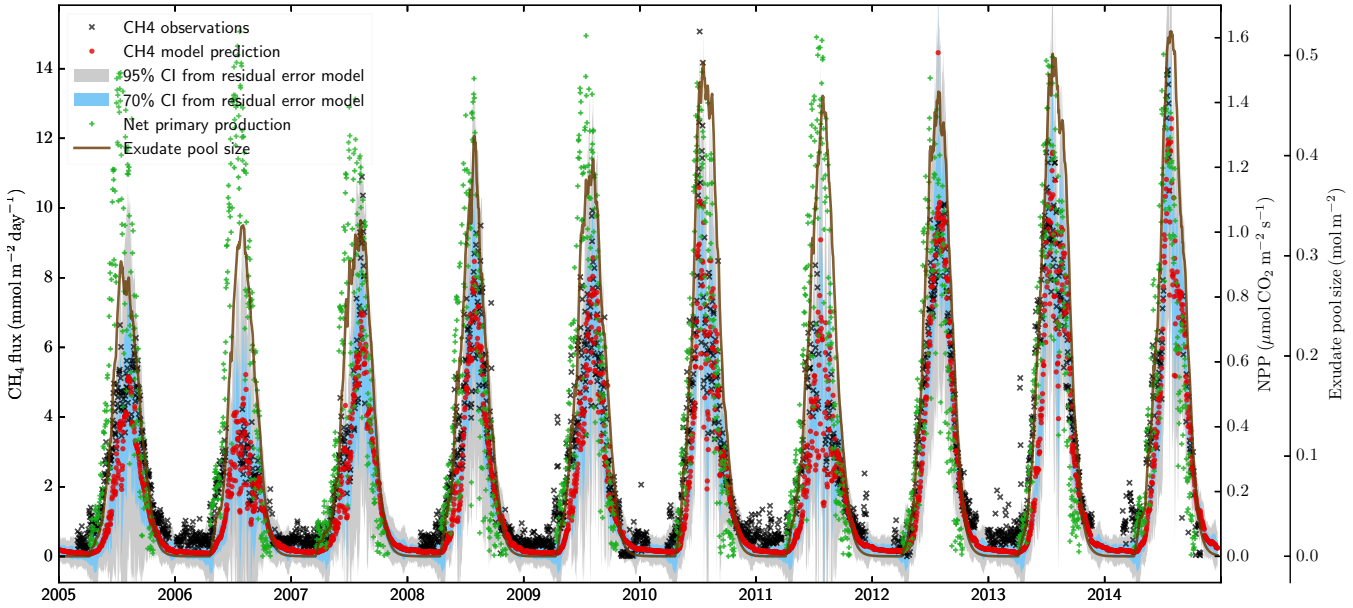

Figure 9. Output ~~fluxes~~ CH_4 flux (red dots) with parameters from the posterior mean~~.~~. Methane observations (black crosses) and predicted fluxes with ~~100 cm~~ confidence intervals from ARMA(2,1) modeling of ~~peat~~a set of 1000 residual timeseries are shown, as are the input net primary production (green dots) and the exudate pool sizes (brown line). Most of the observations are inside the confidence intervals, but note that the effects of the parameter variations in the posterior are not part of these confidence intervals. The constituents of the total flux are shown in Fig. 11.

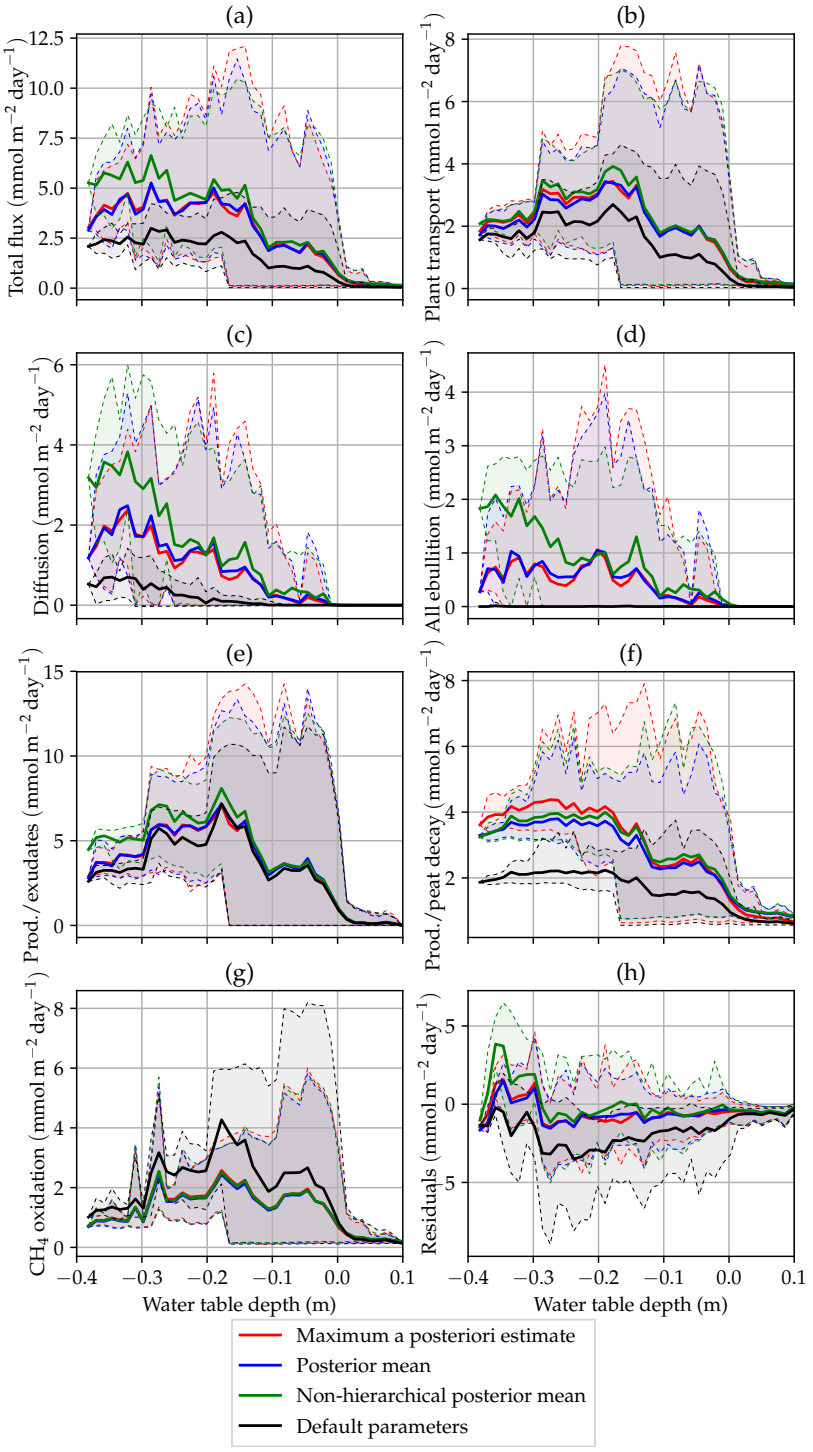

Figure 10. Means of total CH_4 emission (a), its components (b-c), total ebullition taking place (d), CH_4 production (e-f), CH_4 oxidation (g), and model residuals (h) as functions of water table depth. Shaded areas show the 5th and 95th percentiles. To look at the effect of the optimization, compare the black and the ~~green~~ blue/red lines.

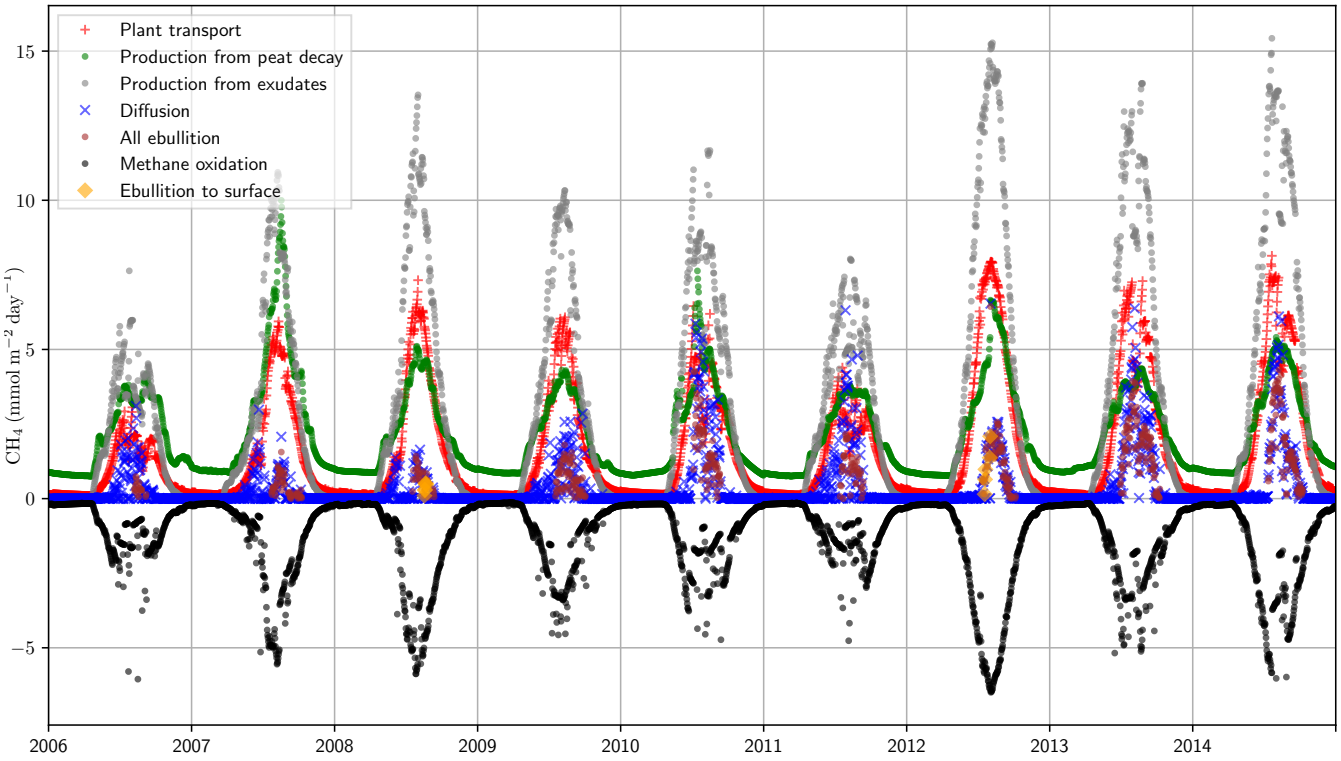

Figure 11. Diffusion, plant transport, ebullition, CH_4 production, and CH_4 oxidation time series for parameter values from the posterior mean estimate~~with 100 cm~~. The figure shows how only a minor part of ~~peat~~ebullition in the end comes to the surface as ebullition. The total flux and the observations are shown in Fig. 9.

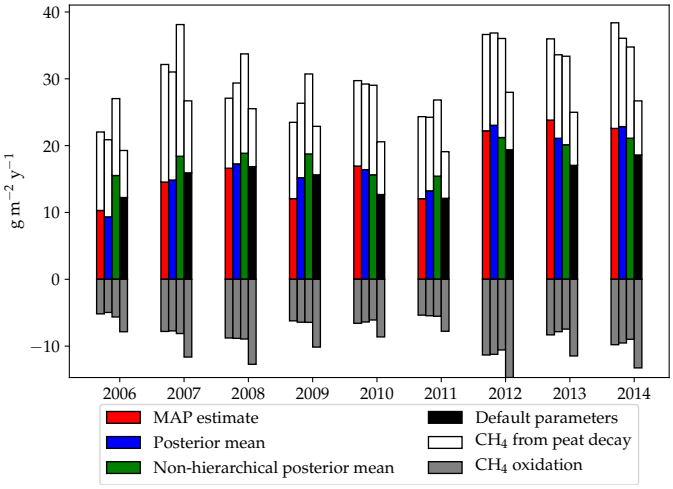

Figure 12. Annual CH_4 production in grams per square meter from root exudates (colored part) and peat decomposition (white part) for the different years. Oxidized CH_4 is shown as gray and negative.

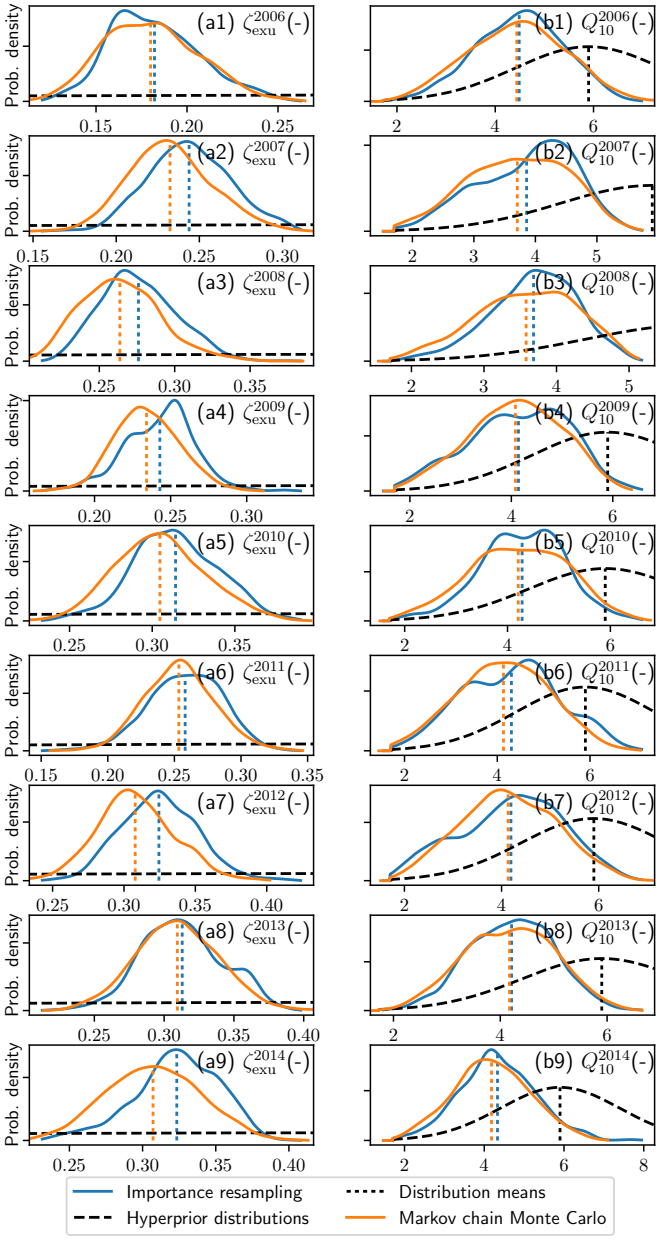

Figure 13. Posterior marginal distributions of the hierarchical parameters ~~for all~~ from both MCMC ~~experiments~~ and importance sampling, along with the hyperpriors. The (~~a~~a-) sub-figures are for the parameters ζ, and the (~~b~~b-) sub-figures for Q_{10}. The curves shown ~~for the MCMC experiments~~ are smoothed slightly using Gaussian kernel estimates for readability. To make these figures, ~~50~~70% from the start of ~~each~~ the MCMC chain was discarded as warm-up. The dotted vertical lines show the default parameter values ~~.Posterior distributions~~ and ~~correlations of~~ the ~~annual means~~ mean values of the ~~output from the modeled processes for the year 2008 with 70 cm peat. The dynamics for the other years and peat depths are mostly similar. The results shown are based on 1000 random samples from the parameter~~ posterior ~~distribution. The two-dimensional marginal~~ distributions~~in the triangle on~~. Importance resampling had the ~~lower left have their labels on~~ tendency of moving the ~~left and at~~ posteriors of the ~~bottom~~ζ-parameters slightly higher, ~~and the correlations between the processes in the upper triangle on the right have their labels on the left and on the top. The images in the lower left triangle show~~ despite the ~~90% (black) 50% (red), and 10% (blue) contours~~weaker prior used for that step.

Table 5. p and r^2 values of the regressions of the Q_{10} (-) parameters against the mean soil temperature of the 10 first weeks of the year at the depth of 35 cm, and the ζ_{exu} parameters against the sum of the net primary production of the first 130 days of the year.

Peat depth	$p_{Q_{10}}$																			
40 cm	0.13	0.30	0.040	0.47	50 cm	0.027	0.53	0.070	0.39	70 cm	0.011	0.63	0.015	0.60	100 cm	0.0068	0.67	0.027	0.53	150 cm	0.34	0.13	0.040	0.48	200

Parameters that were not part of the optimization procedure Parameter Equation Value Units Description Source ΔE_R 6 50000 J mol^{-1} heterotrophic respiration parameter Nedwell and Watson (1995) ΔE_{oxid} 7 50000 J mol^{-1} CH_4 oxidation parameter Nedwell and Watson (1995) $f_{CH_4}^{\mathrm{exu}}$ 15 0.25 - root exudates to CH_4 fraction close to Riley et al. (2011) $g_{CH_4}^{Q_{10}}$ 16 0.4 - peat decay to CH_4 fractionSchuldt et al. (2013) K_R 19 0.22 mol m^{-3} Michaelis-Menten coeff. Nedwell and Watson (1995) K_{CH_4} 20 0.44 mol m^{-3} Michaelis-Menten coeff. Nedwell and Watson (1995) K_{O_2} 20 0.33 mol m^{-3} Michaelis-Menten coeff. Nedwell and Watson (1995) SLA 22 23 m^{2}kg^{-1} specific leaf area Vile et al. (2005) k 23 $\log(2)/1800$ s^{-1} ebullition rate constant - σ 23 0.8 - peat porosity Rezanezhad et al. (2016)MCMC chains from the experiment with 100 cm of peat. The hierarchical parameters in (b) and (d) show the mean value in the middle as a black mass, and the colorful surroundings are the values parameters for the individual years. The last figure (l) shows the value of the objective function.